Coi1 is a novel assembly factor of the yeast complexes III - IV supercomplex

Dissertation

der Mathematisch-Naturwissenschaftlichen Fakultät

der Eberhard Karls Universität Tübingen

zur Erlangung des Grades eines

Doktors der Naturwissenschaften

(Dr. rer. nat.)

vorgelegt von

Ravi Kumar Singhal

aus Jind, Indien

Tübingen

2017

Gedruckt mit Genehmingung der Mathematisch-Naturwissenschaflichen Fakultät der Eberhard Karls Universität Tübingen.

Table of contents

1 List of abbreviations

AAC	ADP/ATP carrier
ADP	adenosine diphosphate
Amp	ampicillin
APS	ammonium peroxodisulfate
ATP	adenosine triphosphate
BN-PAGE	blue native polyacrylamide gel electrophoresis
bp	base pair
BSA	bovine serum albumin
CJs	crista junctions
CM	crista membrane
DDM	*n-Dodecyl-D-Maltoside*
DHFR	dihydrofolate reductase
$DiSC_3(5)$	dipropylthiadicarbocyanine iodide
DTT	dithiotreitol
dNTP	deoxyribonucleoside triphosphate
E. coli	*Escherichia coli*
ECL	Enhanced chemiluminescence
EDTA	ethylendiamine tetraacetate
IMB	inner boundary membrane
IM	inner membrane
IMS	intermembrane space
HA	Haemagglutinin
HEPES	N-2 hydroxyl piperazine-N´-2-ethane sulphonic acid
Hsp	heat shock protein
kDa	kilodalton
LB	Luria Bertani
MIM	mitochondrial inner membrane
MOM	mitochondrial outer membrane
MOPS	N-morpholinopropane sulphonic acid
MPP	mitochondrial processing peptidase
mtHsp	mitochondrial heat shock protein
MTS	mitochondrial targeting sequence

NADH	nicotine amide adenine dinucleotide
ORF	open reading frame
OD	optical density
PAGE	polyacrylamide gel electrophoresis
PCR	polymerase chain reaction
PEG	polyethylene glycol
PK	proteinase K
PMSF	phenylmethylsulfonyfluoride
PVDF	polyvinylidene difluoride
RNasin	ribonuclease inhibitor
RPM	revolutions per minute
RT	room temperature
SAM	sorting and assembly machinery
SAP	shrimp alkaline phosphatase
S. cerevisiae	*Saccharomyces cerevisiae*
SD	standard deviation
SDS	sodium dodecyl sulfate
TBS	TRIS buffered saline
TCA	trichloroacetic acid
TEMED	N,N,N',N'-tetramethylene diamine
TIM	translocase of the inner mitochondrial membrane
TMD	transmembrane domain
TOM	translocase of the outer mitochondrial membrane
TRIS	tris-(hydroxymethyl)-aminomethane
TX-100	Triton X-100
v/v	volume per volume
w/v	weight per volume
wt	wild type
$\Delta\Psi$	membrane potential

2 Summary

Mitochondria are important organelles that are required for generation of ATP, and are also involved in regulation and monitoring various cellular processes. They are divided into several sub-compartments, among them is the mitochondrial inner membrane (IM), which harbors the highly structured multi-subunit respiratory chain complexes. Most of the subunits of these complexes are nuclear-encoded and imported from the cytosol into mitochondria. A small group of the subunits of the respiratory complexes are synthesized within the organelle and are then directed to their proper destination. Components of the respiratory chain complexes from both origins are assembled into the mitochondrial IM with the help of various assembly factors. The integration of the core subunits of cytochrome bc1 complex (complex III) and cytochrome c oxidase complex (complex IV) into the IM is well studied. However, the assembly and organization of their supercomplexes are still not completely understood.

This work characterizes a previously uncharacterized yeast protein (ORF *YDR381C-A*) that we named cytochrome c oxidase interacting protein 1 (Coi1). The protein was found to be a new regulatory factor that is involved in the assembly of complex IV and supercomplexes. The results demonstrated that Coi1 is a small mitochondrial IM protein with a single transmembrane segment toward its N-terminus whereas the C-terminus faces the intermembrane space (IMS). Deletion of *COI1* leads to a severe growth phenotype on non-fermentable carbon sources, a decrease in membrane potential, hampered respiration, and reduced enzymatic activity of complex IV. In addition, the steady-state levels of subunits of complexes III and IV as well as of the assembled complexes and supercomplexes are reduced. Furthermore, Coi1 was found to physically interact with subunits of both complexes, although it appears to be a stoichiometric subunit neither of complex III nor of complex IV. Of note in absence of Coi1, heme A in complex IV was completely diminished. Collectively, this work identifies a novel protein that plays a role in the assembly of the mitochondrial respiratory chain supercomplexes.

3   Introduction

Eukaryotic cells are divided into numerous membrane-surrounded compartments that form different organelles. To function properly, each organelle requires a specific set of proteins in order to functionally contribute to the wide spectrum of biochemical processes in the cell. The vast majority of these proteins are nuclear encoded and synthesized in the cytosol, whereas very few proteins are encoded by mitochondrial or plastid genomes. After or during their synthesis, the nuclear-encoded proteins are targeted to their designated destination where they can properly perform their function (Neupert and Herrmann, 2007; Soll and Schleiff, 2004). Newly synthesized proteins are directed to their target organelles by targeting signals, which are recognized by receptors in the cytosol or on the organelle itself. The proteins are then translocated across or inserted into the organelle's membrane (Schnell and Hebert, 2003). Over the years, our understanding of protein trafficking and organelle biogenesis has significantly increased. This knowledge provides us a better understanding of crucial cellular processes.

3.1   Structure and function of mitochondria

According to the endosymbiont theory, ~1.5 billion years ago mitochondria evolved from α-proteobacteria, which were taken up through endocytosis by an anaerobic primitive eukaryotic cell (Gray et al., 1999). In the course of evolution, the host cell transferred the endosymbiont genes to the nucleus to improve its own survival chances and to regulate the mitochondrial activity in an oxygen-rich environment (Cavalier-Smith, 1987). Mitochondria are present in the majority of eukaryotic cells where they form dynamic, tubular network-like structures surrounded by a double membrane. The mitochondrial network is not static but constantly undergoes processes of fusion and fission (Hoffmann and Avers, 1973; Okamoto and Shaw, 2005). The two mitochondrial membranes give rise to four sub-compartments. The outer membrane (OM), which separates the organelle from the surrounding cytoplasm, and the inner membrane (IM), which separates the inner membrane space (IMS) from the matrix. Mitochondrial proteins are mainly encoded in the nucleus (>99%) and synthesized as precursor proteins on cytosolic ribosomes before their import into the mitochondria. However, a few mitochondrial proteins are also encoded by the mitochondrial genome in the organelle´s matrix. Most of these

mitochondrially-encoded proteins are very hydrophobic IM proteins. Thus, their synthesis in the cytosol and the ensuing transport to the mitochondria via the aqueous environment in the cytosol might pose an immense problem to the cell. This drawback is circumvented by co-translationally inserting these proteins into the inner membrane from the matrix (Neupert and Herrmann, 2007; Soll and Schleiff, 2004).

Mitochondria play a fundamental role in the generation of energy by oxidative phosphorylation. They are further required for various metabolic pathways such as the tricarboxylic acid cycle, β-oxidation of fatty acids, the metabolism of amino acid and lipids, the biosynthesis of heme cofactors and iron-sulphur clusters. In addition to their metabolic function, mitochondria also assist in signaling and act as a central regulatory element of apoptosis, autophagy, and aging (Lill, 2009; Pagliarini et al., 2008; Schmidt et al., 2010; Youle and Karbowski, 2005). Taken together, mitochondria play a prime role in many cellular processes. Their importance is further highlighted by a series of disorders in humans that are caused by mitochondrial dysfunction (Scheffler, 2001).

3.2   Mitochondrial protein translocation

3.2.1   Import of nuclear encoded proteins

Most mitochondrial proteins are encoded by the nuclear DNA and synthesized in the cytosol. The precursor proteins are imported from the cytosol into mitochondria in a post-translational or co-translational manner (Fujiki and Verner, 1991, 1993). The post-translational import of nuclear-encoded proteins into the mitochondria is a widely accepted concept (Ahmed and Fisher, 2009; Borgese et al., 2007). Most likely, cytosolic chaperones stabilizes the precursor proteins during or just after their translation to protect them from aggregating until they have reached their final destination (Neupert and Herrmann, 2007). The precursor proteins are targeted to the mitochondria by recognition sequences. Proteins designated to the IM, the IMS, or the matrix often contain a cleavable N-terminal signal sequence, which is about 10-80 amino acids long (Prokisch et al., 2006). The presequence directs the precursor protein all the way to the matrix where it is usually cleaved off by the mitochondrial matrix processing peptidase (MPP) to complete the import of the protein. As an alternative to a cleavable N-terminal signal, the vast majority of mitochondrial OM proteins and also some proteins found in the mitochondrial IM and

6

the IMS contain internal targeting sequences where the targeting signal remains part of mature protein (Neupert and Herrmann, 2007).
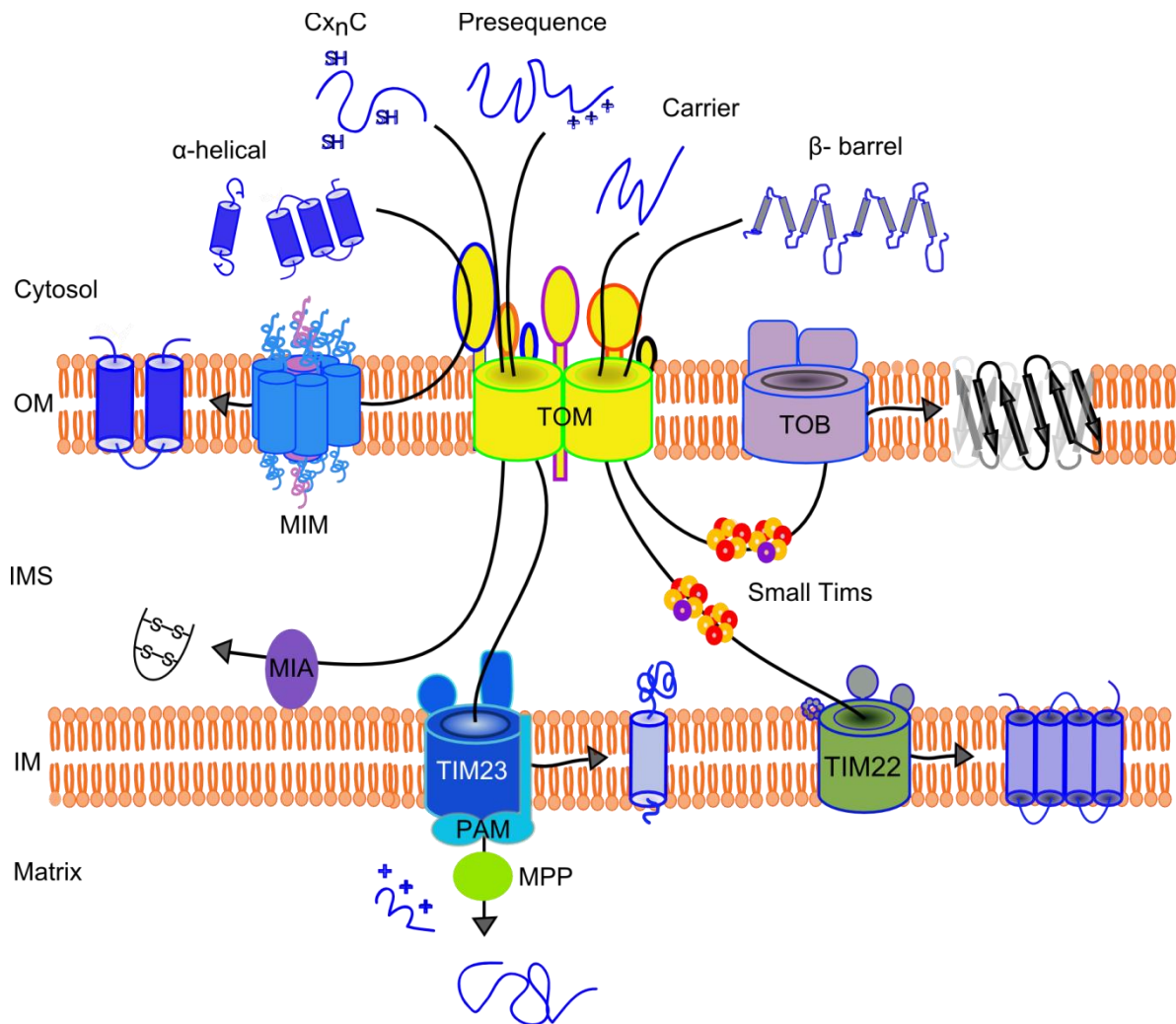
Figure 3.1 Protein translocation machineries in mitochondria. Nuclear encoded proteins are imported into the mitochondria by various import machineries present in the OM and the IM. The precursor proteins are recognized by receptors on the outer membrane and further sorted by different pathways to their final destination. Most of the proteins enter the mitochondria through the TOM complex. The biogenesis of β-barrel proteins requires small Tim chaperones present in the IMS and the TOB machinery that inserts the β-barrel proteins into the OM. α- helical single and multi-span proteins are recognized by OM surface receptor proteins, and the MIM machinery inserts them into the OM. Presequence containing proteins are inserted into the IM or imported into the matrix by the TIM23 complex. For the import into the matrix, the TIM23 complex works together with the PAM module. When presequence-containing proteins reach the matrix, their presequence is cleaved off by MPP. Carrier proteins are transported with the help of small Tim chaperones and are inserted into the IM by the TIM22 machinery. Proteins containing cysteine-rich signals are retained in the IMS by oxidation through the MIA system. Nearly all precursor proteins destined for the IMS, the IM, or the matrix are imported in membrane potential (ΔΨ)-dependent fashion.

Mitochondria contain seven main import machineries that are involved in the translocation of different types of proteins. Three translocase machineries, namely the translocase of the outer mitochondrial membrane (TOM) complex, the topogenesis of mitochondrial outer membrane β-barrel proteins (TOB) complex (also known as sorting and assembly machinery, SAM), and the mitochondrial import (MIM) complex are found in the OM. Almost all mitochondrial precursor proteins are recognized on the mitochondrial surface by the receptor proteins of the TOM complex (Tom20, Tom22 and Tom70) and translocated through a pore formed by the central component of the TOM complex, Tom40 (Chacinska et al., 2009; Neupert and Herrmann, 2007). The TOB complex facilitates the membrane insertion of β-barrel proteins, while the MIM complex is involved in the import of single- and multi-span α-helical proteins of the OM. The mitochondrial IM harbors four import machineries: the translocase of the inner membrane (TIM) 22 complex, the TIM23 complex, the oxidase assembly 1 (OXA1) complex, and the mitochondrial intermediate space assembly protein (MIA) complex (Fig 3.1).

Precursor proteins with a cleavable presequence are translocated across the OM by the TOM complex and handed over to the TIM23 complex which inserts them into the IM or transports them to the matrix. For the import into the matrix, the TIM23 complex interacts with the presequence translocase-associated motor (PAM) machinery. Once the precursor proteins arrive in the matrix, their presequence is cleaved off by MPP (Becker et al., 2012; Dudek et al., 2013; Prokisch et al., 2006; van der Laan et al., 2010). Another class of proteins with a cleavable N-terminal signal is first imported to the matrix in TIM23- and PAM-dependent manner and afterwards inserted into the IM by Oxa1. This process is also known as the conservative sorting pathway (Fig 3.2) (Bohnert et al., 2010; Hell, 2008).

Precursor proteins containing an internal targeting sequence use different import pathways. Multi-span carrier proteins are translocated first by the TOM complex and are then imported into the IM with the assistance of the TIM22 machinery (Brix et al., 1999). IMS proteins containing cysteine rich motifs are imported by TOM complex and retained in the IMS by forming intermolecular disulfide bridges. The disulfide bridge formation is catalyzed by the MIA complex (Chacinska et al., 2004; Hell, 2008).

Mitochondria contain several chaperones to keep proteins that are currently being imported from aggregating. In the IMS, this job is performed by the small Tim chaperone complexes (Tim9/Tim10 and Tim8/Tim13). Additionally, various chaperones present in the matrix support protein folding (Ssc1, Mdj1, Hsp60/Hsp10, Hsp78, and Hep1) (Chacinska et al., 2009; Davis et al., 2007).
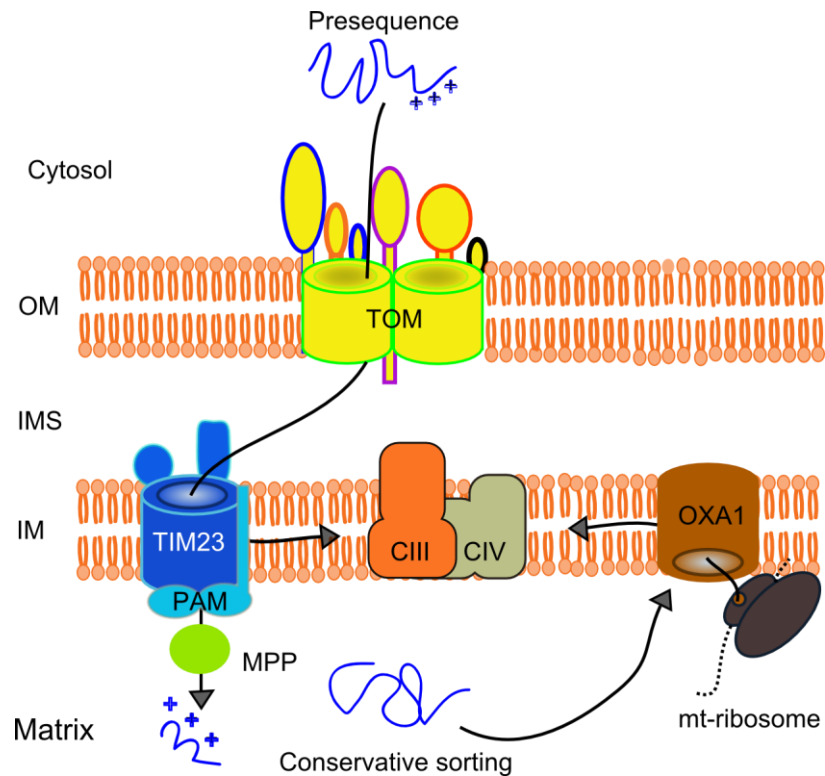
Figure 3.2 Various pathways for the membrane integration of respiratory components. Precursor proteins of the respiratory chain complexes are encoded by both nuclear and mitochondrial DNA. Precursor proteins of nuclear origin are recognized by the receptors on the OM and imported through the TOM and TIM23 complexes. Mitochondrially-encoded precursor proteins are synthesized in the matrix and inserted into the IM in a co-translational manner. To achieve this, the mitochondrial ribosomes are bound to the OXA1 machinery. Some nuclear-encoded precursor protein are first imported into the matrix by the TIM23/PAM complex and then further inserted into the IM by the OXA1 machinery. This import pathway is also known as conservative sorting. After the membrane insertion of precursor proteins, they are assembled into functional complexes.

3.2.2 Membrane insertion of mitochondrially-encoded proteins

The mitochondrial genome of yeast encodes eight proteins. Among them, seven are hydrophobic subunits of the respiratory chain complexes, which are embedded in the IM (Fox, 2012; van der Laan et al., 2010). These proteins are translated on mitochondrial ribosomes associated directly with the membrane and are inserted into

the IM in a co-translational fashion with the help of the assembly factor Oxa1. Oxa1 is also required for assembly of some nuclear-encoded proteins as mentioned above (Fig 3.2) (Bohnert et al., 2010; Fox, 2012; Hell et al., 2001). Oxa1 inserts proteins containing signatures of negatively charged amino acids into the IM, and this process is membrane-potential dependent (Herrmann et al., 1997). Whereas Oxa1 interacts directly with ribosomes, additional factors like Mba1 and Mdm38 are also involved in attaching the translating ribosomes to the IM (Fig 3.2) (Hell et al., 2001; Ott et al., 2006).

3.3   Oxidative phosphorylation system

Under aerobic conditions, eukaryotic cells generate energy in the form of ATP through the process of oxidative phosphorylation in mitochondria. The mitochondrial IM forms heavily folded structures known as cristae. Each crista harbors several copies of respiratory chain components such as NADH dehydrogenase (complex I), succinate dehydrogenase (complex II), cytochrome bc_1 (complex III), cytochrome c oxidase (complex IV), and F_1F_o-ATP synthase (complex V) (Boekema and Braun, 2007).

The oxidative phosphorylation system is powered by electrons derived from the citric acid cycle intermediates NADH and succinate. Complex I catalyzes the oxidation of NADH to NAD^+ and releases four protons into the IMS during the reaction (Fig 3.3). In yeast, complex I is absent and the oxidation of NADH is carried out by Nde1, Nde2, and Ndi1 (Fig 3.3B). This reaction does not release protons into the IMS (Fig 3.3A) (Grandier-Vazeille et al., 2001). Complex II generates electrons by oxidizing succinate to fumarate. The electrons are passed from complex I and complex II to coenzyme Q (CoQ) which delivers them to complex III, where they are transferred to cytochrome c (Cyt C). Complex III not only relays the electrons from CoQ to Cyt C but also pumps protons into the IMS during this process. Complex IV is the final enzyme of the electron transport chain and accepts electrons from Cyt C. These electrons are then utilized to reduce oxygen molecules to water. This also leads to an accumulation of four additional protons in the IMS. As several of the respiratory chain complexes pump protons to the IMS, the electron flux is coupled to the generation of a proton gradient (Δψ) across the mitochondrial IM. This proton gradient is used as a motive force for complex V, which converts it into energy

stored in a chemical bond through phosphorylation of ADP to ATP (Fig 3.3) (Chaban et al., 2014; Saraste, 1999; Yoshida et al., 2001).
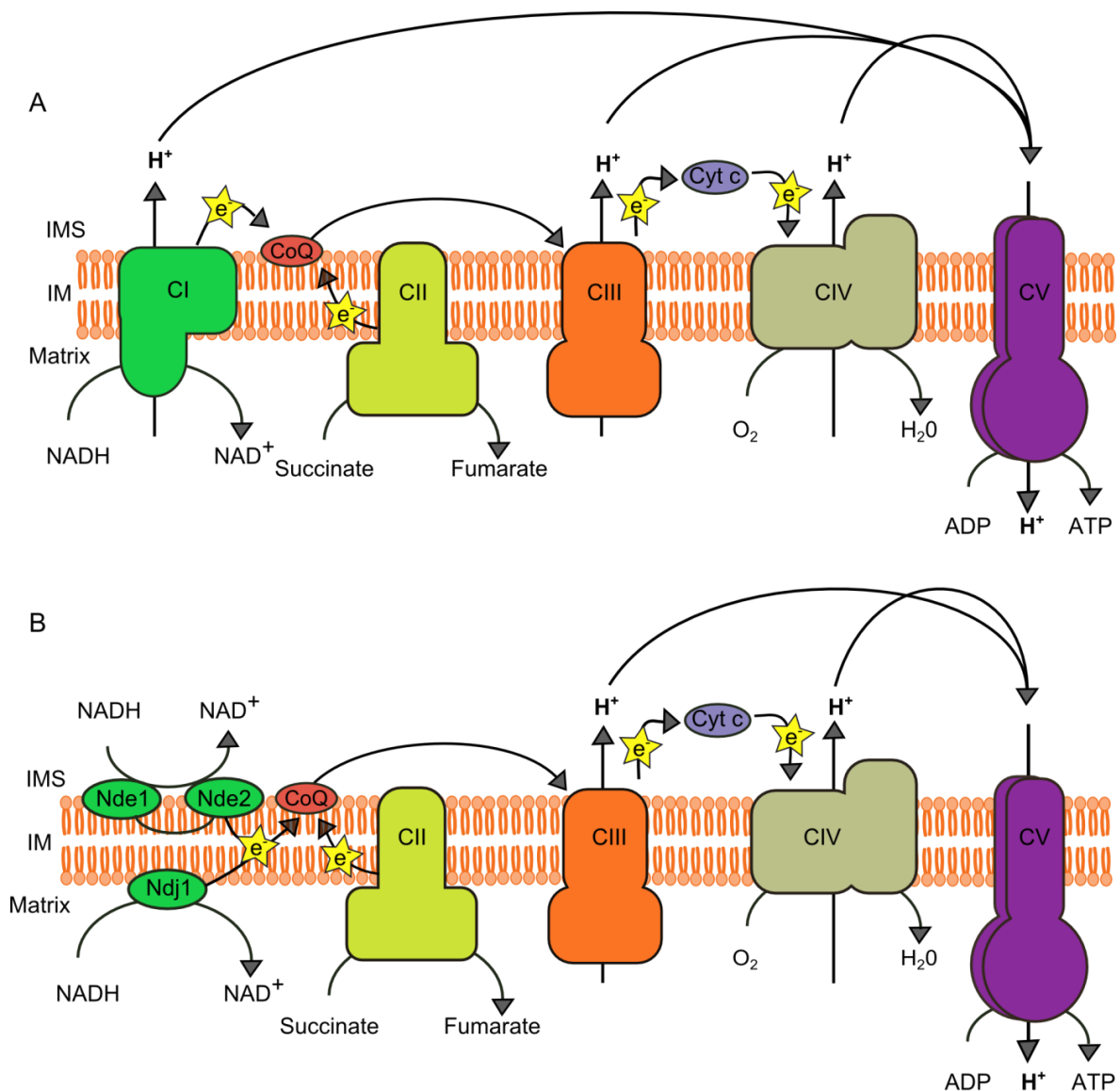
Figure 3.3 Oxidative phosphorylation system in mitochondria based on the fluid model. The mitochondrial IM harbors different enzyme complexes involved in oxidative phosphorylation. **(A)** The mammalian respiratory chain is composed of NADH dehydrogenase (CI), succinate dehydrogenase (CII), cytochrome bc1 (CIII), and cytochrome c oxidase (CIV). These complexes synchronize electron transport from one complex to another leading to the reduction of O_2 to H_2O as the final outcome. With the exception of complex II all other complexes generate proton flux across the IM during this process. The proton gradient is further utilized by the ATP synthase (CV) in production of energy in the form of ATP. **(B)** The oxidative phosphorylation system in *S. cerevisiae* consists of complexes II-IV and the F_1-F_0 ATP synthase. A multimeric complex of Nde1, Nde2, and Ndi1 replaces complex I of higher eukaryotes. In both systems, coenzyme Q (CoQ) and cytochrome c (Cyt C) are involved in electron transport between the complexes. These schematic representations are based on the fluid model (Hackenbrock et al., 1980).

3.4 **Composition and structure of the respiratory chain complexes**

Yeast mitochondria synthesize eight proteins: cytochrome b (Cob) of complex III; Cox1, Cox2, and Cox3 as core components of complex IV; Atp6, Atp8, and Atp9 of complex V, and Var1 which is a ribosomal protein. Complex II is the only respiratory chain complex which does not contain mitochondrially-encoded proteins (Fox, 2012; Mick et al., 2011).

3.4.1 **Assembly of the cytochrome bc_1 complex**

Cytochrome bc_1 complex (complex III) is an essential component of the electron transport chain. It transfers electrons from CoQ to Cyt C, and for each transferred electron, one proton is transported to the IMS. The catalytic core consists of the mitochondrially-encoded Cob with two heme B molecules (low potential b_L and high potential b_H), the nuclear-encoded proteins cytochrome c_1 (Cyt1) that binds heme C, and the Rieske iron-sulphur protein (Rip1) that harbors a 2Fe-2S prosthetic group. Apart from the catalytic core, complex III contains seven additional subunits: Cor1, Cor2, Qcr6, Qcr7, Qcr8, Qcr9, and Qcr10 (Hunte et al., 2000; Smith et al., 2012). For the proper function of complex III, the assembly of nuclear- and mitochondrially-encoded proteins are arranged in a coordinated fashion starting with Cob, which is the sole mitochondrially-encoded subunit. In the next step, as a part of the early assembly subunit, Qcr7 and Qcr8 are added. The intermediate assembly complex is formed by Cor1, Cor2, Cyt1, and Qcr6 together with the early assembly subunits. The assembly of complex III is finished with the addition of Qcr9, Qcr10, and Rip1. Assembly factors such as Cbp3, Cbp4, Cbp6, and Bca1 play a role in the early assembly, whereas insertion and assembly of Rip1 is performed by the assembly factors Bcs1 and Mzm1 (Nobrega et al., 1992; Smith et al., 2012). Complex III is completely functional in a homo-dimer state, which forms supercomplexes with complex IV for efficient electron transport (Dudkina et al., 2010; Hunte et al., 2000).

3.4.2 **Assembly of cytochrome c oxidase**

Cytochrome c oxidase (complex IV) is the terminal enzyme in the electron transport chain that oxidizes Cyt C to reduce molecular oxygen to water. In yeast, cytochrome c oxidase forms a complex comprised of twelve subunits. The core subunits of the complex, Cox1, Cox2, and Cox3 are encoded by mitochondrial DNA

(Castresana et al., 1994). Cox1 and Cox2 contain cofactors that are required for their catalytic activity. Cox1 has a heme a and a bimetallic heme a_3-copper (Cu_B) site, whereas Cox2 has a binuclear copper ion site (Cu_A) (Mick et al., 2010; Soto et al., 2012). In addition to the core components, complex IV comprises nine nuclear-encoded subunits: Cox4, Cox5a/b, Cox6, Cox7, Cox8, Cox9, Cox12, Cox13, and Cox26 (Geier et al., 1995; Levchenko et al., 2016; Soto et al., 2012; Strecker et al., 2016).

The assembly of complex IV is not completely understood, but it is believed to be modulated in a sequential pathway with a number of assembly intermediates. The assembly of complex IV is initiated by the Cox1 translation activators Pet309 and Mss51 (Fox, 2012; Stiburek et al., 2005). Oxa1 co-translationally inserts Cox1 into the IM in association with the assembly factors Cox14, Coa1, Coa3, and Shy1, thereby forming the early assembly complex (Barrientos et al., 2004; Mick et al., 2011; Mick et al., 2010). Coa1 and Shy1 interact with the early assembly complex leading to disassociation of Mss51, which acts as a negative regulatory loop of Cox1 translation (Mick et al., 2011). Prior to the assembly of the nuclear-encoded subunits, cofactors such as heme and metal ions are incorporated into the early assembly complex containing Cox1. The first nuclear-encoded subunits to join the growing complex, Cox5 and Cox6, form a sub-complex before inserting into the early assembly complex (Mick et al., 2011; Stiburek et al., 2005). Matured Cox2 and Cox3 are exported by Oxa1 and associate with the Cox1, Cox5, and Cox6 sub-complex, but the sequential order still remains unclear. Cox7, Cox8, and Cox9 form another sub-complex prior to their incorporation into complex IV. Finally, the structural subunits Cox12 and Cox13 join the holo-complex (Church et al., 2005). Cox13 is assembled by the supercomplex assembly proteins Rcf1 and Rcf2 (Vukotic et al., 2012).

3.5 Respiratory supercomplexes

3.5.1 Organization of supercomplexes

Mitochondria are dynamic structures that reorganize themselves according to variable cues such as external stress or upon a change of nutrient source. Respiratory chain complexes arrange and distribute themselves into individual

complexes or into supercomplexes. Over the years, the organization of these supercomplexes were summarized in three different models namely known as fluid, solid, and plasticity model. The fluid model treats the respiratory chain complexes as individual respiratory units without any physical interactions between each other. In this model, the electron carriers move freely within the lipid membrane (Fig 3.3) (Hackenbrock et al., 1986; Hackenbrock et al., 1980). In contrast to the fluid model, the solid model states that the respiratory complexes are arranged for more efficient transfer of electrons in larger structures formed from complexes I-IV (higher eukaryotes) or complexes III-IV (yeast) (Fig 3.4) (Lange and Hunte, 2002; Lenaz, 2001; Schägger and Pfeiffer, 2000). In mammals and plants, supercomplexes, which are also known as respirasome, are formed from complex I, two copies of complex III, and one to four copies of complex IV ($I+III_2+IV_{1-4}$) (Dudkina et al., 2010; Eubel et al., 2003; Schägger and Pfeiffer, 2000).
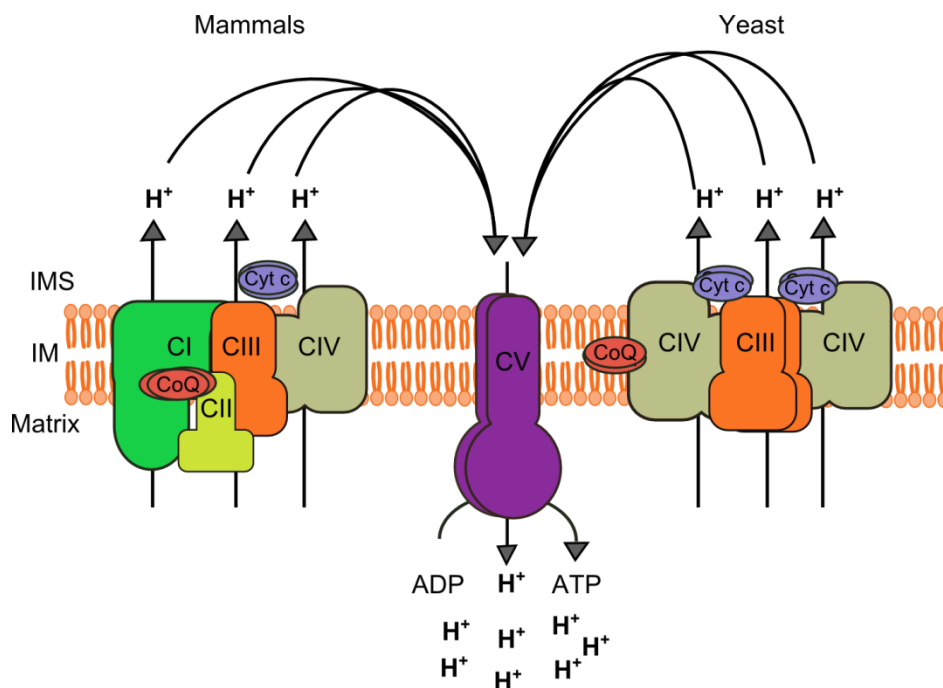
Figure 3.4 Schematic representation of respiratory chain complexes according to the solid model. In the solid model the respiratory chain complexes in higher eukaryotes are composed of complex I, III, and IV and in yeast of complex III and IV. The electrons are transferred with the help of coenzyme Q (CoQ) and cytochrome c (Cyt c), which reside in the inner membrane or in the IMS, respectively. This model is based on Schägger *et al* 2001.

In yeast, supercomplexes are formed from two copies of complex III and one to two copies of complex IV (III_2+IV_{1-2}) (Chaban et al., 2014; Cruciat et al., 2000;

Heinemeyer et al., 2007; Mileykovskaya et al., 2012; Schägger and Pfeiffer, 2000). Complex V in yeast forms dimers, and this dimerization is important for cristae formation (Arnold et al., 1998; Gavin et al., 2004). So far, no study has shown complex II as being part of a supercomplex.

Previous experiments using isolated supercomplexes could show electron transfer supporting the solid model over the fluid model. In addition, the migration behaviour of the complexes when analysed by blue native gel electrophoresis points towards the solid model rather than the fluid model. However, even in these experiments, the supercomplexes were stable only in the mild detergent digitonin, whereas in other detergents such as DDM only the individual complexes were detectable (Schagger, 2001a; Schägger and Pfeiffer, 2000).
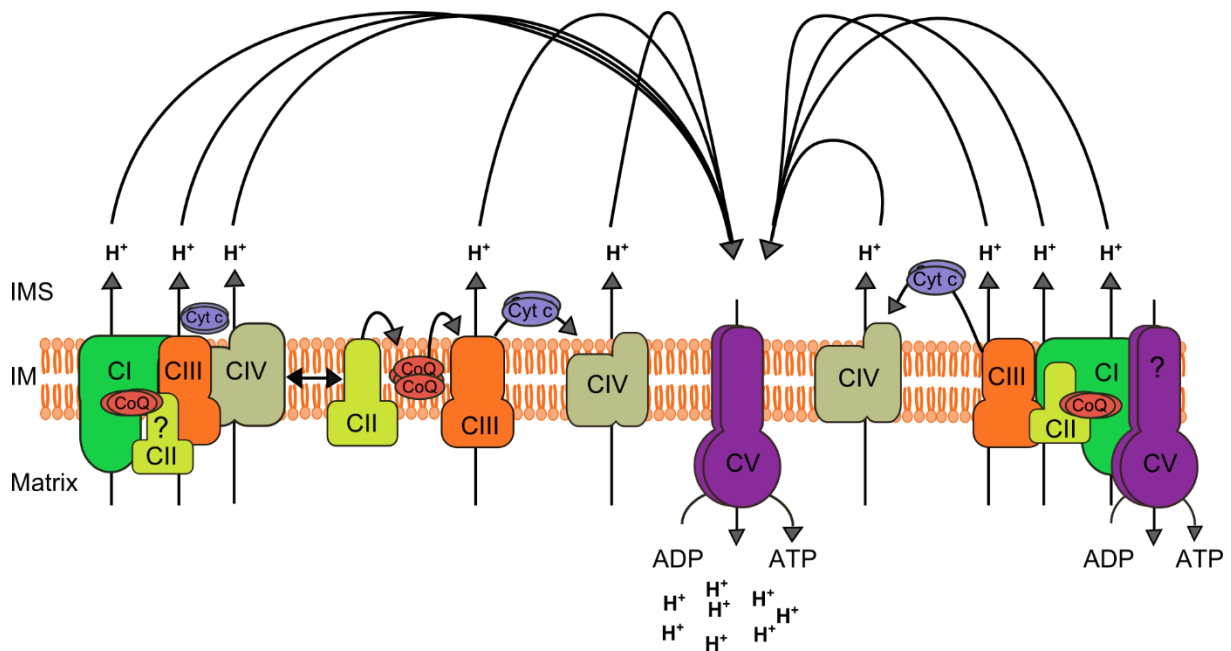
Figure 3.5 Schematic representation of the plasticity model. The plasticity model is a hybrid of both the fluid and the solid model. The respiratory chain complexes are arranged both in individual complexes (fluid model) and in the aforementioned supercomplexes (solid model) in different combinations. The question mark indicates a putative association with the supercomplexes. The plasticity model is based on Schägger *et al* 2001 and Acín-Pérez *et al* 2014.

An *in vivo* evidence for supercomplex formation was lacking until recently when the dynamic assembly of complexes and supercomplexes was monitored in a mammalian cell line. Two independent groups investigated the assembly of respiratory chain complexes by metabolic labeling of mitochondrially-encoded

proteins. The group of Acín-Pérez observed the initial assembly of single complexes, and after a long incubation period, supercomplexes were also observed (Acin-Perez and Enriquez, 2014; Acin-Perez et al., 2008). Similar experiments performed by the group of Ugalde showed partial assembly of complex I, which was completely assembled upon its interaction with complex III and IV (Acin-Perez and Enriquez, 2014; Moreno-Lastres et al., 2012). These experiments led to a new model, termed plasticity model, which includes complexes and supercomplexes being arranged in both fluid and solid models (Fig 3.5) (Acin-Perez and Enriquez, 2014). Although these aforementioned models came as a result of investigations mainly in mammalian systems, to a large extent they can also explain organization of supercomplexes in yeast cells.

3.5.2   Interface between complexes III and IV within their supercomplexes

A pseudo-atomic model of supercomplexes was constructed with the help of X-ray structures of yeast cytochrome c reductase and cytochrome c oxidase from bovine heart (Heinemeyer et al., 2007; Schägger and Pfeiffer, 2000; Tsukihara et al., 1996). Monomeric complex IV was surrounded by two complex III units, one on each side of the complex IV. The predicted interaction interface consists of the complex IV subunits Cox1, Cox2, Cox3, Cox4, Cox5, Cox7, and Cox8 together with the complex III subunits Cob, Cyt1, Qcr6, Qcr7, Qcr8, and Qcr9 (Heinemeyer et al., 2007). Previous experiments could already show an interaction of Cox1, Cox2, and Cox3 (all complex IV) with elements of complex III (Heinemeyer et al., 2007; Stuart, 2008; Winge, 2012).

3.5.3   Physiological relevance of supercomplexes

For the efficient function of the oxidative phosphorylation system, the respiratory chain complexes need to be arranged into a higher-organization state, which is thus of crucial functional importance. In terms of physiology, supercomplexes play an important role in substrate channeling, complex stability and sequestration of reactive intermediates (Schagger, 2001b). Association of complexes III and IV (I, III and IV in higher eukaryotes) improves the electron transfer rate as it reduces the distance that cytochrome c has to cover for the electron transfer between complex III and IV (Fig 3.5). The distance between the binding sites of cytochrome c in complex III and IV

are less than 6 nm in the yeast respirasome and less than 10 nm in the bovine respirasome, which improves the enzyme kinetics of the oxidative phosphorylation (Althoff et al., 2011; Chaban et al., 2014; Dudkina et al., 2011; Mileykovskaya et al., 2012).

Furthermore, the formation of supercomplexes increases the stability of the respiratory chain complexes and the capability of protein insertion into the IM. The dimerization of ATP synthase modulates the cristae structure and creates membrane curvature, which facilitates in turn supercomplex assembly and leads to optimal proton transport for further ATP synthesis (Davies et al., 2012). The characterization of cells with mutated forms of respiratory chain subunits supports a role of supercomplexes in maintaining the stability of the individual respiratory chain complexes. Mutations in subunits of complex III or IV destabilize complex I, suggesting that formation of complex III and IV is required for the stability of complex I in mammals. Interestingly, also in the bacterial system *Paracoccus denitrificans* the assembly of complex I is improved by rearrangement of I+III$_4$+IV$_4$ supercomplexes (Genova and Lenaz, 2014).

In summary, there are many indications that supercomplex formation plays an important role as it (1) increases electron transfer, (2) reduces the release of reaction oxidative species, (3) acts as a regulatory unit in respiration, (4) maintains the ultrastructure of the inner membrane, and (5) plays a role in increasing the stability of the respiratory chain complexes.

3.5.4 Stability and function of supercomplexes

Many studies were undertaken to understand the assembly and stability of the single respiratory chain complexes and of their supercomplexes. Experiments with cells lacking different subunits of the respiratory chain complexes revealed that not all the subunits are essential for supercomplex formation. For example, it was reported that Qcr9 or Rip1 destabilize supercomplexes formed by complex III and IV, whereas Qcr6, Qcr10 (complex III), Cox8, Cox9, Cox12, or Cox13 (complex IV) are required for supercomplex formation (Cruciat et al., 2000; Winge, 2012). Interestingly, the phospholipid cardiolipin was found to play a crucial role in the assembly and stability of supercomplexes (Pfeiffer et al., 2003). Cardiolipin was found at the interaction

interface between complex III and IV, where it associates with Cox3 (complex IV) and Cob (complex III). The loss of cardiolipin destabilizes the yeast supercomplex III-IV, but has no effect on complex V (Pfeiffer et al., 2003; Schägger, 2002). Along this line, an instability of complex IV in the respirasome ($I_1III_2IV_{1-4}$) was observed in cells from human patients with a mitochondrial dysfunction caused by a mutation in the gene taffazin, which is required for cardiolipin remodeling. Taken together, altered cardiolipin levels specifically affect the interaction of complex III and IV both in yeast and human supercomplexes (McKenzie et al., 2006).

3.5.5   Assembly factors of the supercomplexes

A group of proteins, which are not directly associated with the electron transport chain, can influence the assembly of supercomplexes. Among these proteins is also a major isoform of the ADP/ATP carrier, namely Aac2, residing in the mitochondrial IM. This protein associates in yeast cells with complex III-IV supercomplexes and plays a role for their stability (Claypool et al., 2008; Dienhart and Stuart, 2008). ADP/ATP carrier proteins are crucial for the exchange of ADP and ATP across the IM. In addition to Aac2, two assembly factors of complex IV, Shy1 and Cox14, are also involved in formation of complex III-IV supercomplexes in yeast (Barrientos et al., 2004; Glerum et al., 1995; Mashkevich et al., 1997; Stuart, 2008). These proteins are involved in the maturation of Cox1 and also physically interact with complex III-IV supercomplexes. While the exact function of this association is unknown, one assumption is that these factors associate with intermediate assembly forms of the supercomplexes (Winge, 2012). Recently, several groups have identified and characterized two additional proteins, known as respiratory supercomplex factor (Rcf) 1 and 2, which directly interact with complex IV and play a role in the stability of the supercomplexes (Strogolova et al., 2012). Reduced levels of the III_2IV_2 supercomplex and decreased activity of complex IV were observed in cells lacking Rcf1. These phenotypes were even more severe in the absence of both Rcf1 and Rcf2. Of note, monomeric levels of complex IV were not affected by the loss of Rcf1. However, the assembly of a subunit of complex IV, Cox13, was hampered in this mutant, which led in turn to a reduced assembly of the III_2IV_2 supercomplex (Chen et al., 2012; Shoubridge, 2012; Strogolova et al., 2012; Vukotic et al., 2012).

Despite of the aforementioned progress our understanding of the assembly of the respiratory chain complexes and their supercomplexes, a comprehensive picture of the factors involved and their contribution is still missing.

4   Aim of the study

For the proper function of oxidative phosphorylation in yeast cells, the respiratory chain complexes arrange themselves into supercomplexes of complexes III and IV. This study aims to characterize the novel yeast protein Coi1 (ORF *YDR381C-A*), which was found to play a role in the assembly of the respiratory supercomplexes.

Specifically, the following questions will be addressed:

I.   What are the structural and topological characteristics of Coi1?
II. What are the interaction partners of Coi1?
III. What is the molecular function of Coi1?

5 Materials and methods

5.1 Materials

5.1.1 Media

All the media, carbon source and amino acid stock solutions, were autoclaved separately prior to use. Carbon source such as glucose, galactose, and glycerol were added to a final concentration of 2% (v/v). For synthetic media, amino acids (from 100x stock) were used for specific auxotrophic selection markers. The table below summarizes the media used in this study.

Table 1: Media for *S. cerevisiae*

Media	Composition
YP media	2% (w/v) bacto peptone, 1% (w/v) yeast extract, 2% (v/v) carbon source, pH adjusted to 5.5 with NaOH
Lac media	0.3% (w/v) yeast extract, 0.05% (w/v) glucose, 0.05% (w/v) NaCl, 0.1% (w/v) KH_2PO_4, 0.1% (w/v) NH_4Cl, 0.06% (w/v) $MgCl_2 \cdot 6H_2O$, 0.05% (w/v) $CaCl_2 \cdot 2H_2O$, 2.5% (v/v) lactic acid 80%, 0.8% (w/v) NaOH, pH adjusted to 5.5 with NaOH
Synthetic (S) media	0.19% (w/v) yeast nitrogen base without ammonium sulfate, 0.5% (w/v) ammonium sulfate, 0.0055% (w/v) adenine sulfate, 0.0055% (w/v) uracil, 2% (v/v) carbon source, 1% (v/v) amino acid stock solution, pH adjusted to 5.5 with NaOH.
YP agar	2% (w/v) bacto peptone, 1% (w/v) yeast extract, 2% (w/v) agar, 2% (w/v) glucose or 3% (v/v) glycerol, pH adjusted to 5.5
S agar	2% (w/v) agar, 0.19% (w/v) yeast nitrogen base without ammonium sulfate, 0.5% (w/v) ammonium sulfate, 0.0055% (w/v) adenine sulfate, 0.0055% (w/v) uracil, 2% (v/v) carbon source, 1% (v/v) amino acid stock solution, pH adjusted to 5.5 with NaOH.
D-Glucose stock solution	40% (w/v) D-glucose
Glycerol stock solution	100% glycerol
D-Galactose stock solution	40% (w/v) D-galactose

100X amino acid stock	0.2% (w/v) arginine, 0.4% (w/v) tryptophan, 1% (w/v) leucine, 0.4% (w/v) lysine, 0.2% (w/v) histidine, 0.6% (w/v) phenylalanine, 0.2% (w/v) methionine

Table 2: Media for *E. coli*

Media	Composition
LB medium	1% (w/v) bacto-tryptone, 0.5% (w/v) yeast extract and 0.5% (w/v) NaCl in sterile H_2O, pH 7.0.
LB agar	LB media + 2 % (w/v) agar
LB medium with ampicillin	Ampicillin stock solution was made of 100 mg/ml in H_2O and sterilize filtrated. LB medium was supplemented with a final conc. of 100 µg/ml ampicillin. Ampicillin stock solution was added to autoclaved medium or agar solutions only when solutions were below 50°C.

5.1.2   Buffers

The tables below summarize the buffers used in this study**.**

Table 3: Buffers for agarose gel electrophoresis

Name	Composition
1×TAE buffer	40 mM tris-base, 1.14 ml/l acetic acid, 1 mM EDTA, pH 8
10× DNA loading dye	6% (v/v) glycerol, 0.05% (w/v) bromophenol blue, 0.05% (w/v) xylenecyanol

Table 4: Buffers for small scale isolation of plasmid from *E. coli* cells

Name	Composition
E1	50 mM Tris-HCl, 10 mM EDTA, 100 µg/ml RNase A
E2	200 mM NaOH, 1% (w/v) SDS dissolved in H_2O
E3	3 M potassium acetate, pH 5.5 adjusted with acetic acid

Table 5: Buffers for polymerase chain reaction

Name	Composition
10× Pfu buffer with MgSO$_4$	100 mM $(NH_4)_2SO_4$, 100 mM KCl, 1% (v/v) Triton X-100, 1 mg/ml BSA, 20 mM $MgSO_4$, 200 mM Tris, pH adjusted to 8.8 with HCl
10×Taq buffer with $(NH_4)_2SO_4$	200 mM $(NH_4)_2SO_4$, 0.1% (v/v) Tween20, 750 mM Tris, pH adjusted to 8.8 with HCl

Table 6: Buffers for preparation of chemical competent *E. coli* cells

Name	Composition
Tfb1 buffer	30 mM potassium acetate, 100 mM RbCl, 100 mM $CaCl_2$, 50 mM $MnCl_2$, 15% (v/v) glycerol, pH adjusted to 5.8 with acetic acid
Tfb2 buffer	100 mM MOPS, 75 mM $CaCl_2$, 10 mM RbCl, 15% (v/v) glycerol, pH adjusted to 6.5 with NaOH.

Table 7: Buffers for isolation of mitochondria and subcellular fraction

Name	Composition
Re-suspension buffer	100 mM Tris, 10 mM DTT
Spheroplasting buffer	1.2 M sorbitol, 20 mM potassium phosphate, pH 7.2
Homogenization buffer	0.6 M sorbitol, 1 mM EDTA, 1 mM PMSF, 0.2% (w/v) fatty acid-free BSA, 10 mM Tris 7.4 pH adjusted with HCl
SEM buffer	250 mM sucrose, 1 mM EDTA, 10 mM MOPS, pH adjusted to 7.4 with KOH
Percoll gradient buffer	25% (v/v) Percoll, 250 mM sucrose, 10 mM MOPS/KOH pH 7.2, 1 mM EDTA, 2 mM PMSF

Table 8: Buffer for sucrose gradient centrifugation

Name	Composition
Swelling buffer	20 mM HEPES/KOH, 2 mM EDTA, 2 mM PMSF pH 7.4
High sucrose buffer	2.2 M sucrose, 20 mM HEPES/KOH, 2 mM EDTA, 2 mM PMSF, pH 7.4
Low sucrose buffer	0.45 M sucrose, 20 mM HEPES/KOH, 2 mM EDTA, 2 mM PMSF, pH 7.4

Sucrose gradient buffer	2.5 M sucrose, 5 mM MOPS/KOH, 1 mM EDTA, 50 mM KCL

Table 9: Buffers for SDS-PAGE, Western blotting and immunodecoration

Name	Composition
2x Lämmli buffer	4% (w/v) SDS, 20% (v/v) glycerol, 0.02% (w/v) bromophenol blue, 5% (v/v) β-mercaptoethanol, 160 mM Tris, pH adjusted to 6.8 with HCl
SDS-running buffer	50 mM Tris, 1.61 M glycine, 1 g/l SDS
Blotting buffer	20 mM Tris, 150 mM glycine, 0.02% (w/v) SDS, 20% (v/v) ethanol
Ponceau staining solution	8.5 ml of 72% TCA, 0.4 g Ponceau for 200 ml total volume
TBS buffer	10 mM Tris, 154 mM NaCl, pH adjusted to 7.5 with HCl
TBST buffer	TBS buffer, 0.05% (v/v) Tween20
Blocking buffer	5% (w/v) powdered skim milk in TBS buffer
ECL	0.2 mM p-coumaric acid, 1.25 mM Luminol, 100 mM Tris, pH adjusted to 8.5 with HCl. 30% H_2O_2 were added before use in ratio 1:1000 to the ECL solution

Table 10: Buffers for antibody stripping of membranes.

Name	Composition
Stripping buffer	86 mM Tris-HCl, pH adjusted to 6.8, 2.9% (w/v) SDS, 1% (v/v) β-mercaptoethanol

Table 11: Buffers for colloidal Coomassie staining

Name	Composition
Staining solution	50 g aluminum sulfate hydrate, 100 ml ethanol, 0.2 g Coomassie Brilliant Blue G-250 (Serva Blue G), 23.5 ml 85% orthophosphoric acid in total volume of 1000 ml
Destaining solution	100 ml ethanol, 23.5 ml 85% orthophosphoric acid in total volume of 1000 ml

Table 12: Buffers for silver staining

Name	Composition
Fixation solution	40% (v/v) ethanol, 10% (v/v) acetic acid
Sensitizer solution	30% (v/v) ethanol, 8 mM sodium thiosulfate, 500 mM sodium acetate
Silver solution	30 mM silver nitrate
Developing solution	235 mM sodium carbonate, 0.02% (v/v) formaldehvde. 0.003% sodium thiosulfate
Stopping solution	5% (v/v) acetic acid

Table 13: Buffers for cell-free transcription and *in vitro* import of proteins into isolated mitochondria

Name	Composition
Transcription buffer	40 mM Tris-HCl pH 7.5, 10 mM NaCl, 6 mM $MgCl_2$, 2 mM spermidine
F5-import buffer	250 mM sucrose, 10 mM MOPS, 80 mM KCl, 5 mM $MgCl_2 \times 6H_2O$, 3% (w/v) fatty acid free BSA, pH adjusted to 7.2 with KOH
SEM-K^{80} buffer	SEM buffer with 80 mM KCl

Table 14: Buffers for blue native PAGE

Name	Composition
3X Gel buffer	200 mM ε-Amino-n-caproic acid, 150 mM Bis-Tris, pH adjusted to 7.0 with HCL
Solubilization buffer	0.1 mM EDTA, 50 mM NaCl, 10% (v/v) glycerol, 1 mM PMSF, 20 mM Tris, pH adjusted to 7.4 with HCL
10× Cathode buffer A	500 mM Tricine, 150 mM Bis-Tris, 0.2% (w/v) Coomassie G, pH 7.0
10× Cathode buffer B	500 mM Tricine, 150 mM Bis-Tris, pH 7.0
10× Anode buffer	500 mM Bis-Tris, pH adjusted to 7.0 with HCL
10× loading buffer	5% (w/v) Coomassie blue G, 500 mM ε-Amino-n-caproic acid, 100 mM Bis-Tris, pH 7.0

Table 15: Buffers for pull-down assay

Name	Composition
Pull-down buffer	50 mM sodium phosphate, 10 mM MOPS, 20 % glycerol, pH adjusted to 7.5
Solubilization buffer	1% digitonin, 0.5% Triton X-100 or 0.5% DDM in pull-down buffer

Table 16: Solutions for measurement of mitochondrial membrane potential

Name	Composition
Fluorescence dye	2 µM 3,3'- $DiSC_3(5)$ in ethanol
Buffer	0.6 M sorbitol, 0.1% (w/v) BSA fatty acid-free, 0.5 mM EDTA, and 20 mM KPI, pH 7.2
Uncoupler	1 µM valinomycin in ethanol

5.1.3 Enzymes

Restriction enzymes and buffers used in this study were provided by New England Biolabs. Different DNA polymerase such as *ExactRun*, Taq, and Pfu DNA polymerase were provided by Fermentas. Enzymes for yeast cell wall and protein digestion, such as zymolyase (Seikagaku) and proteinase K (Roche) respectively, were used. SP6 was used for transcription of *E. coli* vector, which was provided by Progema. All the enzymes and buffers were used according to the manufacturer recommendations.

5.1.4 Antibodies

Antibodies mentioned below were used for immunodetection. Most of the antibodies were raised in rabbit, apart from HA (abcam), which was raised in rat. The antibodies were diluted in 5% skim milk in TBS buffer (mentioned in Table 9) in appropriate concentration, which is mentioned below in Table 17. Proteins were detected by secondary goat antibody anti-rabbit (BIORAD) or anti-rat (abcam) conjugated to horseradish peroxide (HRP). In this study, antibody against Coi1 was raised against a mixture of two peptides (peptide 1: a.a. 101-114

RGDKLGFLDRRRNE; peptide 2: a.a. 83-96 LVRKSKYE GSGLSA) injected in parallel into two rabbits and serum was obtained from Pineda.

Table 17: Primary antibodies and their dilution factor

Name	Dilution	Cellular localization of antigen
α-Tom40	1:4000	MOM
α-Tom20	1:1000	MOM
α-Tom22	1:1000	MOM
α-Tom70	1:1000	MOM
α-Tob55	1:1000	MOM
α-Fis1	1:1000	MOM
α-Porin	1:4000	MOM
α-Om45	1:1000	MOM
α-Om14	1:4000	MOM
α-Mim1	1:200	MOM
α-Ugo1	1:1000	MOM
α-Coi1	1:2000	MIM
α-Dld1	1:1000	MIM
α-Cor1	1:2000	MIM
α-Cor2	1:2000	MIM
α-Qcr6	1:1000	MIM
α-Cox2	1:1000	MIM
α-Cox4	1:1000	MIM
α-Cox17	1:1000	MIM
α-Pic2	1:1000	MIM
α-AAC	1:1000	MIM

α-Tim23	1:1000	MIM
α-Oxa1	1:1000	MIM
α-Mic60	1:1000	MIM
α-Tim11	1:1000	MIM
α-Cyb2	1:1000	MIM
α-Mcr1	1:1000	MOM/IMS
α-Mge1	1:500	Matrix
α-Aco1	1:4000	Matrix
α-Bmh1	1:1000	Cytosol
α-Erv2	1:1000	ER membrane
α-Ssc1	1:5000	Matrix
α-HA	1:3000	HA-tag

5.1.5 Yeast and *E. coli* strains

Cloning and plasmid isolation were performed in *E. coli* strain XL10 gold. Yeast strains used in this study are mentioned below in Table 18.

Table 18: Yeast strains used in this study

Strains	Genotype	Reference
W303a	MATa; ade2-1; can1-100; his3-11; leu2 3_112; trp1Δ2; ura3-52;	Euroscarf, Frankfurt a. M., Germany
coi1Δ	W303a; *coi1::*HIS3MX6	This study
W303α	MATα; ade2-1; can1-100; his3-11; leu2 3_112; trp1Δ2; ura3-52;	Thesis of J. Dukanovic
mic60Δ	W303α; *mic60*::HIS3MX6	Thesis of J. Dukanovic

5.1.6 Oligonucleotides and constructs

Table 19: Oligonucleotides used in this study

Name	Sequence (5' to 3')	Remarks
coi1Δ FW	G ATA AAT ATA GTA ATA TTT CAT TCT TTG AGC CGT ACT AAG TAT ACA ATG CGT ACG CTG CAG GTC GAC	Amplification of KanMX4 or HISMX6 cassette
coi1Δ RV	T ACA TAA TAC TGC ATT GAA AAA ATG GAT AGG TTG ATT AAA CGT GTG ATC GAT GAA TTC GAG CTC G	Amplification of KanMX4 or HISMX6 cassette
Coi1 no intron FW	GGG GAA TTC ATG TCA AAT CCA TTT CAA AAT ATA GGT AAG AAT TTA CTA TAC ATT TCT GCA GC	Generating Coi1 without the intron: first 26 nucleotide (Exon1) + from nucleotide 221 till the end (exon2)
Coi1 no intron RV	GGG GAA TTC ATG TCA AAT CCA TTT CAA AAT ATA GGT AAG AAT TTA	Amplification of *COI1* ORF. 5' contains *EcoR*I restriction site
Coi1 RV	CCC GGA TCC TTA CTC GTT TCT CCT CCT ATC TAA AAA AC	Amplification of *COI1* ORF. 3' contains *BamH1* restriction site
Coi1 HA RV	CCC GGA TCC CCC TCG TTT CTC CTC CTA TCT AAA AAA C	Amplification of *COI1* ORF. 3' contains *BamH1* restriction site and encoding for HA C-terminal tag
2-9Δ Coi1 FW	GGG GAA TTC ATG AAG AAT TTA CTA TAC ATT TCT GCA GCC	Amplification of *COI1* ORF. 5' 10-114 amino acids contains *EcoR*I restriction site
1-30Δ Coi1 FW	GGG GAA TTC ATG AAA GCT AGA AGA GAT GCT AAA TTT ATA C	Amplification of *COI1* ORF. 5' 31-114 amino acids contains *EcoR*I restriction site
Coi1 4x methionine RV	CCC GGA TCC TTA CAT CAT CAT CAT CTC GTT TCT CCT CCT ATC TAA AAA AC	Amplification of *COI1* ORF. 3' contains *BamH1* restriction site and encoding for 4 methionine

Coi1 FW Cys 77-Ser	GAC AAC ATT GAT TCT TCT GAG GAC C	Amplification of *COI1* ORF. 3' contains Ser at 77 aa position instead of Cys
Coi1 RV Cys77-Ser	GGT CCT CAG A AGA ATC AAT GTT GTC	Amplification of *COI1* ORF. 5' contains Ser at 77 aa position instead of Cys
Coi1 Fw His 81-Ala	GCT CTG AGG ACG CTC AAT TAG TAA G	Amplification of *COI1* ORF. 3' contains Ala at 81 aa position instead of His
Coi1 Rv His81-Ala	CTT ACT AAT TGA GCG TCC TCA GAG C	Amplification of *COI1* ORF. 3' contains Ala at 81 aa position instead of His
Coi1 Fw Cys77-Ser & His 81-Ala	GAT TCT TCT GAG GAC GCT CAA TTA GTA AG	Amplification of *COI1* ORF. 3' contains Ser at 77 aa & Ala at 81 aa
Coi1 RV Cys77-Ser & His 81-Ala	CTT ACT AAT TGA GCG TCC TCA GAA GAA TC	Amplification of *COI1* ORF. 5' contains Ser at 77 aa & Ala at 81 aa
Coi1 RV *85-114 aa coi1Δ*	AAG GGG GAT CCT TAT ACT AAT TGA TGG TCC TCA GAG CAA TC	Amplification of *COI1* ORF. 5' 1-84 amino acids contains *EcoR*I restriction site
Coi1 RV *88-114 aa coi1Δ*	AAG GGG GAT CCT TAA CTC TTT CTT ACT AAT TGA TGG TCC TC	Amplification of *COI1* ORF. 5' 1-87 amino acids contains *EcoR*I restriction site
Coi1 RV *99-114 aa coi1Δ*	AAG GGG GAT CCT TAT GTT ACA GCA CTA AGC CCG CTA	Amplification of *COI1* ORF. 5' 1-98 amino acids contains *EcoR*I restriction site
Coi1 RV *103-114 aa coi1Δ*	AAG GGG GAT CCT TAA CCT CTT TTT CTT GTT ACA GCA CTA AG	Amplification of *COI1* ORF. 5' 1-102 amino acids contains *EcoR*I restriction site
Coi1 RV *109-114 aa coi1Δ*	AAG GGG GAT CCT TAA CCT AAT TTG TCA CCT CTT TTT CTT GTT AC	Amplification of *COI1* ORF. 5' 1-108 amino acids contains *EcoR*I restriction site

Table 20: List of plasmids used in this study

Plasmids	Promoter	Marker(s)	Reference
pYX142	TPI	Leu, Amp	Laboratory stock
pYX142-Coi1	TPI	Leu, Amp	This study
pYX142-Coi1 C-ter HA	TPI	Leu, Amp	This study
pYX142-Coi1 *2-9Δ*	TPI	Leu, Amp	This study
pYX142-Coi1 1-*30Δ*	TPI	Leu, Amp	This study
pYX142-Coi1 Cys77Ser	TPI	Leu, Amp	This study
pYX142-Coi1 His81Ala	TPI	Leu, Amp	This study
pYX142-Coi1 *85-114Δ*	TPI	Leu, Amp	This study
pYX142-Coi1 *88-114Δ*	TPI	Leu, Amp	This study
pYX142-Coi1 *99-114Δ*	TPI	Leu, Amp	This study
pYX142-Coi1 *103-114Δ*	TPI	Leu, Amp	This study
pYX142-Coi1 *109-114Δ*	TPI	Leu, Amp	This study
pGEM4	SP6	Amp	Promega
pGEM4-AAC	SP6	Amp	(Sambrook J., 1989)
pGEM4-Oxa1	SP6	Amp	(Gartner et al., 1995)
pGEM4-pSU9-DHFR	SP6	Amp	(Rapaport et al., 1997)
pGEM4-Porin	SP6	Amp	(Mayer et al., 1993)
pGEM4-Tom40	SP6	Amp	(Paschen et al., 2003)
pGEM4-F1β	SP6	Amp	(Rapaport et al., 1997)

5.2   Methods

5.2.1   Methods in molecular biology

5.2.1.1   Polymerase chain reaction

Polymerase chain reaction (PCR) is a method used to amplify a specific DNA template (Saiki et al., 1988). As a template for PCR, genomic and plasmid DNA were used. A standard PCR reaction contains in total 50 or 100 µl with 100 ng DNA template, 2 µl of 10 mM dNTPs, 1x PCR buffer, 1-2 U of Taq, pfu or *EXACTRUN* DNA polymerase, and H_2O. Buffers used in PCR are mentioned above in Table 5. PCR was performed in a thermocycler (Biometra) according to the two-step program mentioned below in Table 21.

Table 21: General PCR program used in this study

Step	Temperature	Time and cycles
1	95 °C	5'
2	95 °C	1'
3	55 °C	1'
4	75 °C	1' 30" ⟶ Step #2 X 5
5	95 ° C	1'
6	65 °C	1'
7	75 °C	1'30" ⟶ Step #5 X 25
8	75 °C	10'
9	4 °C	Hold

5.2.1.2   Agarose gel electrophoresis

DNA fragments of different molecular masses were separated by agarose gel electrophoresis. They were separated on 0.5 - 2% (w/v) gels prepared in TAE buffer, containing 3% midori green or 2% gel red (Biotium). DNA samples were mixed with 10x loading dye prior to loading onto the gel and electrophoresis was performed in

TAE buffer. To estimate the size of the DNA fragments, 1 kb DNA ladder (Fermentas, Gene Ruler^{TM}) was loaded in parallel. The bands were visualized by UV-light.

5.2.1.3   DNA extraction from agarose gel

DNA fragments of interest were extracted from the agarose gel on UV-light table. The purification was performed with Fast gene^{TM} extraction kit (NIPPON Genetics) as mentioned in the user manual.

5.2.1.4   Restriction digestion of DNA

Endonucleases enzymes were used for restriction digestion of DNA. The restriction setup for PCR cloning or sub-cloning was done with 1-2 µg of DNA and incubation at 37°C for 2h. Inactivation of the enzymes was performed as stated in the user manual.

5.2.1.5   Dephosphorylation of DNA fragments

After restriction digestion of the vector, dephosphorylation was performed with shrimp alkaline phosphate (SAP) at 37°C to avoid re-ligation of the vector. SAP was heat inactivated at 65°C for 20 min before gel extraction of the linearized vector.

5.2.1.6   Ligation with T4 DNA ligase

Linearized vector and insert were purified with peqGOLD extraction kit (VWR). Ligation reaction was prepared in 20 µl final reaction volume containing different ratio of vector to insert (1:3 or 1:6) with 3 µl of PEG 4000, 1 µl of ATP, 1X T4 ligation buffer and 1.5 µl of T4 ligase. Ligation sample were incubated overnight at 4°C in a water bath gradient and transformed into XL10 gold *E. coli* cells.

5.2.1.7   Preparation of chemical competent *E. coli* cells

XL10-gold *E. coli* strain was inoculated for overnight culture at 37°C in LB-chloramphenicol medium. The cells were diluted in 400 ml of fresh LB medium to an $OD_{600}=0.1$ and grown to $OD_{600}=0.5$. The cells were harvested by centrifugation (3000g, 5 min, 4°C) in pre-cooled tubes and the cell pellet was re-suspended in 160 ml of pre-cooled TfbI buffer (Table 6) and incubated on ice for 15 min. The cell

suspension was harvested by centrifugation (4000 g, 10 min, 4°C), the pellet was re-suspended in 16 ml pre-cooled TfbII buffer (Table 6) and incubated for 15 min on ice. Aliquots (100 µl) of the competent cells were snap-frozen in liquid nitrogen and stored at -80°C.

5.2.1.8 Transformation of *E. coli* cells

The plasmid containing gene of interest was transformed into XL10-gold competent cells. The plasmid or ligation mix was added to 100 µl of competent cells and incubated for 30 min on ice. Cells were subjected initially to a heat shock at 42°C for 45 sec and then a cold shock on ice for 2 min. Then, LB medium was added to the cells and incubated at 37°C for 30 min. Next, the cells were harvested by centrifugation (5000g, 5 min, RT) and re-suspended in 100 µl fresh LB medium. The re-suspended cells were plated on LB-Amp agar plates and incubated overnight at 37°C.

5.2.1.9 Plasmid isolation from *E. coli* strain in smaller scale (Miniprep)

Small scale plasmid isolation from *E. coli* cells was done by using alkaline lysis method (Birnboim and Doly, 1979). After transformation, *E. coli* single colonies were picked and grown in 3 ml LB ampicillin medium for 16-18 h at 37°C. 2 ml of cultures were harvested by centrifugation (5000g, 5 min, RT) and re-suspended in 300 µl E1 buffer. The cells were lysed in 300 µl E2 buffer by inverting gently 5 times and were incubated for 5 min at room temperature. Genomic DNA was precipitated by addition of 300 µl E3 buffer, inverting the tube again 5 times, and then by centrifugation step (15000g, 15 min, 2°C). Iso-propanol (96%) was then added to the supernatant in order to precipitate the plasmid, and the solution was centrifuged (15000g, 15 min, 2°C). The pellet was washed with 70% ethanol and centrifuged again (15000g, 15 min, 2°C). The pellet was re-suspended in 30 µl of H_2O or directly into restriction digestion mix.

5.2.1.10 Large scale plasmid DNA preparation (Midiprep)

E. coli cells were shaken overnight in 50 or 100 ml culture at 37 °C. Isolation of plasmid-DNA was done by using PureYield Plasmid Midiprep System (Promega) as

mentioned in the user manual. DNA concentration was determined by photometer and the solution was stored at -20 °C.

5.2.2 Methods in yeast genetics

5.2.2.1 Cultivation of *S. cerevisiae*

Yeast cells were grown in complete (YP medium) or synthetic medium (S medium) with fermentable (glucose or galactose) or non-fermentable (glycerol or lactate) carbon source according to published protocol (Sambrook J., 1989). Some auxotrophic markers were eliminated when strains were grown on synthetic selective medium (without leucine and histidine). In this study, all strains were grown in liquid medium at 30°C with constant shaking at 120 rpm. The cells were also grown on plates containing solid media at different temperature (15°C, 24°C, 30°C, and 37°C). The cells were stored for longer time periods in 15% glycerol solution in -80°C freezer, and on plates for short term at 4°C.

5.2.2.2 Yeast transformation with the lithium acetate method

Yeast cells were transformed by the lithium acetate method as previously described (Gietz et al., 1995). Cells were harvested by centrifugation (5000g, 5 min, RT) from freshly growing cells from liquid medium or small amount of cells from a plate. The cell pellet was re-suspended in 1 ml of 100 mM lithium-acetate and incubated for 5 min at 30°C with constant shaking at 500 rpm. The cells were collected again by centrifugation (5000g, 5 min, RT) and re-suspended in 240 µl of 50% (w/v) polyethylene glycol 3350, 55 µl H_2O, 36 µl 1 M lithium-acetate, 10 µl salmon sperm DNA (5 mg/ml) and 5 µl plasmid DNA or PCR product (100- 600 ng/µl). The cell suspension was mixed and incubated at 42°C for 30 min with shaking at 800 rpm. The cells were centrifuged (5000g, 5 min, RT) and streaked on a plate with appropriate selective medium. The plates were incubated at 30°C for 2-4 days until single colonies appeared.

5.2.2.3 Gene targeting in yeast by homologous recombination method

Knockout of specific genes was obtained by the homologous recombination technique with the pFA6a-*HIS3MX6* plasmid (Wach et al., 1997). For *COI1*

(*YDR381C-A*) deletion, the ORF was replaced in W303a background by the *HIS3MX6* cassette with a PCR product obtained by using the specific primers mentioned in Table 19. The deletion cells were selected on SD plates lacking histidine at 30°C, and the genotype was confirmed by colony PCR with specific primers mentioned in Table 19.

5.2.2.4   Site-directed mutagenesis

COI1 was mutated with single or double point mutations by using *ExtactRUN* DNA polymerase. The primers were designed with 10-15 bp upstream and downstream of the mutated codon and are indicated in Table 19. The efficiency of the PCR was monitored on 1-2% agarose gel, and the PCR product was treated at 37°C for 1 h with 1 µl of *Dpn1*. The samples were heat inactivated for 20 min at 80°C, and 5-10 µl of the PCR product was transformed into *E. coli* cells.

5.2.3   Cell biology methods

5.2.3.1   Drop dilution assay

For drop dilution assay, cells were grown overnight at 30°C in 20 ml of synthetic or complete medium. On the next day, the cells were diluted to OD_{600} of 0.1 or 0.2 and grown again until cells reached an OD_{600} of 1.0. Cells were then harvested by centrifugation (3000g, 3 min, RT) and washed with 1 ml sterile water. The cell pellet was re-suspended with sterile H_2O to an OD_{600} of 2.0, and 5 µl of serial dilutions of fivefold increments were spotted on solid media. The plates were incubated at different temperatures (15°C, 24°C, 30°C and 37°C) for 2-3 days.

5.2.3.2   Isolation of yeast crude mitochondria

Yeast cells were inoculated into 50 ml culture and incubated overnight at 30°C. On the next day, the culture was diluted into 200 ml of fresh medium to an OD_{600} of 0.1- 0.2. Once the cells reached the logarithmic phase (OD_{600} of 0.8- 1.0), they were harvested (3000 g, 5 min, RT) and re-suspended in 2.4 ml of SEM buffer supplemented with 2 mM PMSF. The cell suspension was distributed in four Eppendorf tubes containing each 600 mg of glass beads. Cells were broken open by vortexing five times for 1 min with interval of 1 min on ice in between. Cell debris and

beads were sedimented by centrifugation (1000g, 3 min, 2°C), and the supernatant corresponding to the whole cell lysate (WCL) was collected in a fresh tube. Protein concentration of the WCL was measured with the Bradford method, and the WCL fraction was centrifuged (20000g, 15 min, 2°C) to isolate crude mitochondria at the pellet, whereas the supernatant represents the cytosol fraction. Aliquots of 200 µl of WCL and cytosol fractions were precipitated by chloroform-methanol method. The samples representing the crude mitochondria, WCL and cytosol, were re-suspended in 2x Lämmli buffer, cooked for 5 min at 95°C and stored at -20°C until they were analyzed on the SDS-PAGE.

5.2.3.3   Isolation of mitochondria from yeast cells

Isolation of *S. cerevisiae* mitochondria was performed as previously described (Daum et al., 1982) with minor modification. The cells were grown at 30°C in total volume of 2-10 l of suitable medium to an OD_{600} of 0.8-1.5 and harvested by centrifugation (3000g, 5 min, 20°C). The cell pellet was washed with 200 ml H_2O and cells were centrifuged again (3000g, 5 min, 20°C), the pellet was weighted and then re-suspended in suspension buffer (Table 7) to a ratio of 2 ml per g cells. Cell suspension was incubated at 30°C for 10 min with a constant shaking, and the cells were harvested by centrifugation (5 min, 3000g, 20°C). The cells were re-suspended to a ratio of 2 ml/g of cells in spheroblasting buffer and centrifuged again (5 min, 3000g, 20°C). Next, the cell wall was digested by re-suspending the cells with spheroblasting buffer containing 4.5 mg zymolyase (per g of wet cells weight) and was incubated at 30°C for 60 min. The spheroblasting efficiency was monitored photometrically by adding 20 µl of the spheroblasting solution to 1 ml of either H_2O or 1.2 M sorbitol. The OD_{600} in water should be eight to ten-fold less compared to that in 1.2 M sorbitol, upon complete spheroblasting of the cells. The cells were re-isolated by centrifugation (2000g, 5 min, 2°C) and re-suspended in 13 ml/g cells in homogenization buffer. Cells were homogenized by 10 strokes in tight fitting glass homogenisator on ice, and homogenized cells were centrifuged (2000g, 5 min, 2°C) twice to get rid of cell debris.

Mitochondria were isolated from clarified supernatant with higher centrifugation step (18000g, 15 min, 2°C). The mitochondrial pellet was further centrifuged twice at lower centrifugation (2000g, 5 min, 2°C), and at the final step, mitochondria were

isolated again at higher centrifugation (18000g, 15 min, 2°C). The mitochondrial pellet was re-suspended in 1 ml SEM buffer supplemented with 2 mM PMSF. Aliquots of appropriate concentration were snap-frozen in liquid nitrogen and stored at -80°C.

5.2.3.4 Subcellular fractionation of yeast cells

Isolation of mitochondria was performed as mentioned above (5.2.3.3). After the homogenization step, 2 ml of sample, which corresponds to whole cell lysate (WCL), was collected. After the first centrifugation step to obtain mitochondria (18000g, 15 min, 2°C) the supernatant was collected, which corresponds to post-mitochondrial supernatant (cytosolic and light ER fraction). To isolate highly pure mitochondria, the mitochondria fraction was loaded onto 17.5 ml Percoll gradient solution (25% Percoll) (Table 7) and separated by ultracentrifugation (80000g, 45 min, 2°C). The purified mitochondria migrate in the lower half of the gradient, which was transferred with the glass tip into a fresh tube, containing 30 ml of SEM buffer. Pure mitochondria were isolated by centrifugation (15000g, 15 min, 2°C), and the pellet was re-suspended in 500 µl SEM buffer. Aliquots (50 µl) were flashed frozen in liquid nitrogen and stored at -80°C until further use.

Microsomes were isolated from post-mitochondrial supernatant with an initial clarifying spin (15000g, 15 min, 2°C). The supernatant was centrifuged (130000g, 1 h, 2°C), and the microsomes were re-suspended in 500 µl SEM buffer and subjected to another clearing spin (8000g, 10 min, 2°C). Aliquots (50 µl) were stored at -80°C until further use.

5.2.3.5 Separation of mitochondrial outer and inner membrane proteins by sucrose gradient

Isolated mitochondria (3 mg), obtained from cells grown on lac medium were re-suspended in 1 ml SEM supplemented with 2 mM PMSF, and the organelles were re-isolated by centrifugation (12000g, 5 min, 2°C). The mitochondria were swollen at 4°C for 1 h in 10 ml of swelling buffer in a 15 ml falcon tube placed on an overhead shaker. Next, the density of the sample was adjusted by adding high sucrose buffer to a final concentration 0.4 M. The swollen mitochondria were ruptured by sonication

(8x 3 sec; 2 min intervals, on ice) by using mini sonication tip (70% duty cycle, output 6) immersed 2 cm into the sample solution. The mitochondrial vesicles were harvested by ultracentrifugation in 60Ti tubes (Beckmann) (20000g, 2h, 2°C), and the pellet was thoroughly re-suspended in 400 µl of low sucrose buffer. The pellet was sonified at 4°C in a water bath for 5-10 min and centrifuged (35000g, 15 min, 2°C) to get clarified vesicles. In the meantime, the sucrose gradient was prepared in SW60 tubes (Beckmann). The pipetting scheme of the gradient is mentioned in the Table 22 below. To obtain the outer and inner membrane proteins, the supernatant was loaded on the sucrose gradient and centrifuged (230000g, 16 h, 2°C) in SW60 rotor (Beckmann). The gradient was carefully harvested from top to bottom in aliquots of 90 µl that were further mixed with 4x Lämmli and analyzed by SDS-PAGE.

Table 22: Pipetting scheme for sucrose gradient

Molarity (M)	Gradient buffer (in µl)	Sucrose gradient buffer (in µl)
0.9	959	541
1.0	900	600
1.1	840	660
1.2	779	721
1.3	720	780
1.4	660	840

5.2.3.6   Fluorescence microscopy of yeast cells

Yeast cells were transformed with pVT100U-mtGFP vector (Westermann and Neupert, 2000), harboring mitochondrial targeted green fluorescent protein. Yeast cells containing the vector were grown to logarithmic phase, and 5 µl of culture were used to examine the mitochondrial morphology under fluorescence microscope (Zeiss Axioscope) with 100x magnification.

5.2.4 Biochemical methods

5.2.4.1 Determination of protein concentration

To determine protein concentration, the Bradford method was applied (Bradford, 1976). The protein solution (10 µl) was diluted in 1 ml of Roti-Quant Bradford solution (1:5 dilution in SEM buffer) and incubated at room temperature for 5 min in darkness. To determine standard curve, 2-10 µg of BSA from 1 mg/ml stock were used. The absorbance of the samples was measured at 595 nm, and protein concentration was estimated according to the calibration plot.

5.2.4.2 Protein precipitation by trichloroacetic acid (TCA)

Aqueous protein solution was precipitated by adding 72% TCA to a final concentration of 12%. The samples were vortexed and then incubated on ice for 30 min and centrifuged (30000g, 20 min, 2°C). A volume of 500 µl of 90 % acetone was used to wash the pellet, and subsequently, the pellet was dried at 50°C for 10 min. The pellet was re-suspended in 2x Lämmli buffer and incubated at 95°C for 5 min.

5.2.4.3 Protein precipitation by chloroform-methanol

To precipitate higher amounts of protein, chloroform-methanol precipitation was performed (Wessel and Flugge, 1984). Four volumes of methanol, three volumes of chloroform, and three volumes of water were added to the samples and vortexed thoroughly. The samples were separated by centrifugation (16000g, 1 min, RT) into two phases. The upper phase was carefully removed and three volumes of methanol were added to the lower phase. After vortexing, the samples were centrifuged (16000g, 1 min, RT) and the pellet was air dried at 50°C. Then, the pellet was re-suspended with 2x Lämmli buffer and incubated at 95°C for 5 min.

5.2.4.4 Carbonate extraction

Mitochondria were subjected to alkaline extraction as published before (Fujiki et al., 1982). Isolated mitochondria (50 µg) were re-suspended in 50 µl of 20 mM HEPES/KOH pH 7.5, and then 50 µl of freshly prepared pre-cooled 200 mM sodium carbonate solution was added. The samples were incubated on ice for 30 min prior to separation of soluble and membrane proteins by ultracentrifugation (120000g, 1 h,

2°C). The supernatant containing soluble fraction was precipitated by the TCA method, whereas the pellets were re-suspended directly in 50 µl 2x Lämmli and incubated for 5 min at 95°C.

5.2.4.5   Proteinase K treatment of mitochondria

Mitochondria (50 µg) were re-suspended in 100 µl SEM buffer, and the solution was supplemented with Proteinase K (50 and 200 µg/ml). The samples were incubated on ice for 30 min. As a control, mitochondria were treated on ice with 0.2% Triton X-100 in SEM buffer for 20 min and subjected to PK treatment as described above. To stop the reaction, 2 µl of 200 mM PMSF were added to all samples. Mitochondria were re-isolated (18,000g, 20 min, 2°C), while proteins from the Tx-100 containing samples were precipitated by TCA. The pellet was re-suspended in 50 µl of 2x Lämmli buffer, incubated for 5 min at 95°C and further analyzed by SDS-PAGE.

5.2.4.6   SDS-PAGE

Protein samples were analyzed on denatured condition in 10-15 % SDS-PAGE gels. The SDS gel was casted between two glass plates with 1 mm spacing in between, and to avoid leakage, the bottom gel was separately prepared. The composition of bottom, running, and stacking gel are described in Table 23, and buffer composition in Table 9 above. The protein samples were prepared in 2x Lämmli with concentration of 2 µg/µl (15 µg- 100 µg) and denatured at 95°C for 5 min before being subjected to SDS-PAGE. Electrophoresis was performed at 20 mA per gel, for approximately 3 h until the dye front reached the bottom gel. A protein ladder (PAGE Ruler[TM], Fermentas) was used as a molecular weight markers.

5.2.4.7   Western blotting

Proteins from SDS-PAGE were transferred onto the nitrocellulose membrane (Whatman) by semi-dry blotting technique as described previously (Kyhse-Andersen, 1984; Towbin et al., 1979). Three filter papers (3 mm) were soaked in blotting buffer (Table 9) and placed on the blotting apparatus followed by the nitrocellulose membrane. The SDS gel was placed on the membrane, and additional three filter papers were placed on top of the gel. Air bubbles were removed by rolling a glass pipette over the assembled blot. The proteins were transferred for 1.5 h at 220 mA.

The efficiency of the protein transfer was monitored by incubating the membrane in Ponceau staining solution (Table 9) for 1-2 min, followed by several washes.

Table 23: Composition of gels used for SDS-PAGE

Components	Bottom gel	Running gel			Stacking gel
	15%	10%	12.5%	15%	
40% aa/bis-aa (29:1)	3.75 ml	3.13 ml	3.91 ml	4.69 ml	563 µl
1M Tris pH 8.8	3.75 ml	4.69 ml	4.69 ml	4.69 ml	-
1M Tris pH 6.8	-	-	-	-	625 µl
water	2.39 ml	4.55 ml	3.77 ml	2.99 ml	3.76 ml
10% APS	100 µl	125 µl	125 µl	125 µl	50 µl
TEMED	8 µl	10 µl	10 µl	10 µl	4 µl
Total volume	10 ml	12.5 ml	12.5 ml	12.5 ml	5 ml

5.2.4.8 Immunodetection of proteins

To avoid unspecific binding of antibodies, membranes with blotted proteins were incubated at room temperature with 5% skim-milk in TBS buffer for 1 h. Membranes were briefly washed with TBS before incubating them with primary antibodies at 4°C overnight or at room temperature for 1 h. The membranes were then washed twice with TBS and once with TBST before their incubation at room temperature with secondary antibodies (1:10000) in 5% skim-milk for 1 h. To detect the specific proteins, the secondary antibody was conjugated to HRP. A chemiluminescence signal was obtained upon adding ECL and H_2O_2. This signal was detected by X-ray films (Super RX, Fuji) and these were developed by an X-ray film developing machine (SRX-101A Konica Minolta).

5.2.4.9 Colloidal Coomassie staining

After gel electrophoresis, proteins were visualized by Coomassie staining. The gel was shortly washed with water before incubating in staining solution for either 1-2

h or overnight. De-staining solution was then added to remove excess of Coomassie staining, and the bands of interest were cut out for protein analysis by mass spectrometry.

5.2.4.10 Blue native PAGE (BN-PAGE)

Membrane proteins were analyzed under native conditions by applying blue native gel electrophoresis (BN-PAGE) as mentioned previously (Schagger and von Jagow, 1991). Isolated mitochondria (50 - 100 µg protein) were re-isolated in SEM buffer by centrifugation (12000g, 10 min, 2°C), and the pellet was lysed in sample buffer containing 1% digitonin (protein: detergent ratio of 1:10 (w/w)), or 0.5% solution of either Triton X-100, or DDM (resulting in protein: detergent ratio of 1:3). The solubilized samples were incubated on ice for 20-30 min and centrifuged (30000g, 20 min, 2°C) to get rid of non-solubilized material in the pellet. The solubilized mitochondrial proteins in the supernatant were mixed with 5 µl of 10x loading buffer and analyzed on 3-13% acrylamide gradient gel. BN-PAGE (Table 24) was performed at 4°C as described previously (Schägger, 2002). Whereas, the first part of the gel was run at 150 V and 15 mA for 2 h in cathode B buffer. Next, the buffer was switched to cathode A buffer, and the gel was ran further at 50 V, 15 mA overnight. The native gel was either blotted to PVDF membranes or stained with Coomassie.

Table 24: Composition of gels used for BN-PAGE

Components	Bottom gel	Stacking gel	3.5%	4 %	6%	8%	10%	13%
48%AA/1.5% Bis-AA	5 ml	0.417 ml	0.44 ml	0.5 ml	0.75 ml	1 ml	1.25 ml	1.625 ml
3X gel buffer	3.3 ml	1.67 ml	2 ml	2 ml	2 ml	2 ml	2 ml	2 ml
water	1.7 ml	2.88 ml	3.4 ml	3.47 ml	3.22 ml	1 ml	0.75 ml	-
60% (V/V) glycerol	-	-	-	-	-	2 ml	2 ml	2.355 ml
10% APS	50 µl	30 µl	50 µl	30 µl	25 µl	20 µl	20 µl	20 µl
TEMED	25 µl	3 µl	3 µl	3 µl	2 µl	2 µl	2 µl	2 µl

5.2.4.11 *In vitro* transcription and translation of radiolabeled precursor proteins

Transcription was done in the presence of SP6-polymerase as mentioned previously (Melton et al., 1984; Trochimchuk et al., 2003). *In vitro* transcription was performed in a mixture of total volume of 50 µl containing: 10 µl SP6-buffer, 5 µl 10 mM DTT, 2 µl (80U) RNAse inhibitor (Promega), 10 µl 2.5 mM rNTP-mix (GE Healthcare), 2.6 µl of 0.8 mM methyl G(5´)ppp(5´)G cap (Amersham), 5 µg plasmid DNA, and 1.5 µl (75 U) SP6 Polymerase. The Transcription reaction was performed at 37°C for 1 h, and the resulting mRNA was precipitated by adding 5 µl of 10 M LiCl and 150 µl ethanol p.A. for 4-5 h at -20°C. The mRNA was further isolated by centrifugation (37000g, 20 min, 2°C) and washed with 500 µl ice-cold 70% ethanol. The dry mRNA was re-suspended in 37 µl H_2O with 2 µl RNAse inhibitor, and aliquots of suitable volumes were stored in -80°C.

Translation of mRNA was performed in a mixture containing: 50 µl rabbit reticulocyte lysate (Promega), 12.5 µl mRNA, 1.75 µl amino-acid without methionine, 3.5 µl Mg-acetate, 0.5 µl RNAse inhibitor, and 6 µl ^{35}S-methionine (10 mCi/ml). The reaction was incubated for 1 h at 30°C, and then 6 µl of 58 mM methionine and 12 µl of 1.5 M sucrose were added to the reaction. Precursor proteins were obtained at the supernatant of a centrifugation step (90000g, 50 min, 4°C, TL45).

5.2.4.12 *In vitro* import of radiolabeled precursor proteins into mitochondria

The import of precursor proteins were performed at 25°C in the presence of isolated mitochondria (50 µg) for the indicated time periods in import buffer. The import reaction was stopped by diluting the import mixture with SEM K[80] buffer (Table 13), and mitochondria were re-isolated (12,000g, 2 min, 4°C). In some experiments, the organelles were treated with PK as described in section 5.2.4.5 before re-isolation. Mitochondrial pellets were re-suspended in 2x Lämmeli buffer and analyzed by SDS-PAGE.

5.2.4.13 Autoradiography and quantification of bands

The radiolabeled proteins separated on the SDS-PAGE were transferred to nitrocellulose membrane and detected by X-ray film (Kodak Bio Max MM). The signal of radiolabeled proteins depends on number of methionine present in the protein. Therefore, the detection of a signal varied from 2 to 30 days. The bands were quantified by using AIDA image analyzer tool.

5.2.4.14 Measurement of mitochondrial membrane potential

The membrane potential across the inner membrane ($\Delta\psi$) was measured by fluorescence quenching of the membrane potential sensitive dye $DiSC_3(5)$ (Sigma) by a modified published procedure (Gartner et al., 1995). $DiSC_3(5)$ dye (3 µl) was added at 25°C to a cuvette with 3 ml buffer. The fluorescence was monitored by fluorescence spectrometry (F-800, Jasco) with excitation at 622 nm and emission at 670 nm, and the data was taken at 2 sec intervals. Once the fluorescence of the dye was stabilized, 50 µg of mitochondria in SEM buffer were added to the cuvette, and flurorescence was further measured until a stable signal was obtained. The complete dissipation of the membrane potential was achieved by adding 3 µl of valinomycin, and the increase in the fluorescence was monitored. For the assessment of the membrane potential, the difference between the fluorescence level before and after adding the valinomycin was estimated.

5.2.4.15 Pull-down assay

Isolated mitochondria (1 mg) were solubilized at 4°C for 30 min in 600 µl of lysis buffer containing 1% (w/v) digitonin, 0.5% (w/v) Triton X-100, or 0.5% (w/v) DDM. Anti-HA magnetic beads (Pierce ^{TM} ThermoFischer Scientific) were washed twice with lysis buffer and then equilibrated with the buffer at 4°C for 30 min. The solubilized organelles were subjected to a clarifying spin (30,000xg, 20 min, 4°C), and the supernatant was incubated at 4°C overnight with the equilibrated anti-HA beads. The unbound material was removed, and the beads were washed thoroughly with lysis buffer containing 0.1% Triton X-100, digitonin, or DDM. Bound proteins were eluted with 2x Lämmeli without reducing agent and analyzed by SDS-PAGE.

6   Results

As part of my efforts to better understand the assembly of the cytochrome c oxidase complex, I decided to investigate the uncharacterized ORF *YDR381C-A*. This protein was found in the interactome of Cox4 of the inner membrane (Bottinger et al., 2013), but was previously also described in a high-throughput study to be included in the proteome of the MOM (Zahedi et al., 2006). The protein has a molecular mass of 12.7 kDa and lacks homologs in higher eukaryotes. According to *in silico* prediction, Ydr381C-A has a putative transmembrane segment in its N-terminal region (a.a. 11-30) (Quick2D, http://toolkit.tuebingen.mgp.de) (Fig 6.1). I wanted to understand the biological role and the mechanism of action of this protein, and due to reasons described below, I re-named *YDR381C-A* to Cytochrome c Oxidase Interacting protein 1 (*COI1*).
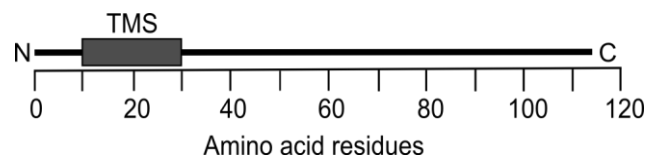

Figure 6.1 Schematic depiction of Coi1. Coi1 is predicted to have a single transmembrane segment (TMS) that includes a.a. residues 10-30. The putative TMS is indicated with a grey box.

6.1   Coi1 is an inner mitochondrial membrane protein

To better characterize Coi1, a specific antibody is an essential tool. I obtained several sera from the company Pineda and monitored by Western blotting the specificity of the antibodies.
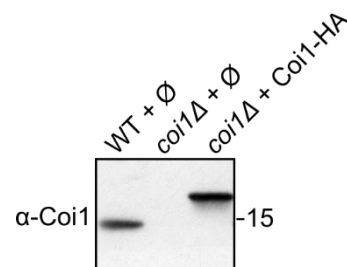

Figure 6.2 Serum raised in rabbit against Coi1. WT or *coi1Δ* cells were transformed with an empty plasmid or with a plasmid encoding C-terminally HA-tagged Coi1. Mitochondria were analyzed by SDS-PAGE and immunodecorated with antibody against Coi1.

The quality and specificity of coi1 antibody is demonstrated in Figure 6.2. It shows a signal at the expected size of the protein at ~15 kDa, the absence of a signal in a deletion strain, and a shift in the protein´s migration upon usage of HA-tagged version. This antibody was used in the experiments described in this thesis.

To confirm the reported mitochondrial location of Coi1 at a single gene level, subcellular fractionation of wild type cells was performed. The obtained fractions were analyzed by immunoblotting with an antibody against Coi1. Similarly to the known mitochondrial protein Tom40, Coi1 was enriched in the mitochondrial fraction (Fig 6.3 lane 4). This observation confirms that Coi1 is a mitochondrial protein. Since the protein harbors a putative TMD, four different topologies of the protein with respect to the mitochondrial membranes can be considered (Fig. 6.4A). However, I wondered whether the protein is indeed inserted into a membrane. To address this issue, isolated organelles were subjected to alkaline extraction, where soluble and peripheral membrane proteins were separated from integral membrane proteins. Coi1 was present in the membrane fraction like known MOM proteins such as Tom20 and Om45 (Fig 6.4B lanes 6 and 7). Thus Coi1 is a membrane-embedded protein.
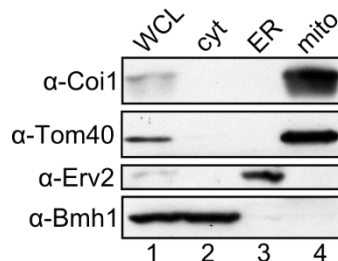

Figure 6.3 Coi1 is a mitochondrial protein. Coi1 is a mitochondrial protein. Whole-cell lysate (WCL) and fractions corresponding to cytosol (cyt), light microsomal fraction (ER) and mitochondria (mito) were analyzed by SDS-PAGE and immunodecorated with antibodies against Coi1, Bmh1 (cytosolic protein), Erv2 (ER protein), and Tom40 (mitochondrial protein).

To address the topology of Coi1 and to discriminate among the aforementioned topological possibilities, proteinase K (PK) was added to isolated mitochondria. Proteins exposed to the cytosolic side such as Tom20 were cleaved by PK, whereas the signal of Coi1 was still detectable. On the other hand, Coi1 could not be detected in lysed mitochondria treated with PK, suggesting that Coi1 is protected from the action of PK in intact mitochondria (Fig 6.4B lanes 1-5). Thus, topology #1 as depicted in Figure 6.4A can be excluded. To further investigate the orientation of Coi1,

mitochondria were swollen in hypo-osmotic conditions to disrupt the outer membrane and subsequently were treated with PK. These conditions eliminated the signal of both Coi1 and the IMS protein Dld1. In contrast, the matrix protein Aco1 remained resistant under these conditions, demonstrating the intactness of inner membrane (Fig 6.4C lane 4). Considering that the antibody against Coi1 was raised against C-terminal peptides, this outcome suggests that the C-terminus of Coi1 is facing towards IMS (options #2 or #3 in Fig 6.4A).
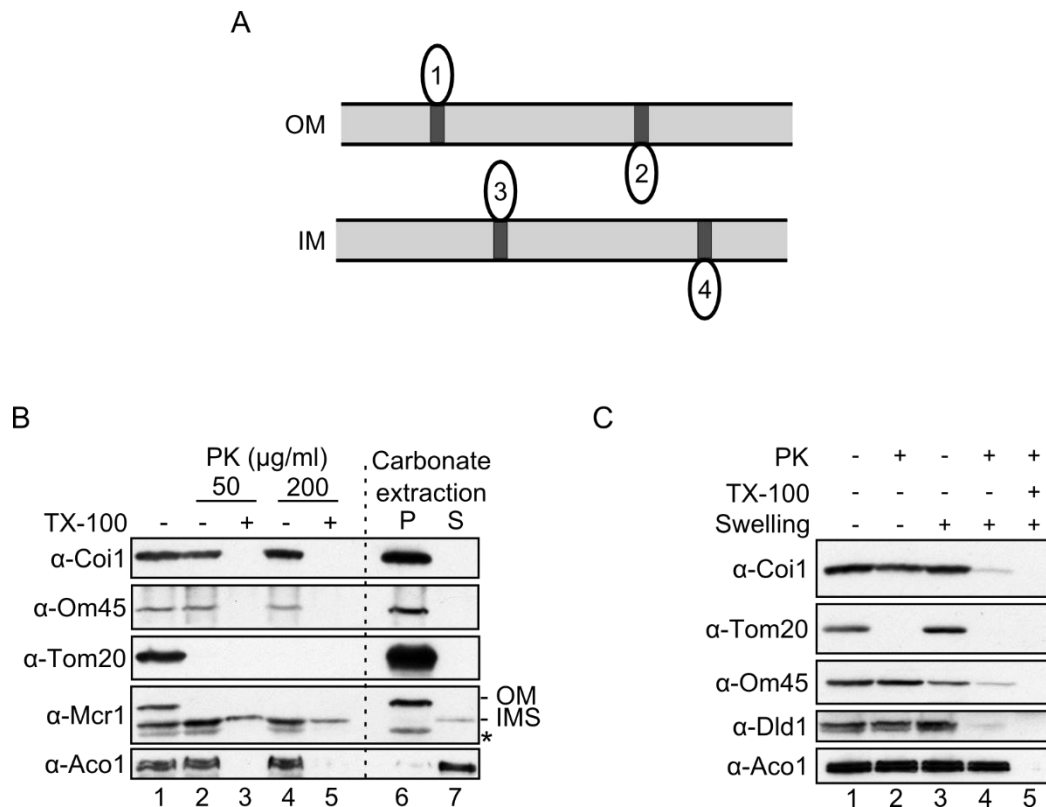

Figure 6.4 Coi1 is membrane embedded and facing towards the IMS. (A) Schematic representation of the four theoretical possibilities for the membrane topology of Coi1. **(B)** Coi1 is membrane embedded and protected from external protease. Isolated mitochondria were subjected to externally added proteinase K (PK) in the presence or absence of the detergent Triton X-100 (lanes 1-5). Other samples were subjected to alkaline extraction (lanes 6-7 right). The pellet (P) and the supernatant (S) fractions were analyzed by SDS-PAGE and immunoblotting. Om45, OM protein facing towards IMS; Tom20, OM protein exposed towards the cytosol; Mcr1, has two isoforms, a 34 kDa OM form and a 32 kDa IMS form; Aco1, soluble matrix protein. **(C)** Coi1 is exposed to the IMS. Isolated mitochondria were left untreated or were swollen before PK was added in the presence or absence of Triton X-100. Samples were analyzed by SDS-PAGE and immunodecoration with antibodies against the indicated proteins. Dld1, an IM protein facing the IMS. *, indicates degradation product.

49

To find out in which membrane Coi1 is embedded, mitochondrial OM and IM vesicles were obtained by hypo-osmotic swelling and sonication. The vesicles were separated by sucrose gradient centrifugation and the collected fractions were analyzed. Coi1 was predominately detected in heavier fractions very similar to the IM protein Cox2. In contrast, the OM protein Tom20 was mainly found in the lighter fractions (Fig 6.5). Taken together, these results suggest that Coi1 is embedded in the mitochondrial IM, facing towards the IMS (Fig 6.4A, topology #3).
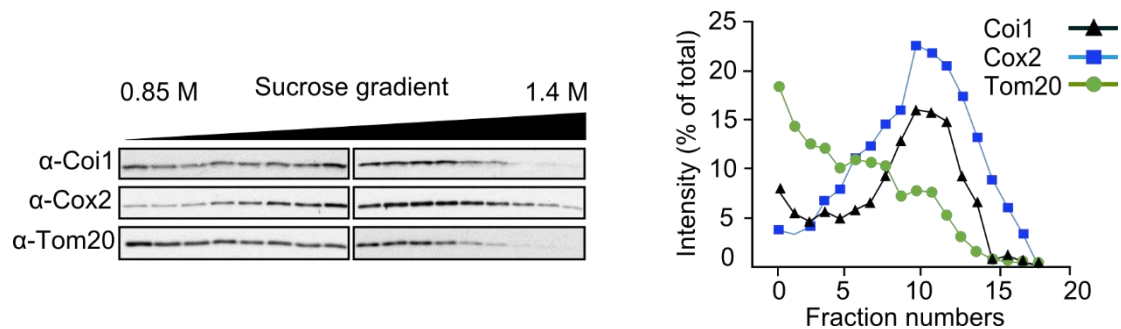

Figure 6.5 Coi1 is inner membrane protein. Isolated mitochondria were subjected to sonication followed by sucrose density gradient centrifugation. Fractions of the gradient were collected and analyzed by SDS-PAGE and immunodecorated with antibodies against the indicated proteins. Right panel: the intensities of the various bands were quantified and depicted. The sum of all intensities of each protein was set to 100%.

6.2 Loss of *COI1* has a severe growth effect on yeast cells

To investigate the function of Coi1 in yeast cells, the chromosomal copy of *COI1* was deleted, and the growth of the deletion strain was analyzed. The *coi1Δ* strain showed a severe growth phenotype on both non-fermentable (YPG and SG-Leu) and fermentable (YPGal and SGal-Leu) carbon sources at all temperatures tested. (Fig 6.6A). This growth phenotype is a direct result of the *COI1* deletion as it could be complemented by overexpression of either native Coi1 or C-terminally HA-tagged Coi1 (Fig 6.6A). These observations further verify that ectopically expressed Coi1 and Coi1-HA are functional. Accordingly, Coi1-HA was found to be in the mitochondrial fraction upon subcellular fractionation (Fig 6.6B lane 4). Altogether, the loss of Coi1 results in a severe growth phenotype, and overexpression of the protein can rescue this growth phenotype.
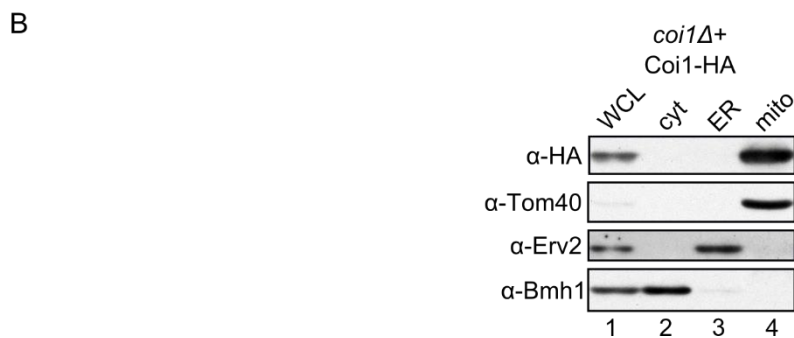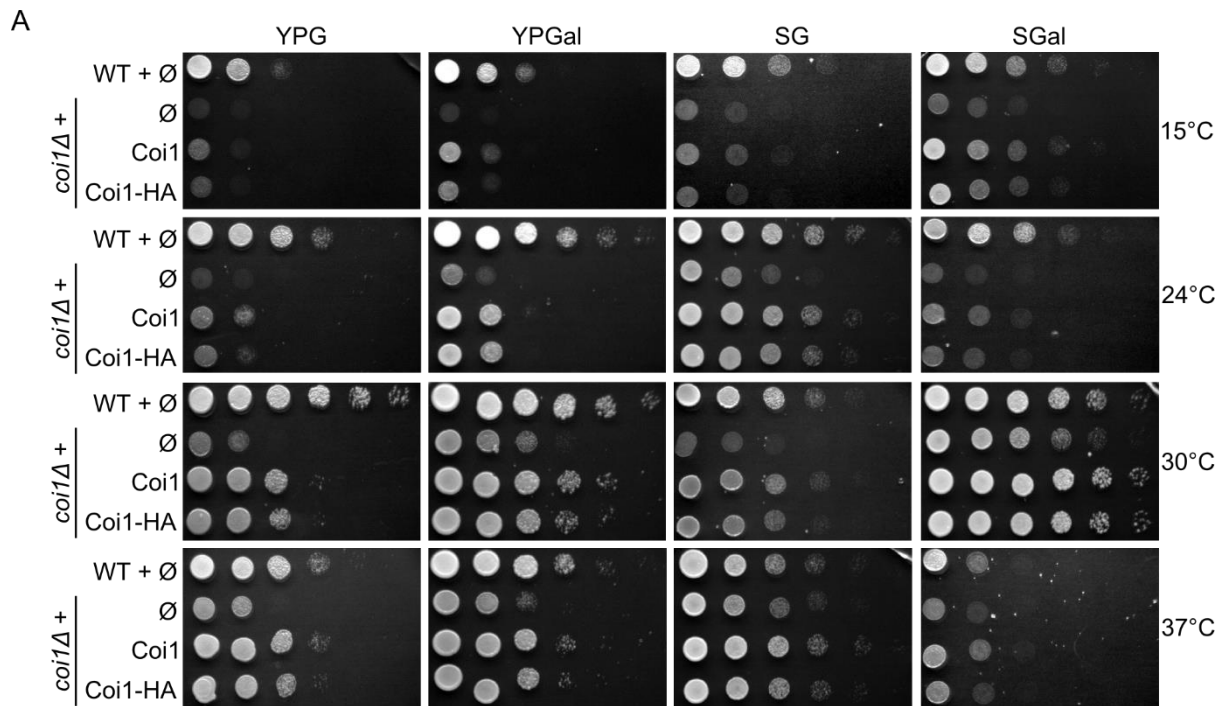
Figure 6.6 Deletion of *COI1* results in a severe growth phenotype. Wild type and *coi1Δ* cells were transformed with an empty plasmid, whereas the latter cells were transformed also with a plasmid encoding either Coi1 or Coi1-HA. **(A)** Cells were tested by drop dilution assay at the indicated temperatures on medium containing either the non-fermentable carbon source, glycerol (YPG and SG-Leu), or the fermentable carbon source, galactose (YPGal and SGal-Leu). **(B)** Coi1-HA is localized to mitochondria. Whole-cell lysate (WCL) and fractions corresponding to cytosol (cyt), light microsomal fractions (ER) and mitochondria (mito) from *coi1Δ* cells expressing Coi1-HA were analyzed by SDS-PAGE and immunodecoration with antibodies against HA (Coi1-HA), Tom40 (mitochondrial protein), Erv2 (ER protein), and Bmh1 (cytosolic protein).

Next, I wondered whether overexpression of Coi1 might have a harmful effect on the cell growth. To this end, either native Coi1 or C-terminally HA-tagged Coi1 was overexpressed in wild type cells. The results of the drop dilution assay indicate that ectopically expressed Coi1 and Coi1-HA had no negative functional effect on wild type cells (Fig 6.7). Hence, Coi1 in higher amounts has no adverse effect on the yeast cells.
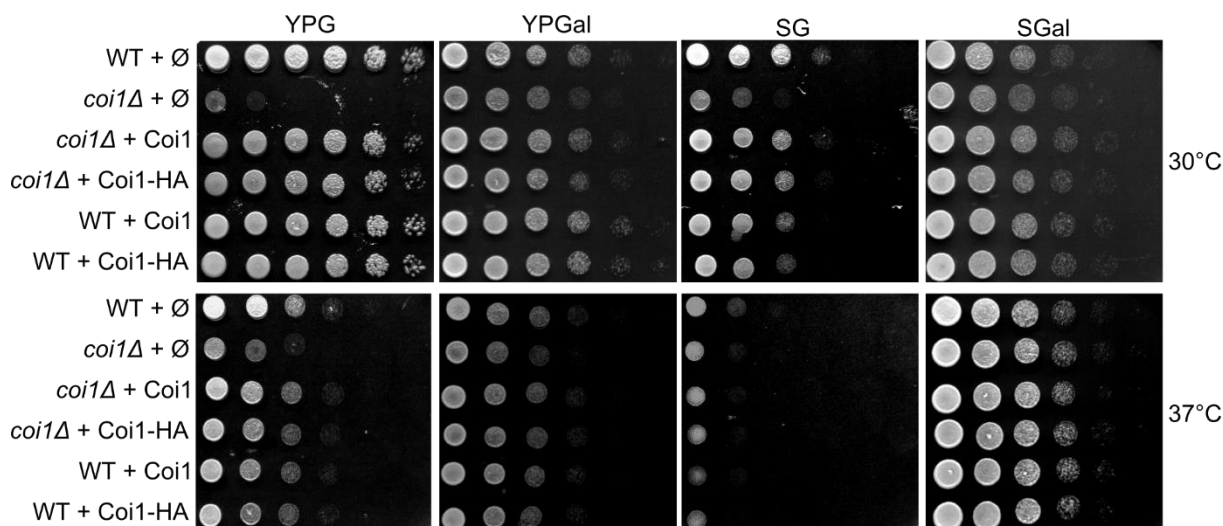
Figure 6.7 Overexpression of Coi1 has no negative effect on wild type cells. Wild type and *coi1Δ* cells were transformed with an empty plasmid or plasmid encoding either Coi1 or Coi1-HA. Cells were tested at 30°C or 37°C by drop dilution assay on rich medium containing either non-fermentable carbon source glycerol (YPG and SG-Leu) or the fermentable carbon source galactose (YPGal and SGal-Leu).

6.3 The transmembrane domain of Coi1 is crucial for its function

Coi1 has a single putative transmembrane segment of 20 amino acids towards its N-terminus region (a.a. 11-30). It also does not have a canonical presequence (Fig 6.8A). To understand more about the importance of the N-terminal region, two N-terminal truncated versions of Coi1 lacking either amino acids 2-9 (*coi1-2-9Δ*) or 2-30 (*coi1-2-30Δ*) were generated (Fig 6.8A). To test whether the deleted amino acids play a role in targeting and localization of the protein, the mutated variants were ectopically expressed in *coi1Δ* cells and complementation assay was performed. The growth phenotype from deletion of *COI1* was not rescued by *coi1-2-30Δ*, whereas *coi1-2-9Δ* showed only slightly reduced complementation capacity (Fig 6.8B). In agreement with the moderately reduced functionality, the steady state levels of *coi1-2-9Δ* were somewhat reduced in both WCL and mitochondrial fraction in comparison to overexpressed full length Coi1. The *coi1-2-30Δ* variant was not detected at all, suggesting that loss of the putative TMS probably leads to rapid degradation of the truncated version (Fig 6.9A).
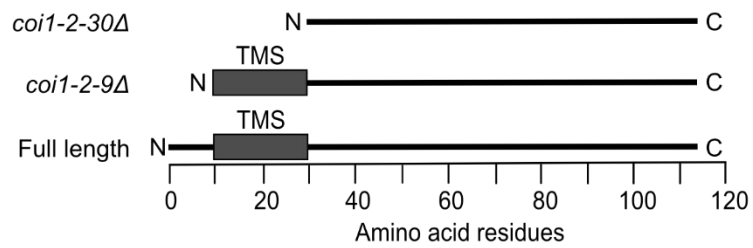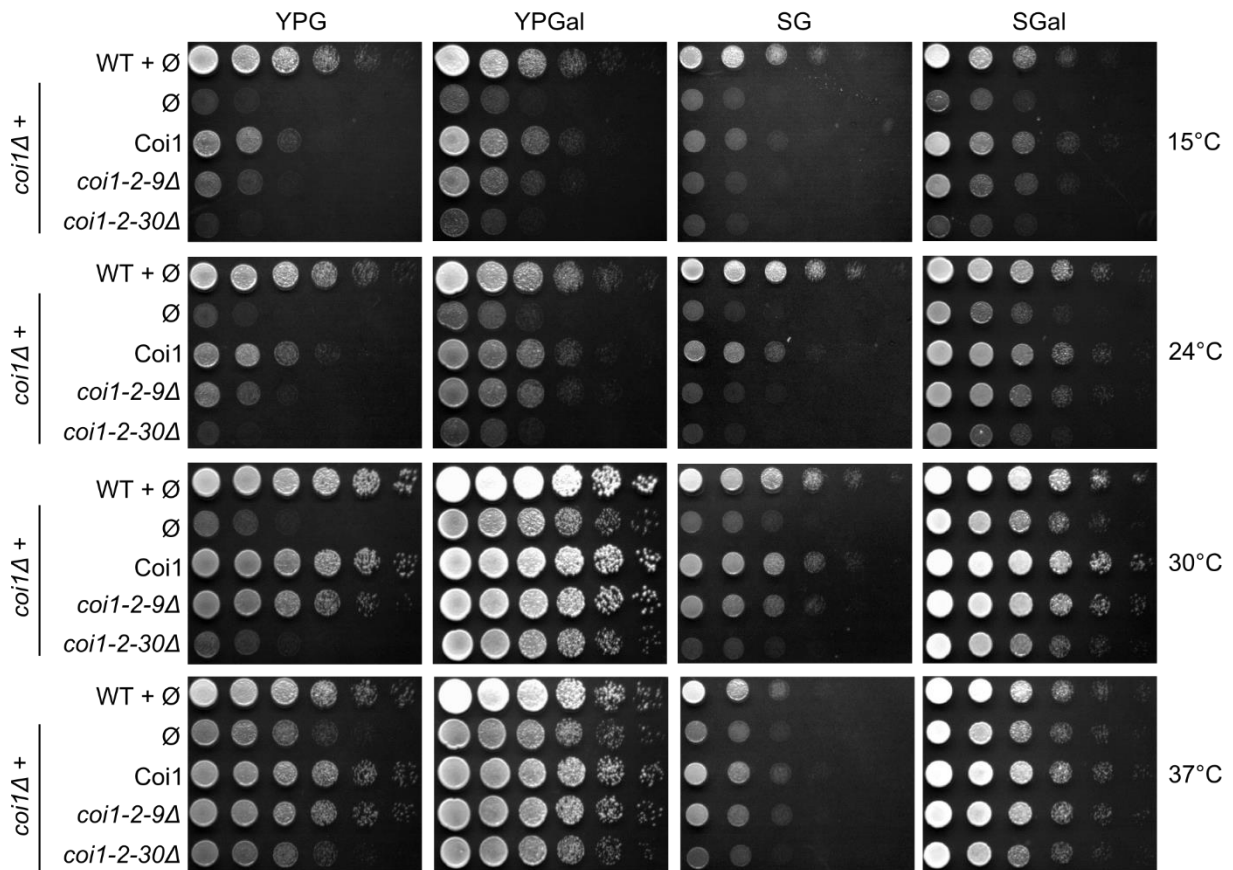
Figure 6.8 The transmembrane domain of Coi1 is required for its function. (A) Schematic illustration of full length and truncated forms of Coi1. **(B)** *coi1Δ* cells were transformed with an empty plasmid or with plasmid encoding Coi1 or its truncated variants. DDA was performed at the indicated temperatures on the specified medium.

To test if *coi1-2-9Δ* is embedded in the membrane, alkaline extraction was performed to separate soluble and membrane proteins. Despite its reduced steady-state levels, *coi1-2-9Δ* was inserted into the membrane similarly to full length Coi1 and the MOM protein Tom40 (Fig 6.9B). These findings indicate that residues 2-9 of Coi1 have only a slight effect on the stability and function of the protein, whereas residues 11-30 appear to be crucial for stability of the protein and its correct mitochondrial targeting.
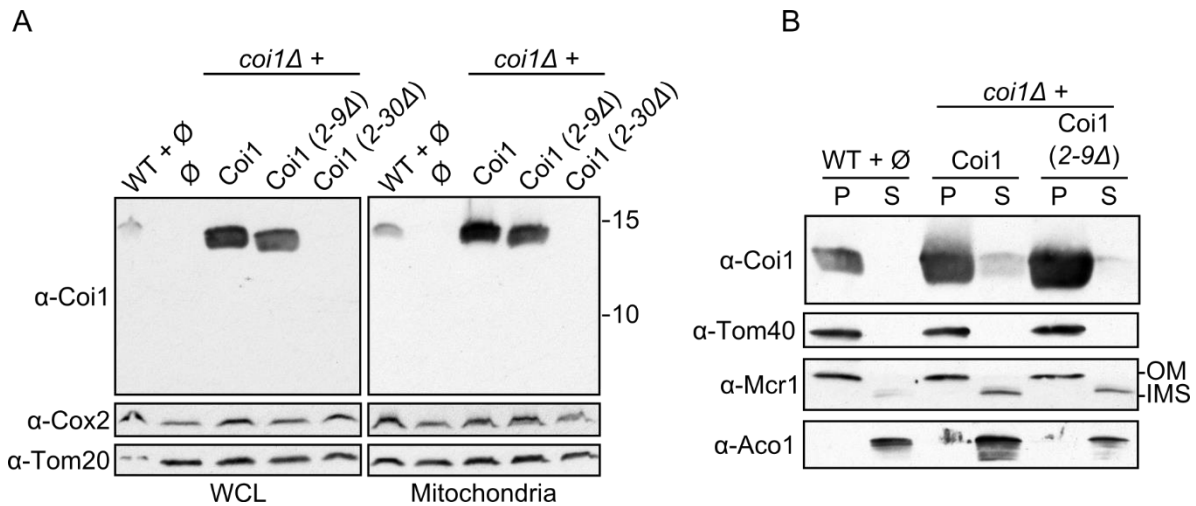
Figure 6.9 The transmembrane domain of Coi1 is crucial for the stability of the protein. **(A)** Crude mitochondria and whole cell lysate (WCL) were isolated from the indicated strains. Samples were analyzed by SDS-PAGE and immunodecoration with antibodies against Coi1, Cox2 (IM protein), and Tom20 (OM protein). **(B)** Isolated mitochondria were subjected to alkaline extraction. The pellet (P) and the supernatant (S) fractions were analyzed by SDS-PAGE and immunodecorated with the antibodies against the indicated proteins.

6.4   Conserved residues of Coi1 have a functional role

Coi1 has homologs in many fungi and it contains several conserved, positively charged amino acids at its C-terminus (Fig 6.10). To understand the role of these amino acids, different C-terminal truncations of Coi1 were generated, and a complementation assay was performed. Truncated versions of Coi1 lacking amino acids 85-114 (*coi1-85-114Δ*), 88-114 (*coi1-88-114Δ*), 99-114 (*coi1-99-114Δ*), 103-114 (*coi1-103-114Δ*), or 109-114 (*coi1-109-114Δ*) were constructed (Fig 6.10). Next, these variants were ectopically expressed in *coi1Δ* cells. The growth phenotype of *coi1Δ* cells was not rescued by *coi1-85-114Δ, coi1-88-114Δ,* and *coi1-99-114Δ*, whereas *coi1-103-114Δ* and *coi1-109-114Δ* showed a partial rescue capacity (Fig 6.11A). As a positive control, full length Coi1 was able to rescue the *coi1Δ* phenotype (Fig 6.11A). Obviously, lack of complementation capacity can result from low expression level of these variants. To test the steady state levels of the various Coi1 forms, mitochondria were isolated and the levels of the truncated Coi1 versions were compared to those of plasmid-encoded full length Coi1. The steady state levels of *coi1-99-114Δ* and *coi1-103-114Δ* were only slightly reduced compared to the full-length protein, but the levels of *coi1-109-114Δ* were moderately reduced (Fig 6.11B).
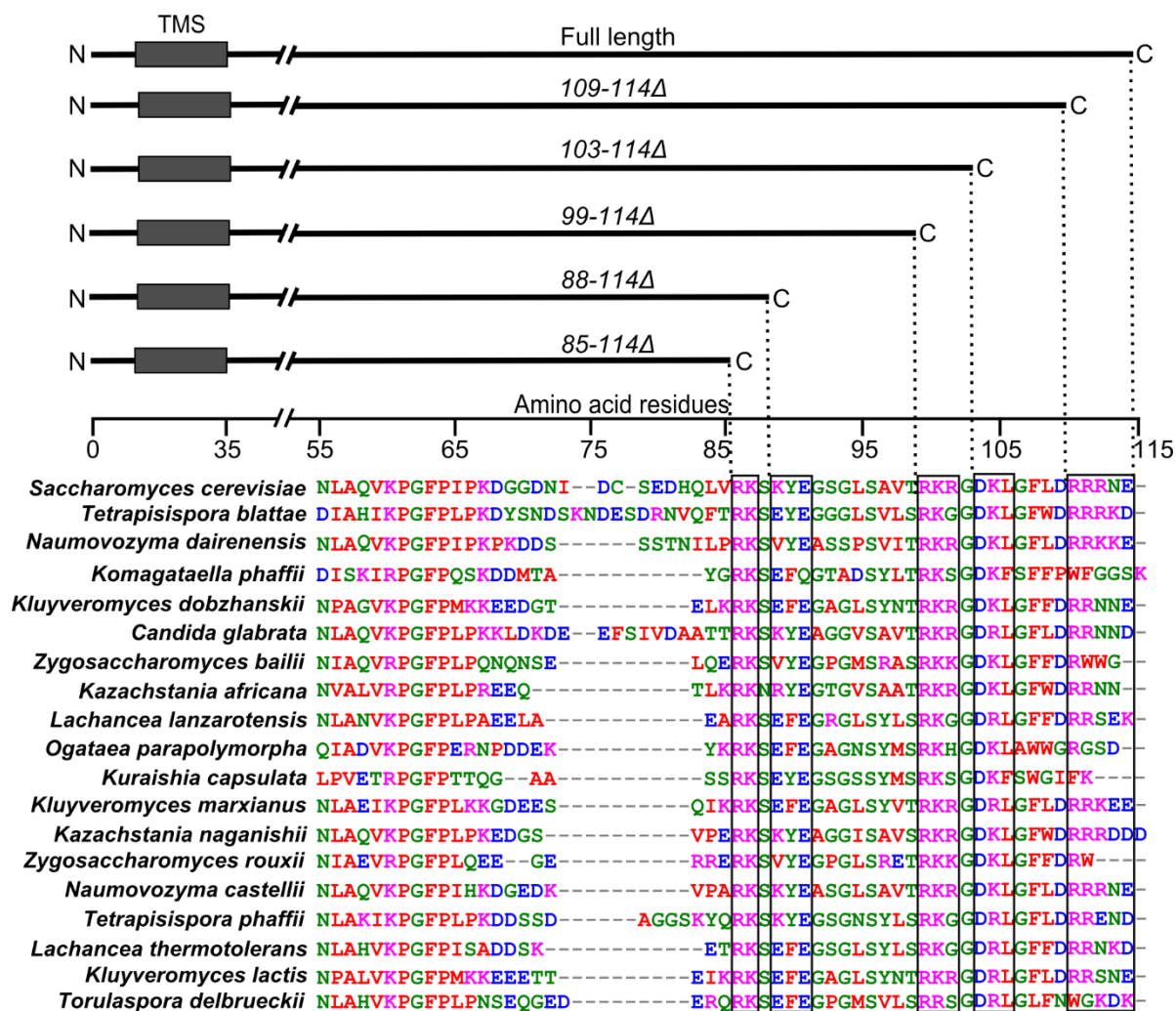
Figure 6.10 Conserved residues at the C-terminus of Coi1. Top panel: Schematic representation of full length and truncated versions of Coi1 used in this study. Bottom panel: Sequence similarity alignment by PSI blast of Coi1 in different fungi (https://toolkit.tuebingen.mpg.de /psi_blastp).

Of note, using the anti-Coi1 antibody, no signal could be detected for the truncated versions *coi1-85-114Δ* and *88-114Δ*. As a control, the levels of mitochondrial matrix protein Ssc1 and Tom40 were not affected by the absence or truncation of Coi1 (Fig 6.11B). Since the Coi1 antibody was raised against a mixture of two C-terminally peptides (81-100 and 101-114 amino acids), it might well be that the lack of detection of these versions results from the absence of the appropriate epitopes in these proteins.
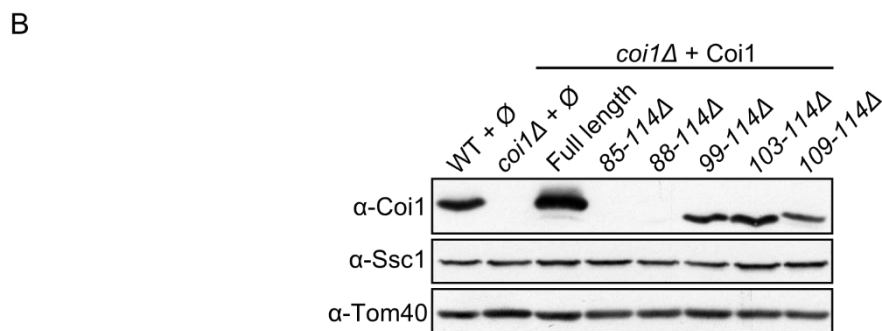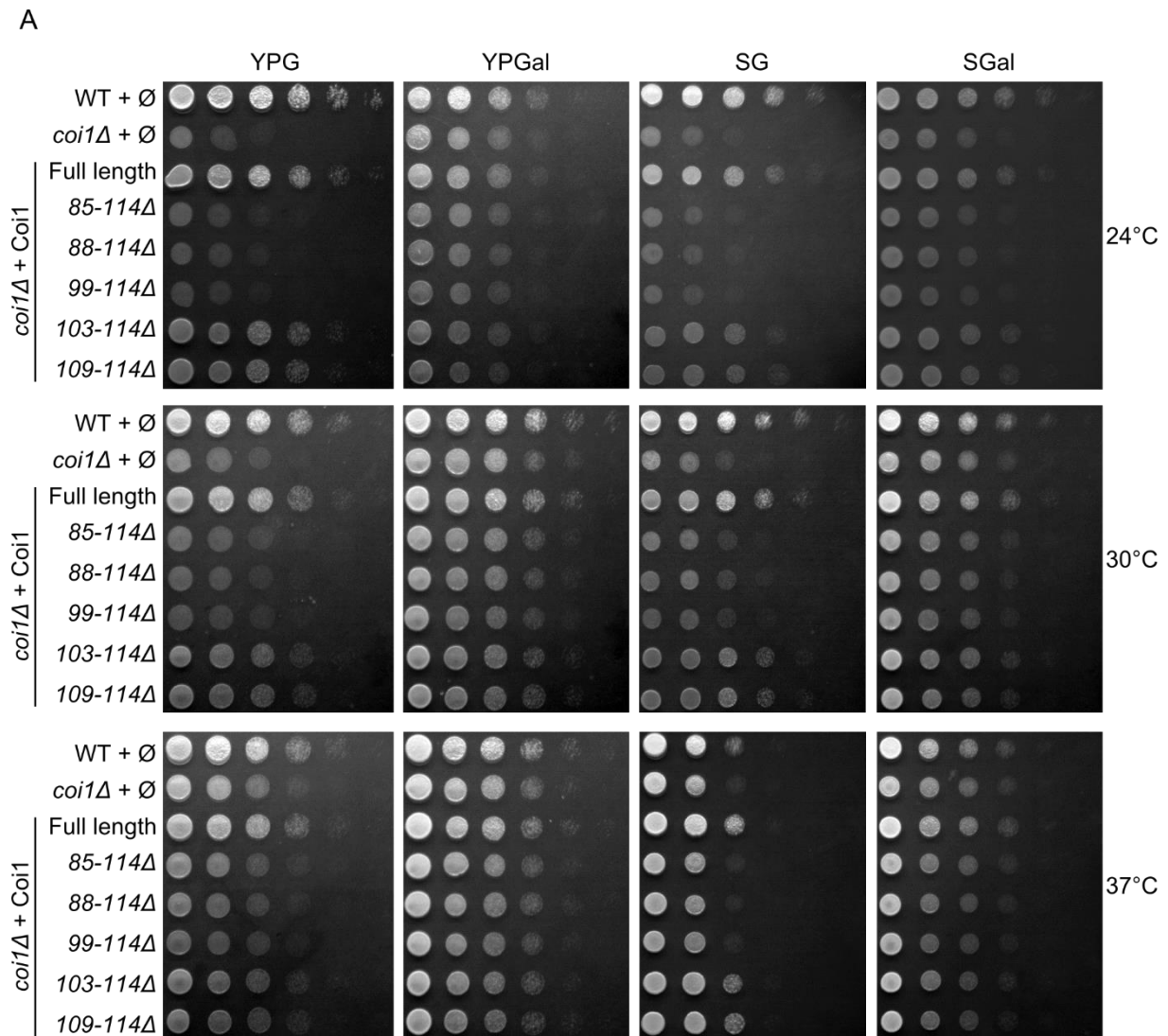
Figure 6.11 Conserved residues at the C-terminus of Coi1 are required for its function.
(A) WT or *coi1Δ* cells were transformed with an empty plasmid or with a plasmid encoding full length or truncated Coi1. The cells were subjected to a drop dilution assay at the indicated temperatures on the specified medium. **(B)** Crude mitochondria were isolated from the strains described in (A). Samples were analyzed by SDS-PAGE and immunodecoration with the indicated antibodies.

To verify this point, the truncated versions of Coi1 were C-terminally tagged with HA. These constructs were ectopically expressed in *coi1Δ* cells, and a complementation assay was performed. In this case, only the *coi1-HA-109-114Δ* partially rescued the growth phenotype of *coi1Δ* cells, while it was not rescued by the other four variants (Fig 6.12A). These findings indicate that the HA-tag has a negative effect on the function of the protein.
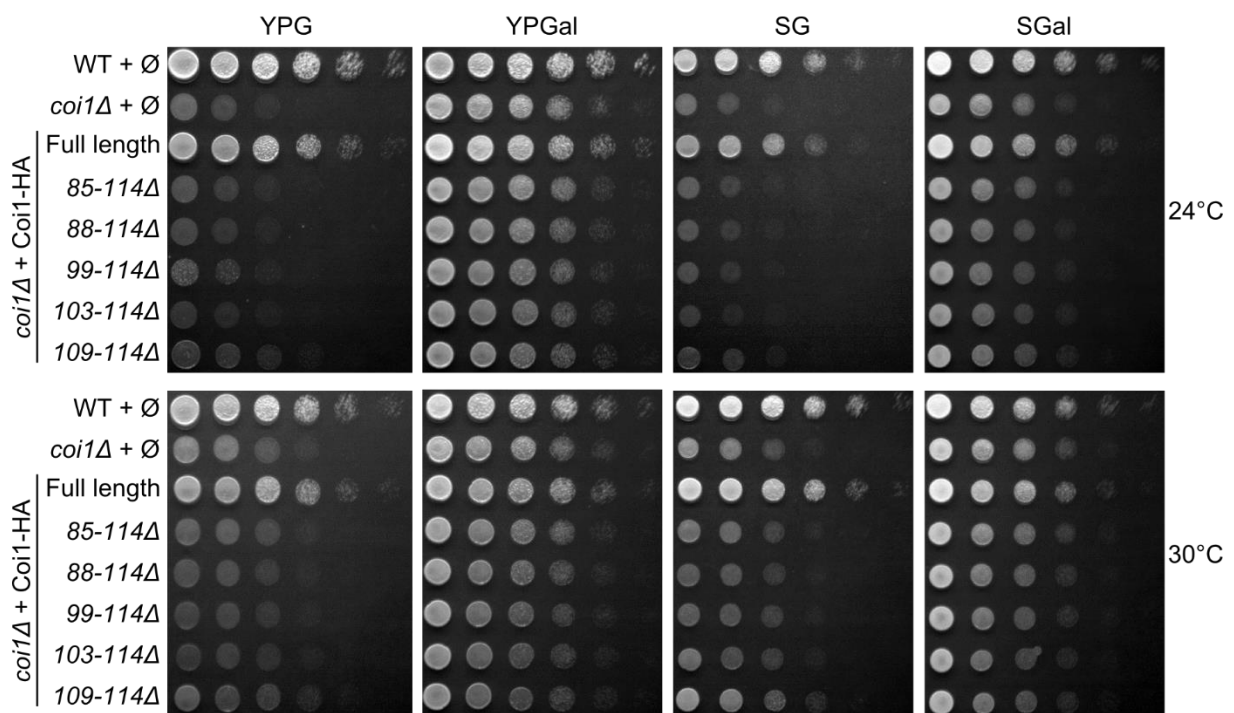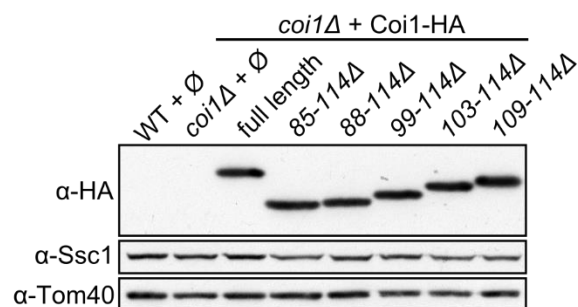
Figure 6.12 Truncated versions of conserved residues at the C-terminus of Coi1 leads to altered function of the protein. (A) WT or *coi1Δ* cells were transformed with an empty plasmid, plasmid encoding full length, or truncated Coi1 with a C-terminally HA-tag. Drop dilution assay was performed at the indicated temperatures on the specified medium. **(B)** Crude mitochondria were isolated from strains expressing HA-tagged Coi1 variants in *coi1Δ* cells. Samples were analyzed by SDS-PAGE and immunodecoration with antibodies against HA, Ssc1 (mitochondrial matrix protein), and Tom40 (OM protein).

The steady state levels of the HA-tagged proteins were also tested in these strains, and interestingly, the HA decoration showed that all the truncated versions of Coi1-HA were expressed at the same levels of the full length Coi1-HA (Fig 6.12B). This suggests that the truncation of the different segments at the C-terminal region does not affect the expression levels or the stability of the protein. This, in turn indicates that the reduced signal observed with the Coi1 antibody is due to the loss of the epitopes in the shorter proteins. Therefore, the effects observed on the growth phenotype are not due to different protein levels but rather due to altered functionality. Taken together, the positively charged amino acid region between positions 85 to 99 are essential for the functionality of the protein.

6.5   *In vitro* import assay to monitor the import of Coi1 into mitochondria

To better understand the biogenesis of Coi1, an *in vitro* assay to monitor its import into mitochondria was developed. To improve the detection of radiolabeled Coi1, four additional methionine residues were added to its C-terminus. The radiolabeled precursor protein was precipitated from the reticulocyte lysate and refolded in urea containing buffer to remove the abundant hemoglobin, which interferes with detection as it has the same molecular weight of Coi1.

Isolated mitochondria were incubated at 16°C with radiolabeled Coi1 for different time points and after the import reaction, mitochondria were re-isolated and subjected to PK (Fig 6.13A lane 5-8) or trypsin (Fig 6.13A lane 9-12) treatment to remove non-imported proteins. As control to test the proteolytic activity on the precursor protein, reticulocyte lysate in the absence of mitochondria was subjected to similar PK (Fig 6.13A lane 1-2) or trypsin (Fig 6.13A lane 3-4) digestion. Such experiments demonstrate that radiolabeled Coi1 was protected against PK or trypsin treatment with no clear difference between the various time points or the incubation temperature tested (4 or 25°C) (data not shown).

Experiments described above confirmed that Coi1 is an inner membrane protein (Fig 6.4B, C). I next aimed to test, if the *in vitro* imported Coi1 is indeed found in the membrane. To differentiate between non-imported (on the surface of mitochondria) and imported precursor protein, the mitochondria were re-isolated after import and

treated with PK or trypsin with or without Triton X-100. Most of the Coi1 precursor proteins was not imported into the mitochondria and was digested by PK or trypsin.
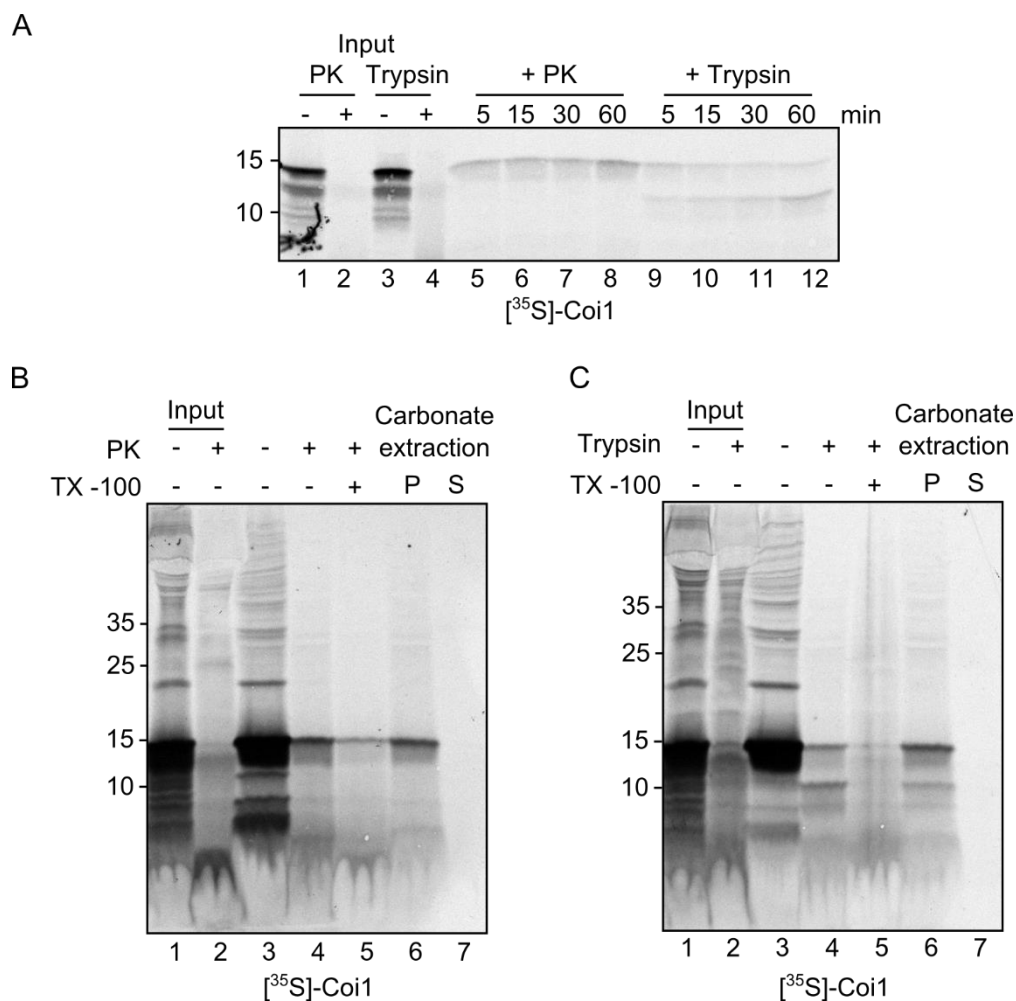

Figure 6.13 *In vitro* import of Coi1 into wild type mitochondria. (A) Radiolabeled Coi1 was incubated at 16°C with isolated mitochondria for the indicated time points. At the end of the import reactions, mitochondria were re-isolated and treated with proteinase K (PK) or trypsin to remove non-imported material. As a control, import reactions lacking mitochondria were treated in a similar manner. Imported proteins were analyzed by SDS-PAGE and autoradiography. The input lane represents 20% of the radiolabeled protein used in each import reaction. **(B, C)** Mitochondria were incubated at 16°C for 10 min in import reaction, and at the end of the import reaction, mitochondria were re-isolated and subjected to PK (B) or trypsin (C). In some samples Tx-100 was added to solubilize the organelle. Other samples were subjected to alkaline extraction, and the pellet (P) and the supernatant (S) fractions were analyzed by SDS-PAGE and autoradiography.

To verify that the protection of Coi1 from external proteases is not resulting from aggregation, mitochondria upon import were lysed with Triton X-100 after import. This should allow full access to the proteases. Indeed, Coi1 was completely digested in presence of trypsin in lysed mitochondria (Fig 6.13C lane 5), whereas with PK it was

only partially digested (Fig 6.13B lane 5). Furthermore, to confirm the insertion of Coi1 into the membrane, alkaline extraction was performed to separate membrane bound and soluble proteins. In agreement with previous experiments (Fig 6.4B), newly imported Coi1 was found in the pellet fraction after alkaline extraction (Fig. 6.13B- C lane 6).

In conclusion, Coi1 was not efficiently imported *in vitro* into isolated mitochondria However, a small portion of the molecules reached the IM and remained protease-protected and membrane-bound.

6.6 Coi1 forms higher molecular weight complexes

Next, it was investigated by blue native PAGE whether Coi1 forms a complex under native conditions. Isolated mitochondria from wild type, *coi1Δ*, and a strain overexpressing Coi1-HA in *coi1Δ* background were lysed with 1% digitonin and analyzed in 6-13% gel. Although Coi1 has a molecular mass of 12.7 kDa, it could be also detected as part of a higher molecular weight complex (Fig 6.14). As Coi1 antibody had cross-reactive signal with other proteins, samples were also decorated with anti-HA antibody. In both decorations, a specific signal for Coi1 at a higher molecular mass of approximately 300 kDa could be observed.
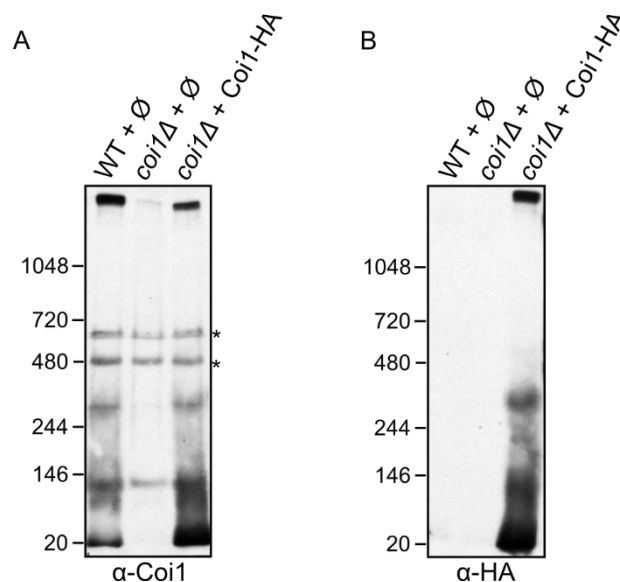

Figure 6.14 Coi1 forms higher molecular weight complex. Mitochondria isolated from wild type, *coi1Δ, and coi1Δ* strain overexpressing Coi1-HA were lysed with 1% digitonin, analyzed by BNGE and immunodecorated with the specified antibodies. *, indicates cross reactivity of the anti-Coi1 antibody.

6.7 Deletion of *COI1* causes reduction of both the mitochondrial membrane potential and oxygen consumption

6.7.1 *coi1Δ* cells have reduced mitochondrial membrane potential

The severe growth phenotype of *coi1Δ* cells suggests alterations in mitochondrial functions (Fig 6.6A). To further study such possible alterations, the membrane potential of isolated mitochondria from either wild type or *coi1Δ* cells was measured by employing the membrane potential-sensitive dye DiSc3(5). This fluorescent dye undergoes self-quenching upon its migration to energized mitochondria. As expected, reduction of the fluorescence signal was observed immediately upon addition of mitochondria. This reduction was restored by the addition of the uncoupler valinomyin. Of note, the fluorescence quenching was about twofold lower in organelles lacking Coi1, in comparison to wild type mitochondria (Fig 6.15). This indicates that Coi1 is required for the optimal function of the respiratory complexes.
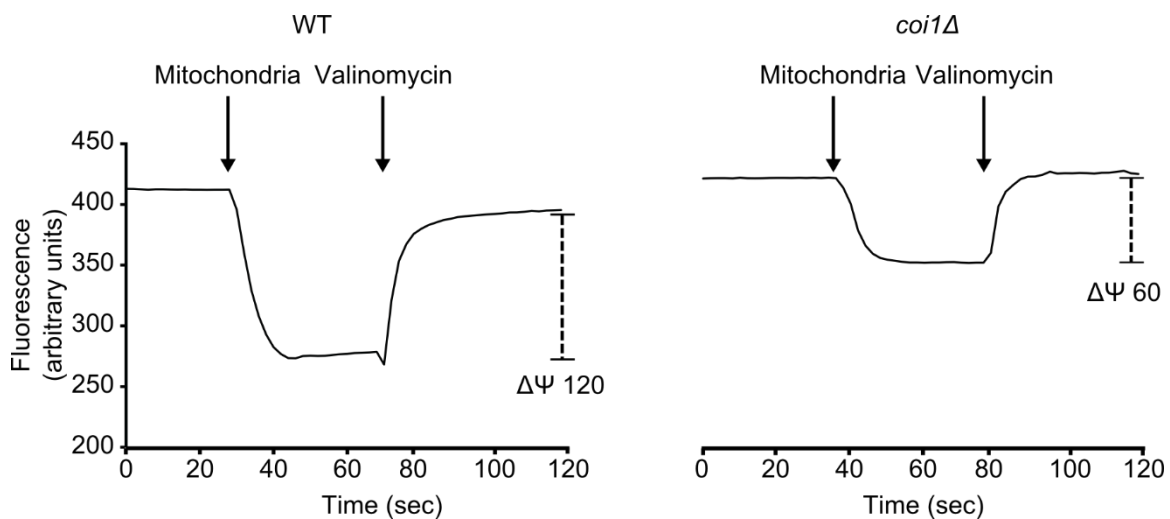
Figure 6.15 Mitochondria lacking Coi1 have lower membrane potential. Membrane potential (ΔΨ) of mitochondria isolated from either wild type or *coi1Δ* cells was monitored by a fluorescence assay with the dye DiSC3(5). The first arrow indicates the time point of the addition of mitochondria to the dye-containing buffer. The second arrow points to the time point when valinomycin was added to dissipate the membrane potential. A reduction of the fluorescence signal was observed upon adding mitochondria, which was restored by addition of valinomycin. The ΔΨ, represented by the difference in the fluorescence levels before and after the addition of valinomycin is indicated.

6.7.2 Absence of Coi1 hampers the *in vitro* import of mitochondrial proteins

To check if deletion of *COI1* affects the biogenesis of other mitochondrial proteins, the *in vitro* import efficiency of newly synthesized radiolabeled precursor proteins was analyzed by importing them into organelles isolated from either wild type or *coi1Δ* cells.
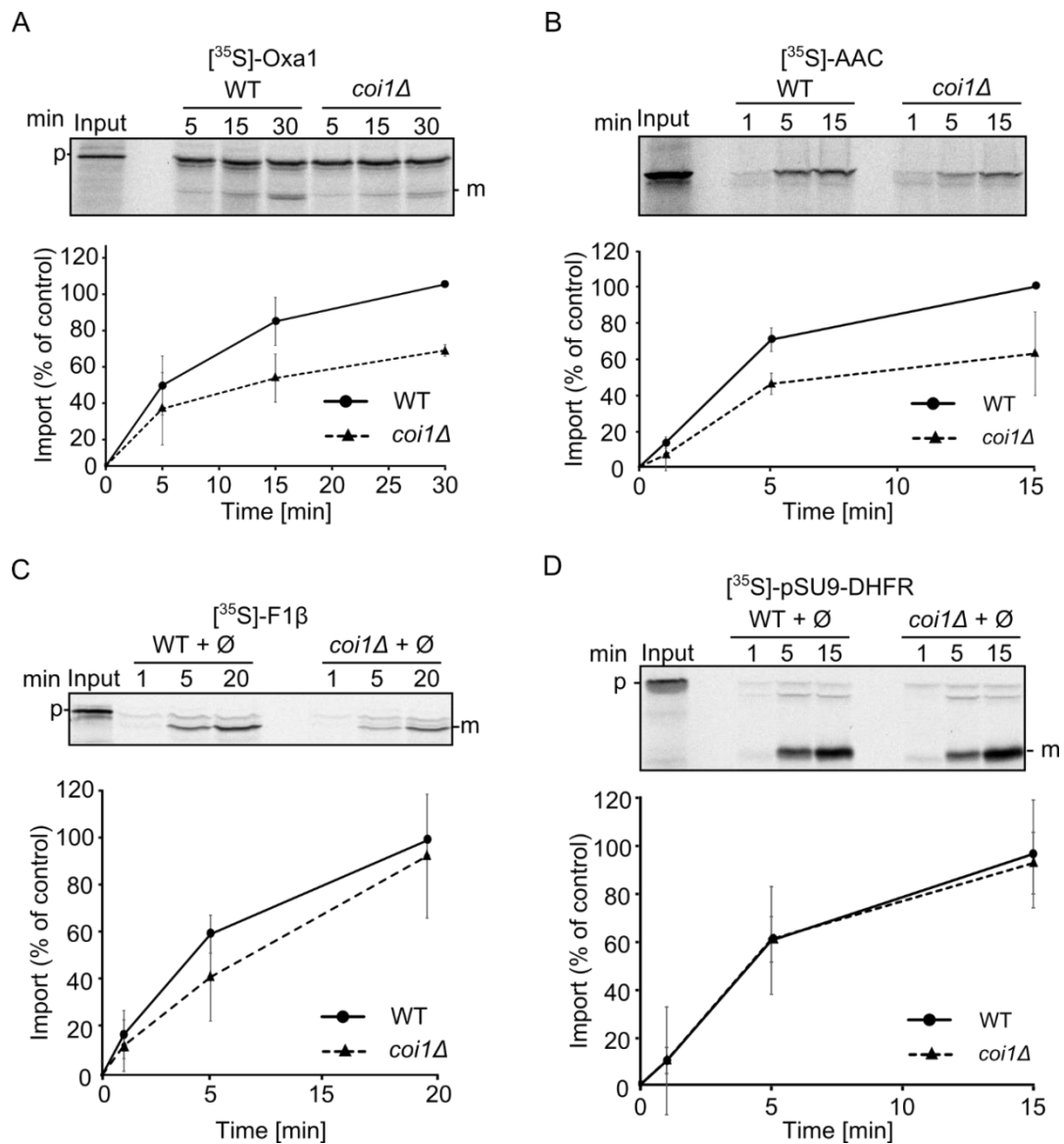
Figure 6.16 The absence of Coi1 affects the import of several mitochondrial IM proteins. Radiolabeled precursors of Oxa1 **(A)**, AAC **(B)**, F1β **(C),** and pSU9-DHFR **(D)** were imported for the indicated time periods into mitochondria isolated from either wild type or *coi1Δ* cells. At the end of the import reactions, mitochondria were re-isolated and treated with PK to remove non-imported material. Imported proteins were analyzed by SDS-PAGE and autoradiography. The input lane represents 20% of the radiolabeled protein used in each import reaction. All the experiments were performed in three independent repeats. Bands from three independent experiments were quantified and the amount of protein imported for the longest time point into control organelles was set to 100%.

Loss of Coi1 reduced the efficiency of the *in vitro* import of several IM proteins like Oxa1, AAC, and F1β, which requires membrane potential for their import (Fig 6.16A-C). pSu9-DHFR, a matrix-targeted model substrate with a strong MTS, was not affected by the absence of Coi1 (Fig 6.16D). The OM proteins, Porin and Tom40, which do not require membrane potential for their import, were not affected by the deletion of *COI1* (Fig 6.17A, B). These findings suggest that absence of Coi1 affects the overall membrane potential and this in turn influences the import efficiency of mitochondrial proteins, which are membrane potential dependent.
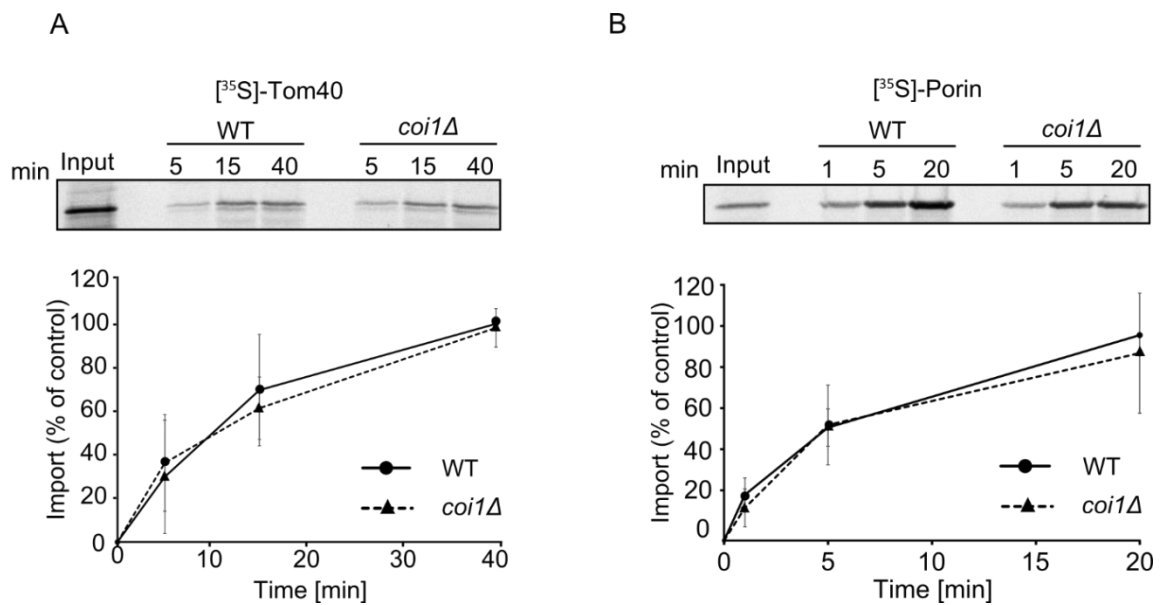
Figure 6.17 The absence of Coi1 has no effects on the import of mitochondrial outer membrane proteins. Radiolabeled precursors of Tom40 **(A)** and Porin **(B)** were imported for the indicated time periods into mitochondria isolated from either wild type or *coi1Δ* cells. At the end of the import reactions, mitochondria were re-isolated and treated with PK to remove non-imported material. Imported proteins were analyzed by SDS-PAGE and autoradiography. The input lane represents 20% of the radiolabeled protein used in each import reaction. All the experiments were performed in three independent repeats, bands were quantified and the amount of protein imported for the longest time point into WT organelles was set to 100%.

6.8   Deletion of *COI1* hampers mitochondrial respiration.

To substantiate the reduced respiration in the absence of Coi1, mitochondrial oxidative phosphorylation was examined by measuring oxygen consumption in wild type and *coi1Δ* cells. These experiments were performed in collaboration with Dr. Ilka Wittig's group (Goethe University, Frankfurt) and Prof. Johannes M. Herrmann's group (University of Kaiserslautern). The whole cell oxygen consumption was measured by high-resolution respirometry in two steps; first the routine respiration was monitored then, the maximal uncoupled respiration. Under both conditions the respiration in *coi1Δ* cells was significantly impaired in comparison to wild type cells (Fig 6.18A). Next, the respiration activity of isolated organelles was also measured. Reduced respiration capacity in mitochondria lacking Coi1 in comparison to the wild type organelles was observed. Of note, mitochondria lacking Coi1 had higher ability to respire than non-respiring organelles lacking Oxa1 (Fig 6.18B). This observation suggest a residual respiration capacity in *coi1Δ* cells. Altogether these results demonstrate that Coi1 is required for maintenance of the mitochondrial respiration activity.
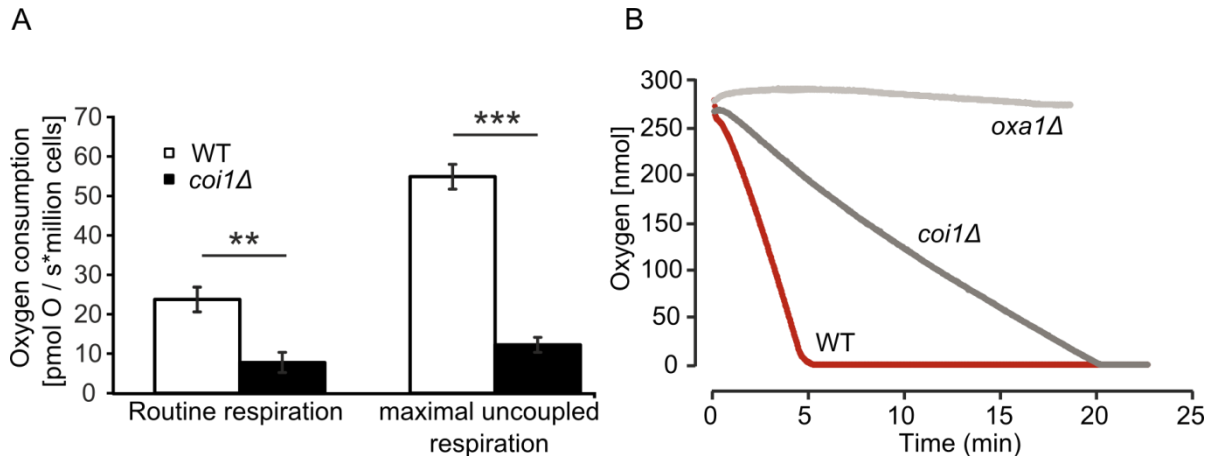
Figure 6.18 Lack of Coi1 affects oxygen consumption. **(A)** Measurement of oxygen consumption in yeast cells. Wild type and *coi1Δ* cells were grown in YPGal and the oxygen consumption was analyzed by high-resolution respirometry at 30°C. Error bars indicate standard deviation of three independent experiments. ** $p < 0.01$, *** $p < 0.001$. These results were obtained in collaboration with Dr. I. Wittig. **(B)** Oxygen consumption in mitochondria isolated from wild type, *coi1Δ*, or *oxa1Δ* cells was measured over time by oxygen measurement system at 24°C. These measurements were done in cooperation with the group of Prof. J. Herrmann.

6.9   Deletion of *COI1* influences the steady state levels of mitochondrial proteins

6.9.1   Absence of Coi1 affects the steady state levels of a sub-set of mitochondrial proteins

Lack of Coi1 causes altered mitochondrial function in terms of reduced *in vitro* import of IM proteins and hampered respiration. In order to further investigate the effect of *COI1* deletion, the steady state levels of proteins in mitochondria isolated from *coi1Δ* cells were monitored. The levels of inner membrane respiratory chain complex proteins such as Cox2, Cor1, Qcr6, and Cyb2 were reduced in the mutant organelles (Fig 6.19A, B). In addition, the steady state levels of the OM protein OM14 (Fig 6.20A, B), the matrix protein Aco1, and carrier proteins such as AAC and Pic2 were affected by the deletion of *COI1* (Fig 6.19A, B).
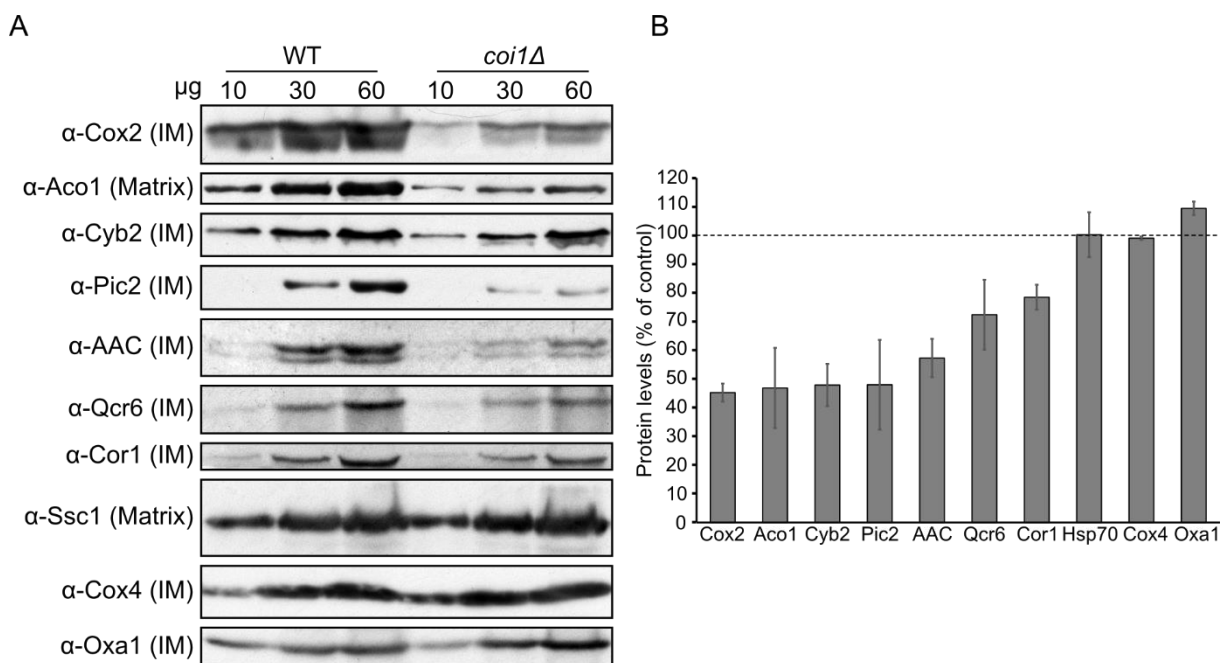
Figure 6.19 Deletion of *COI1* affects the steady-state levels of IM proteins. (A) The indicated amounts of mitochondria isolated from either wild type or *coi1Δ* cells were analyzed by SDS-PAGE and immunodecoration with the indicated antibodies. **(B)** The intensity of the bands from three independent experiments as those presented in (A) was determined, and the amounts of proteins in mitochondria lacking *COI1* are presented as mean percentages of their levels in wild type organelles. Error bars represent ±s.d.

In contrast, the levels of mitochondrial outer membrane proteins like Tom40, Tom20, and Tom70 as well as inner membrane proteins like Oxa1 and Cox4 or of the matrix protein Ssc1 were not affected (Fig 6.19 and 6.20). In conclusion, the absence of Coi1 has an effect on the steady state levels of respiratory chain complex proteins and some other mitochondrial components.
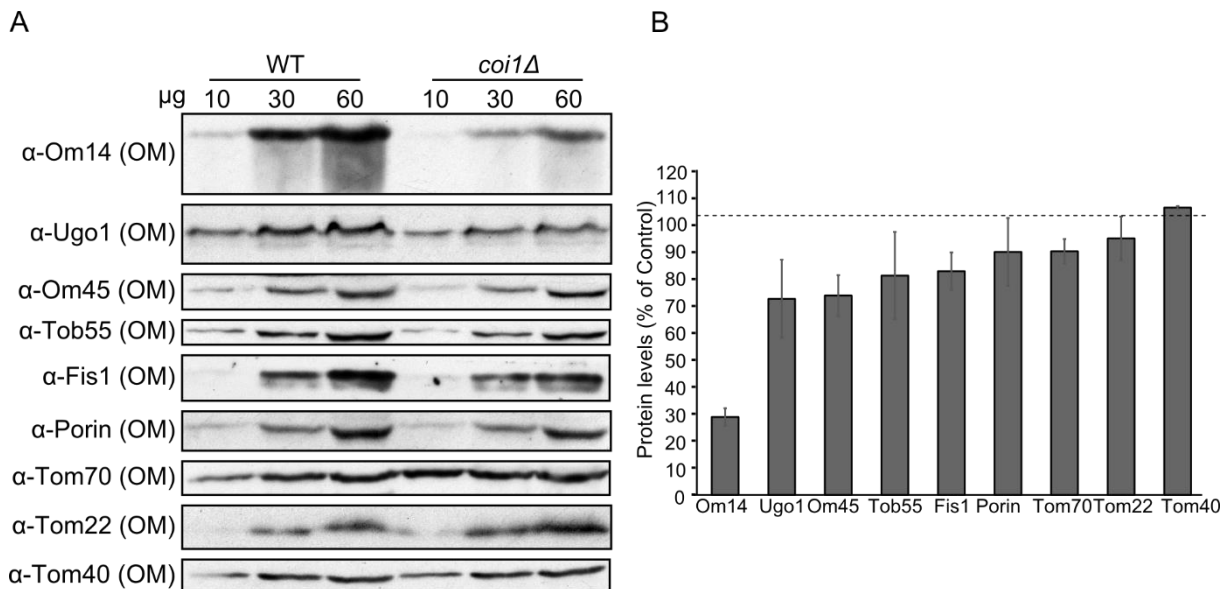
Figure 6.20 The absence of Coi1 affects some mitochondrial OM proteins. (A) The indicated amounts of mitochondria isolated from either wild type or *coi1Δ* cells were analyzed by SDS-PAGE and immunodecoration with the indicated antibodies. **(B)** The intensity of the bands from three independent experiments as presented in (A) was determined, and the amounts of proteins in mitochondria lacking Coi1 are presented as mean percentages of their levels in wild type organelles. Error bars represent ±s.d.

6.9.2 Coi1 is not involved in translation of mitochondrial encoded proteins

Steady state levels of mitochondrial-encoded IM proteins were drastically reduced in the absence of Coi1. To further investigate the role of Coi1 in the biogenesis of such proteins, translation of these proteins in *coi1Δ* strain was tested (in collaboration with Prof. J. Herrmann, University of Kaiserslautern). In either galactose or glucose, the translation capacity of mitochondria lacking Coi1 was similar or only slightly reduced in comparison to that of control organelles (Fig 6.21). Thus, it can be concluded that Coi1 affects the steady state levels of mitochondrial IM proteins, but it is hardly involved, or not at all, in the translation of mitochondrial encoded proteins.

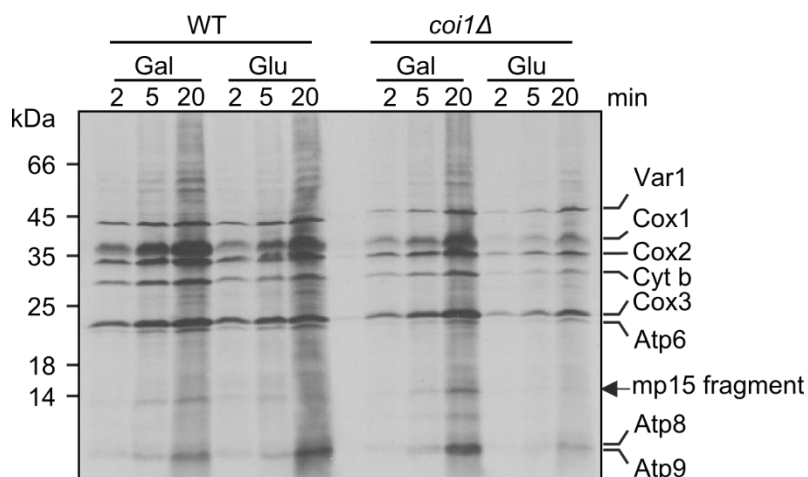**Figure 6.21 Coi1 is not required for mitochondrial-encoded protein synthesis.** Wild type and *coi1Δ* cells were grown in rich media containing galactose (gal) or glucose (glu). Cells were re-suspended in synthetic medium lacking methionine and treated with cycloheximide to block cytosolic translation. Radiolabeled methionine was added and cells were incubated at 30°C. At the indicated time points samples were subjected to alkaline extraction and analyzed by SDS-PAGE followed by autoradiography. The translated mitochondria proteins are indicated on the margin. These results were obtained in collaboration with the group of J. Herrmann.

6.10   Interaction partners of Coi1

6.10.1   Coi1 physically interacts with components of complexes III and IV

Our aforementioned results demonstrate that the absence of Coi1 affects the levels of some respiratory components and respiration activity. In search of interaction partners of Coi1, a yeast strain expressing C-terminally HA tagged Coi1 was generated, and the functionality and the correct location of this tagged version was verified (Fig 6.6B). Isolated mitochondria from this strain were solubilized with various detergents such digitonin (1%), DDM (0.5%), or Triton X-100 (0.5%). Affinity purification was performed using anti-HA magnetic beads. Interestingly, various components of complex III (Cor1, Qcr6), complex IV (Cox2, Cox4), the carrier protein Pic2, and the contact site protein, Mic60 were co-eluted with Coi1-HA (Fig 6.22A-C).
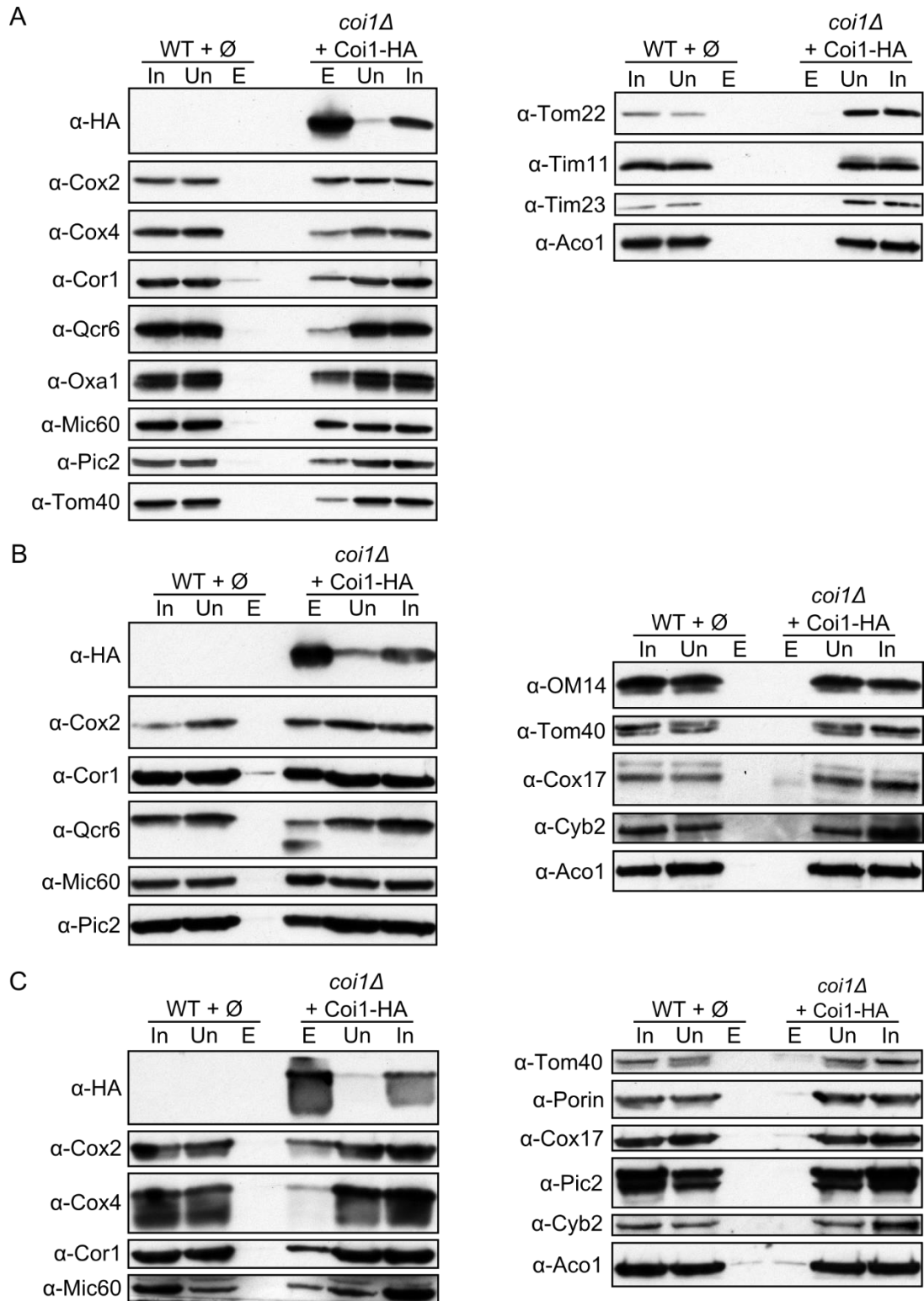
Figure 6.22 Coi1-HA interacts with components of complexes III and IV. Mitochondria were isolated from either wild type or *coi1Δ* cells expressing Coi1-HA. The organelles were lysed with buffer containing 0.5% Triton X-100 **(A)**, 0.5% digitonin **(B),** or 0.5% DDM **(C).** The lysates were subjected to a clarifying spin, and the supernatants were used in a pull-down assay with anti-HA magnetic beads. Supernatant (In, 2% of total), unbound material (Un, 2% of total), and material eluted from the beads (E, 33.3% of total) were analyzed by SDS-PAGE and immunodecoration with the indicated antibodies.

These interactions with Coi1 were specific, as they were not observed in the control strain. Furthermore, other mitochondrial proteins such as the soluble matrix protein Aco1, the IM protein Tim23, complex V protein Tim11, and the OM protein Tom22 were not co-eluted with Coi1-HA (Fig 6.22A-C). Interestingly, the interaction between Coi1 and the partners was very stable even in a harsh detergent such as Triton X-100. These findings suggest that Coi1 physically interacts with subunits of complexes III and IV.

6.10.2 The interactome of Coi1 as analyzed by mass spectrometry

To obtain a more comprehensive picture of the interactome of Coi1, proteins interacting with Coi1-HA were analyzed by mass spectrometry. This analysis was done in collaboration with Dr. Ilka Wittig's group (Goethe University, Frankfurt). Affinity pull-downs were performed as mentioned in section 6.10.1 using mitochondria isolated from either wild type or *coi1Δ* cells expressing Coi1-HA that were solubilized with 0.5% Triton X-100. Proteins interacting with Coi1-HA were digested with trypsin and analyzed by liquid chromatography and mass spectrometry. The data from the mass spectrometric analysis is plotted on volcano plot, and the proteins were sorted to 0.03 false discovery rate (FDR) showing highly significant interaction partners of Coi1 (Fig 6.23). In agreement with the previous results (Fig 6.22), the volcano plot demonstrated that components of complexes III and IV like Qcr1, Qcr2 (complex III), Cox2 (complex IV), and Rcf1 (regulator factor of supercomplex III-IV) are highly enriched in the group of strong interactors of Coi1. Interestingly, the central component of the TOM complex, Tom40 also appears to interact with Coi1-HA (Fig 6.23), in contrast to what previously shown (Fig 6.22). However, this interaction probably represents an import intermediate when newly synthesized molecules of Coi1 are translocated via the TOM complex. Taken together, the mass spectrometry analysis confirms that Coi1 interacts with components of the respiratory chain complexes.
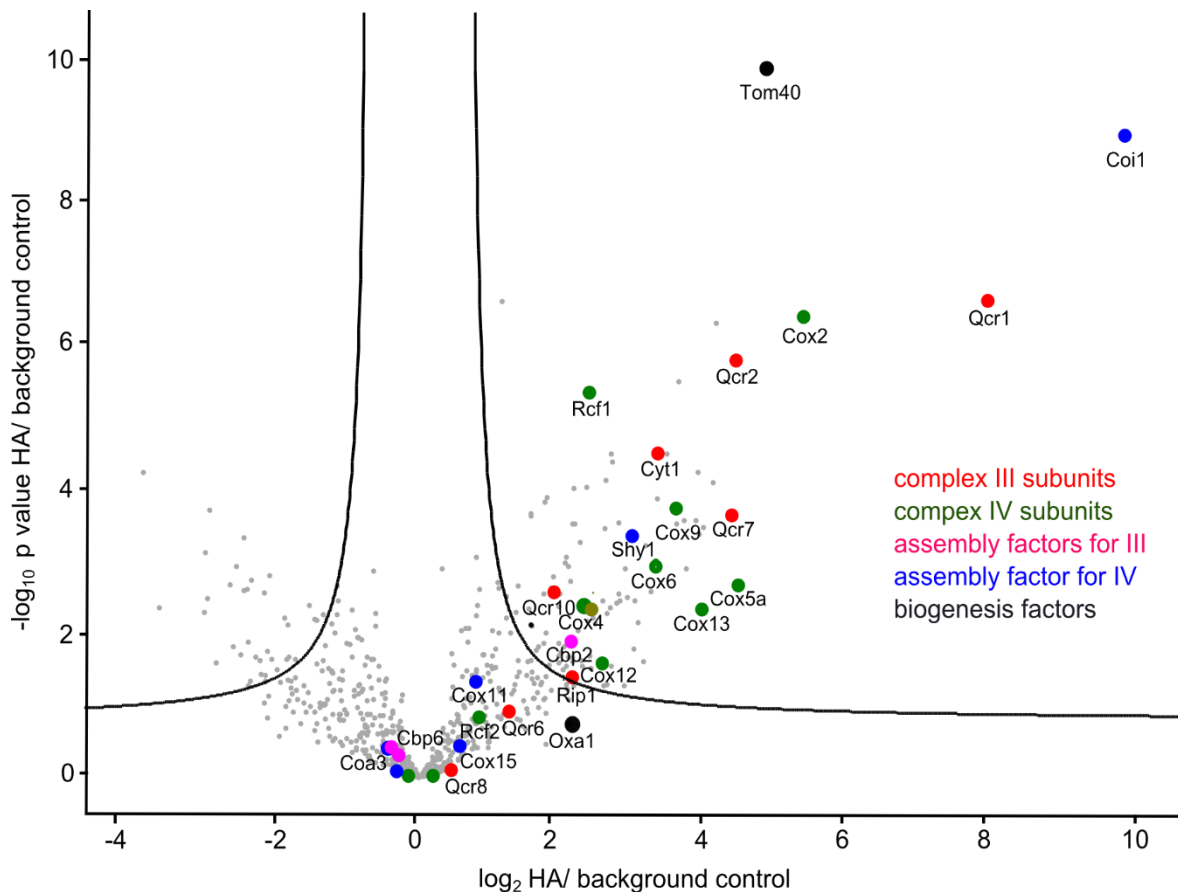
Figure 6.23 Coi1 interacts with respiratory chain complex proteins. Mitochondria isolated from *coi1Δ* cells expressing Coi1-HA were solubilized with 0.5% Triton X-100 and subjected to affinity purification. Eluted fractions were trypsinized and analyzed by quantitative mass spectrometry. The log fold change and the negative $\log_{10}$ p-value of six independent experiments were determined and plotted. Proteins belonging to the same complex are shown in the same color; complex III subunits in red, complex IV subunits in green, assembly factors of complex III in pink, assembly factors of IV in blue, and biogenesis factors in black.

6.10.3 Mic60 stabilizes the interaction between respiratory chain complexes and Coi1

An interesting finding from the affinity pull-down assays was that the central subunit of the mitochondrial contact site complex (MICOS), Mic60 was also co-eluted with Coi1-HA. To understand the relevance of this physical interaction, affinity pull-down with a strain expressing Coi1-HA in the absence of Mic60 was performed as described in section 6.10.1. Surprisingly, in the absence of Mic60, the interactions between Coi1-HA and its partners were drastically reduced (Fig 6.24). Of note, the HA-tagged form of Coi1, brings down also the native form of the protein suggesting that the Coi1 containing functional unit harbors at least two copies of the protein. This

interaction was also reduced in the absence of Mic60. Collectively, it appears that Mic60 is stabilizing, directly or indirectly, the interactions of Coi1 with its partner proteins.
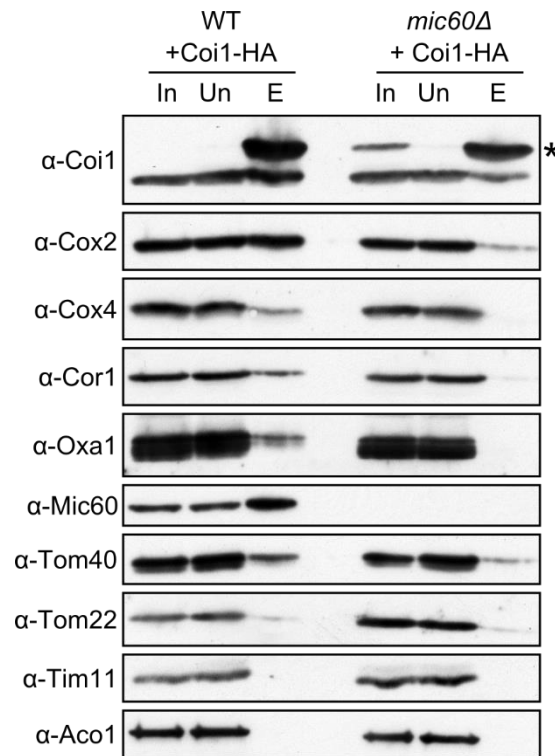
Figure 6.24 Mic60 stabilizes the interactions of Coi1 with its partner proteins. Mitochondria were isolated from either wild type or *mic60Δ* cells expressing Coi1-HA. Organelles were treated as described in section 6.10.1. Supernatant (In, 2% of total), unbound material (Un, 2% of total), and material eluted from the beads (E, 50% of total) were analyzed by SDS-PAGE and immunodecoration with the indicated antibodies. * indicates detection of HA-tagged Coi1 with anti-Coi1 antibody.

6.11   The importance of Coi1 for the formation of supercomplexes

6.11.1 Coi1 plays an important role in the formation and stability of respiratory supercomplexes

The aforementioned results suggest strong physical and functional interactions between Coi1 and complexes III and IV. To investigate whether Coi1 is involved in regulation of the assembly or stability of these complexes, they were examined by blue native PAGE (in collaboration with Dr. Ilka Wittig, Goethe University, Frankfurt). BN-PAGE of organelles solubilized in digitonin revealed that the absence of Coi1 resulted in reduced levels of complex IV and its super complexes with complex III

(Fig 6.25). To further confirm the defect in complex IV, a specific heme staining was performed. In the absence of Coi1, complex IV in its monomeric form or as a part of supercomplexes exhibited almost no heme staining, pointing to an impaired complex IV assembly or heme integration (Fig 6.25B).
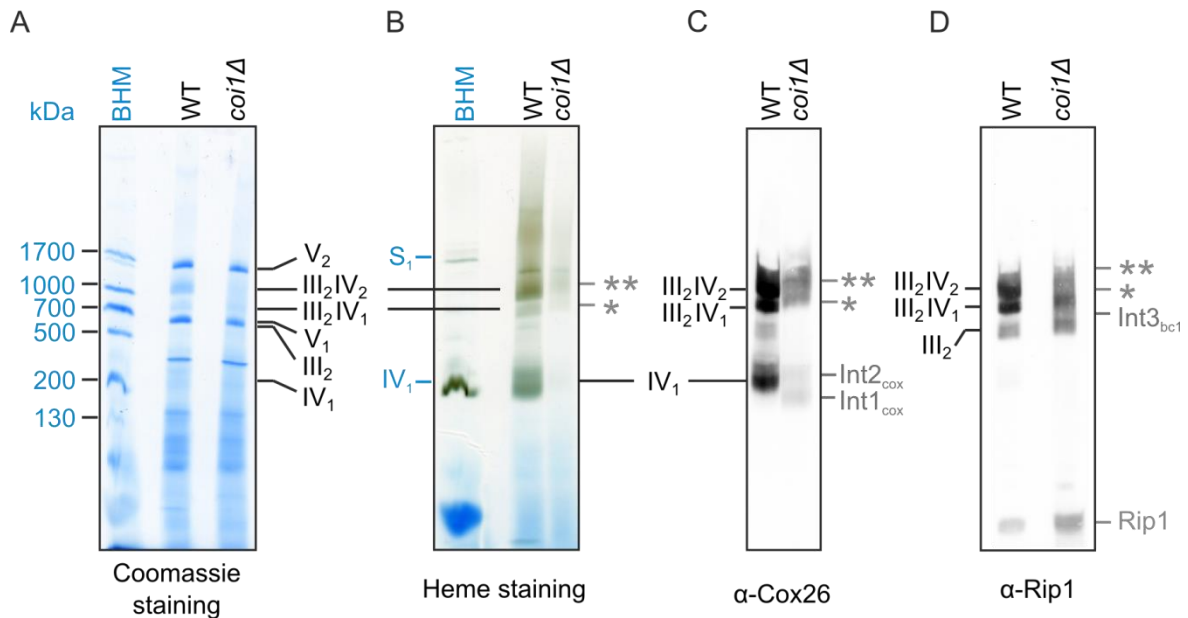

Figure 6.25 Coi1 is essential for assembly of complexes III and IV and their supercomplexes. Mitochondria isolated from wild type and *coi1Δ* cells were analyzed by blue native PAGE. **(A)** Samples were solubilized using 2.5% digitonin and the gels were stained with Coomassie. **(B)** Samples were analyzed as in (A) and the complex IV was detected by a specific heme staining. **(C, D)** Samples were analyzed as in (A) and then immunodecorated with antibodies against either the complex IV subunit Cox26 (C) or the complex III component Rip1 (D). Black annotations describe yeast complexes and blue annotations represent a mass ladder of mitochondrial complexes from bovine heart mitochondria (BHM). Complexes and proteins marked in grey highlights the altered appearance of supercomplexes III_2IV_1 (*), III_2IV_2 (**), Rieske protein of complex III (Rip1), complex IV and its assembly intermediates ($Int1_{cox}$, $Int2_{cox}$), complex III and its assembly intermediate ($Int3_{bc1}$). Assignment of mitochondrial complexes: V_1 and V_2, monomeric and dimeric ATP synthase; III_2, dimeric complex III; IV_1, monomeric complex IV; III_2IV_1, supercomplex containing complex III dimer and one copy of complex IV; III_2IV_2, supercomplex with two copies of complex III and two of complex IV; S_1, mammalian supercomplex containing complex I, two complex III, and one copy of complex IV.

The complexes were further analyzed by immunodecoration with antibodies against subunits of either complex IV (Cox26) or complex III (Rip1) (Fig 6.25C, D). The results indicated alterations in these complexes upon deletion of *COI1*. Cox26 was detected in two weak bands ($Int1_{cox}$ and $Int2_{cox}$) in the migration range of monomeric complex IV, and a size shift was observed in the supercomplexes (Fig

6.25C). In addition to the size shift, a considerably lower amount of supercomplexes III/IV were detected. These observations indicate assembly problems in the absence of Coi1 that are manifested as an altered composition or a dead-end assembly intermediate.

Complex III was also analyzed by immunodecoration with antibody against Rip1. Similarly, a defect in assembly of complex III subunits in absence of Coi1 was observed (Fig 6.25D). Deletion of *COI1* resulted in lower abundance of complex III dimers (Int3$_{bc1}$) and supercomplexes III/IV, as well as in change in their migration behavior. In line with reduced assembly, an accumulation of Rip1 monomer was detected in the absence of Coi1 (Fig 6.25D).

6.11.2 Overexpression of Coi1 rescues the assembly defect of respiratory chain complexes

Since the overexpression of either Coi1 or Coi1-HA rescues the growth phenotype of *coi1Δ* cells (Fig 6.7), I wondered whether such overexpression would also reduce the altered assembly of the supercomplexes III$_2$IV$_2$ (Fig 6.25). Isolated mitochondria from wild type, *coi1Δ*, and *coi1Δ* overexpressing Coi1-HA cells, were solubilized with 1% digitonin and analyzed by blue native PAGE. The gels were either stained with Coomassie or immunodecorated with antibodies against complex III or IV subunits. In absence of Coi1, almost no Coomassie staining was observed at the levels of supercomplexes, while overexpressed Coi1 could restore the levels of supercomplexes back to wild type amounts (Fig 6.26A).

Additionally, immunodecoration against the core complex IV subunit (Cox2) revealed that, Cox2 was not assembled into monomeric complex state and the supercomplexes in the absence of Coi1. Overexpression of Coi1 reversed these effects (Fig 6.26B). The absence of Coi1 had similar influence on complex III (Cor1), and overexpression of Coi1 reversed the levels of III$_2$IV$_2$ supercomplex (Fig 6.26C). To control for specificity, absence of Coi1 has no influence on the assembly of the TOM complex (Fig 6.26D). These observations clearly show that overexpressed Coi1 can rescue altered assembly of supercomplexes and monomeric complex IV in mutant cells. This rescue capacity demonstrates that the observed alterations are direct outcome of the absence of Coi1.
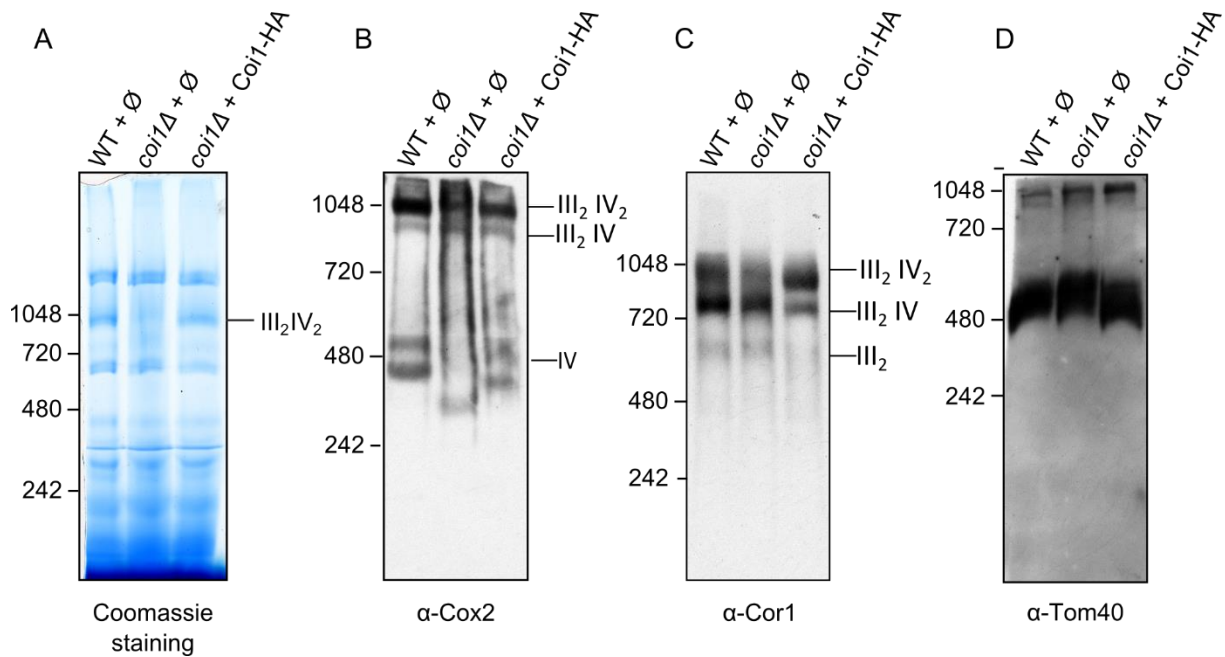
Figure 6.26 Overexpression of Coi1 in *coi1Δ* cells rescues the assembly of III₂IV₂ supercomplexes. Isolated mitochondrial from the indicated strains were lysed with 1% digitonin and analyzed by blue native PAGE. Gels were stained with Coomassie **(A),** or immunodecorated with specific antibodies against the core subunit of complex IV, Cox2 **(B)**, the Cor1 subunit of complex III **(C)**, or the central TOM component, Tom40 **(D)**.

6.12   Coi1 is required for the function of complex IV

6.12.1 Lack of Coi1 reduces complex IV activity

The results described above suggest that the altered monomer complex IV and supercomplex formation in the absence of Coi1 lead to respiratory defects. Next we asked whether the presence of Coi1 is required for the enzymatic function of complex IV. To that goal the activities of cytochrome c oxidase (COX) and citrate synthase (CS) as a control were measured (in collaboration with Dr. Ilka Wittig's group, Goethe University, Frankfurt). The enzymatic activity of COX and CS were measured in isolated mitochondria from either wild type or *coi1Δ* cells. Since CS activity (Fig 6.27B) was slightly affected, COX activity was normalized to the CS activity. In mitochondria lacking Coi1, COX activity was significantly reduced compared to wild type mitochondria (Fig 6.27A). This finding suggests an essential role for Coi1 in normal function of complex IV.
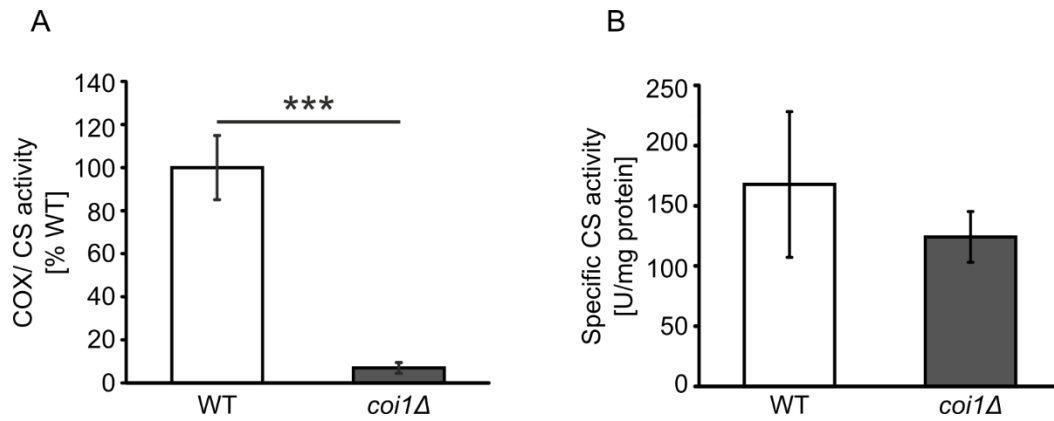
Figure 6.27 Coi1 is required for function of complex IV. Enzymatic activity of Cytochrome c Oxidase (COX) **(A)** and Citrate Synthase (CS) **(B)** were analyzed by spectroscopy at 30°C in mitochondria isolated from either wild type or *coi1Δ* cells. Error bars indicate standard deviation of three independent experiments. *** p<0.001 (Student t-test).

6.12.2 Coi1 is required for the optimal assembly of heme A into complex IV

The altered assembly of complexes III and IV in organelles lacking Coi1 (Fig 6.25) and the absence of heme staining of complex IV (Fig 6.25 B) led us to investigate the heme absorbance spectra in these organelles. Interestingly, the intensity of absorbance of heme types B and C were higher in the organelles from the mutated cells as compared to control mitochondria (Fig 6.28).

Figure 6.28 Coi1 is required for the optimal assembly of the heme A into complex IV. The absorbance spectra of different heme types was measured in mitochondria isolated from either wild type or *coi1Δ* cells. Heme C, B, and A are detected at wavelengths of 551, 561, and 603 nm, respectively.

75

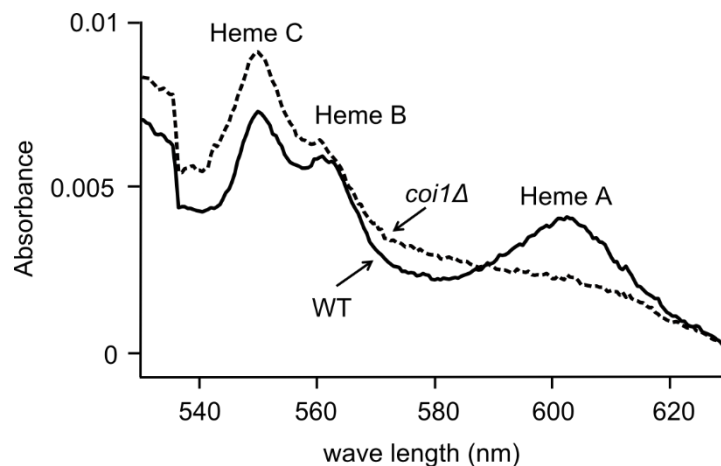In contrast, heme A absorbance was drastically reduced in the absence of Coi1. Collectively, the heme staining results and the heme absorbance measurements suggest that Coi1 is required for the proper transfer of heme A to complex IV and/or the assembly of heme A into this complex.

6.12.3 The putative heme binding domain of Coi1 is not crucial for its function

To investigate the relevance of Coi1 for heme assembly, the amino acid sequence of Coi1 was screened for a possible heme binding domain. Heme binding domains usually consist of the motif CXXCH, but it was also reported that the motifs CXXXH or XXCH, lacking one of the two cysteines of the classical heme binding motif, can still lead to a transient interaction with heme (Allen et al., 2004; Mavridou et al., 2012). Interestingly, CXXXH motif (residues 77 to 81) was identified in Coi1. To investigate the role of these amino acids in the function of Coi1, single point mutations replacing either cysteine at position 77 by serine (C77S) or histidine at position 81 alanine (H81A) as well as the double replacement were introduced (Fig 6.29A). Coi1 versions containing the single or double mutations were expressed in yeast cells lacking the native protein and the steady state levels of the Coi1 variants were analyzed. The mutations had no effect on the protein levels of Coi1 when compared to the native protein (Fig 6.29B). Next, the rescue capacities of the different mutated Coi1 versions were analyzed by a drop dilution assay (Fig 6.29C). Both variants with single mutant and the one with the double replacement could rescue the growth phenotype of *coi1Δ* cells to a similar extent as the native protein (Fig 6.29C). Taken together, the putative heme binding domain in Coi1 does not play a major role in the function of the protein.
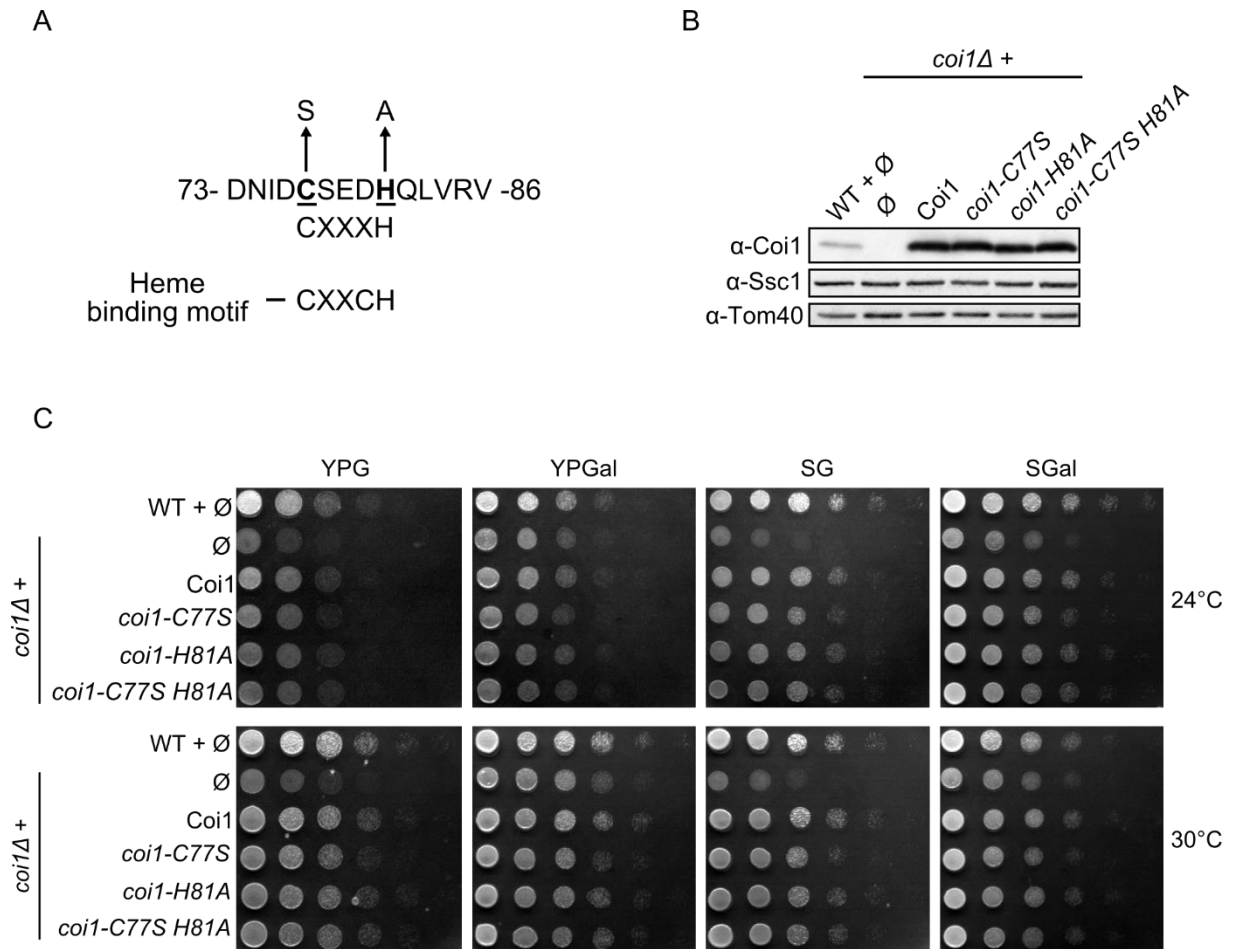
Figure 6.29 CXXXH motif in Coi1 has no direct functional role. (A) Schematic representation of the mutations performed at the putative heme binding domain in Coi1 sequence. Cysteine 77 was mutated to serine (C77S), histidine 81 to alanine (H81A). The sequence of the canonical heme binding motif is indicated. **(B)** Crude mitochondria was isolated from the indicated strains. Proteins were analysis by SDS-PAGE and immunodecoration with the specified antibodies. **(C)** Cells lacking Coi1 were transformed with an empty plasmid or plasmid encoding full length Coi1, single mutant (C77S and H81A) or double mutant (C77S/H81A). The growth on the specified medium of the transformed cells and WT as control was monitored at the indicated temperatures by drop dilution assy.

7 Discussion

The mitochondrial respiratory chain complexes are arranged in series of supercomplexes for their flawless functions. These multifaceted structures are assembled by an array of factors bringing the individual complexes together to a working state. Although several such assembly factors have been identified and characterized, the complete picture of the assembly process as well as a comprehensive list of the proteins involved are still lacking. In the current study we identified a novel protein Coi1 that is required for the assembly of the respiratory chain supercomplexes.

7.1   Coi1 is a small single transmembrane domain protein

Coi1 is a small protein with a molecular mass of 12.7 kDa that is conserved in fungi but has no apparent homologues in higher eukaryotes. From *in silico* prediction, Coi1 has a putative transmembrane segment in its N-terminal region (a.a. 11-30). The experiments performed in this study suggest that Coi1 has indeed a transmembrane domain that is embedded in the IM. The short N-terminal region of Coi1 is facing the matrix and the C-terminal domain resides in the IMS. Some of the IM precursor proteins contain an N-terminal targeting sequence which directs them to the TIM23 machinery (Fig 3.1) (Becker et al., 2012; Dudek et al., 2013). IM proteins are also sorted by hydrophobic internal signal which is laterally released into the membrane by the TIM23 complex (Diekert et al., 1999; Rehling et al., 2003). Coi1 has no predicted canonical cleavable presequence, but might be target with internal targeting signal, which remains unknown. To better understand the targeting of Coi1, I constructed different truncated versions of Coi1 (Fig 6.8). These experiments show that the transmembrane domain of Coi1 is crucial for the correct topology and stability of the protein. However, whether the transmembrane domain is also required for the targeting of Coi1 to mitochondria remains unclear. Nevertheless, I could show that the first nine amino acids of Coi1 are not essential for the correct targeting of the protein, as the corresponding truncated version of Coi1 (*coi1-2-9Δ*) is targeted to and inserted into the mitochondrial IM.

7.2   Structural organization of Coi1

According to multiple sequence alignment, the hydrophilic C-terminal region of Coi1 has relatively low sequence conservation but contains highly charged amino acids which are conserved in various species (Fig 6.10). To understand the relevance of these conserved segments, truncated versions lacking them were generated. Nearly all truncated versions have a severe impact on the function of Coi1 as they were not able to rescue the growth phenotype of *coi1Δ* cells expect from 109-114 (*coi1-109-114Δ*), which would partially complement the *coi1Δ* phenotype (Fig 6.11A, B). Steady state levels of truncated versions of Coi1 beyond *85-114Δ* and *88-114Δ* were not able to be detected by anti-Coi1, due to loss of recognition site (antibody was raised against 81-100 and 101-114 amino acids peptides) (Fig 6.11B). Therefore proteins levels were compared to HA-tagged variants. Notably, the protein levels of truncated version with HA-tag were similar to full length protein, suggesting that the removed segments are not crucial for the stability of the protein (Fig 6.12B). The positively charged amino acid region might play a structural role in Coi1 or potentially involved interacting with the other proteins containing patches of negatively charged residues of its function. Another speculation might be that positively charged residues of Coi1 may interact with polar head groups of lipids.

Coi1 interacts with respiratory complexes III and IV that are composed from core subunits and accessory subunits (Fig 6.22). These accessory subunits are mostly small nuclear-encoded proteins, which assist in the regulation, assembly or stabilization of respiratory chain complex subunits (Zickermann et al., 2010). The amino acid sequences of these subunits are relatively low conserved between mammals and yeast, and also some subunits are completely absent in other eukaryotes (Das et al., 2004). Despite their low sequence similarity, several small subunits of the respiratory chain complexes with a molecular mass ranging from 6 to 19 kDa are predicted to have a common topology. These subunits are mainly integral membrane proteins containing a hydrophobic α-helical region buried in the phospholipids core of the membrane and soluble, hydrophilic domains at the N- and C-termini (Zickermann et al., 2010). The hydrophilic region of these subunits contains an unusually high percentage of charged residues. For example, the bovine ATP synthase e, f, and k subunits contain around 50% of charged residues in their C-terminal domains (McCaldon and Argos, 1988; Turakhiya et al., 2016; Zickermann et

al., 2010). Coi1 has a similar topology as a single-span protein. Around 34% of Coi1's sequence is made up of aspartate, glutamate, lysine or arginine. These residues are especially enriched in the hydrophilic, C-terminal region that resides in the IMS. The lack of Coi1 homologues in higher eukaryotes is also not an unusual feature of the accessory factors. Collectively, Coi1 shares several structural features with other accessory subunits of respiratory complexes such as membrane topology and amino acid composition point to a possible role of Coi1 as an of accessory subunit of the respiratory chain complexes.
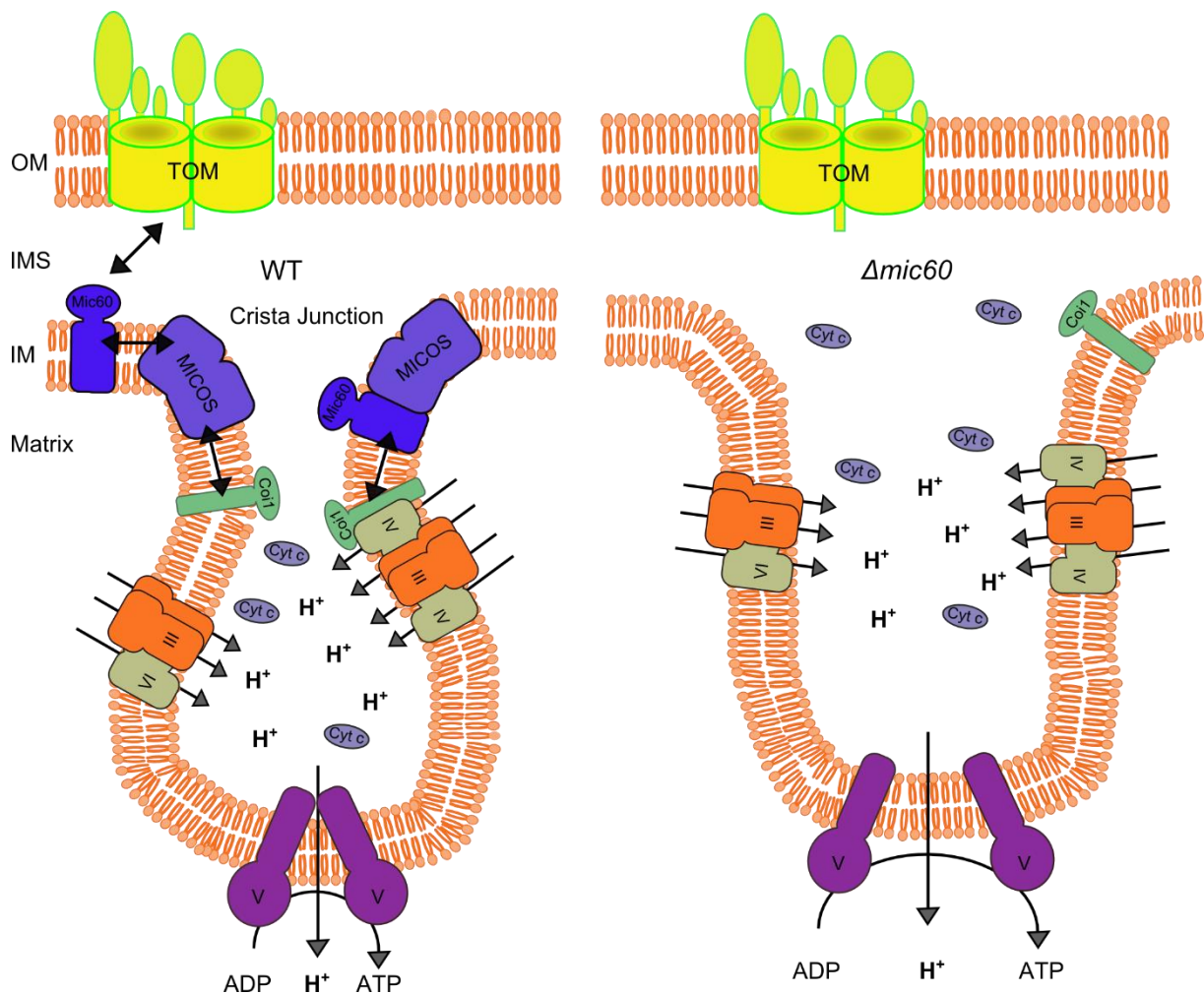
Figure 7.1 Mic60 retains the cristae junction and its architecture. Cristae organizing system (MICOS) is a multi-subunit complex which is enriched in cristae junctions. Mic60, which is a core subunit of MICOS complex is essential for normal cristae architecture. Mic60 complex forms contacts with the outer membrane by interactions with Tom40 and SAM. In wild type condition when Mic60 is present, Coi1 interacts with respiratory chain complexes. In the absence of Mic60, the interactions between Coi1 and the respiratory chain complexes are drastically reduced. Such a reduction might affect the assembly of respiratory supercomplexes.

The deletion of *COI1* results in cell growth retardation, dissipation of the mitochondrial membrane potential, and defects in oxidative phosphorylation activity. To better characterize the precise function of Coi1, I searched for its interaction partners. Affinity pull-down experiments showed that Coi1 interacts with various components and assembly factors of the respiratory chain complexes III and IV, with the contact site protein Mic60, with carrier proteins, and with the OM protein Tom40 (Fig 6.22). The strongest interaction partners of Coi1 were Qcr1, Qcr2, Cox2, Rcf1, and Tom40 (Fig 6.23). In another study, Coi1 was also identified in the interactome of Cox4 (Bottinger et al., 2013), confirming the interaction of Coi1 with Complex IV. Interestingly, I could show that Coi1 interacts with Mic60, which is a core component of the MICOS complex in the IM (Friedman et al., 2015). Furthermore, I also observed that the interactions of Coi1 with the respiratory complexes subunits were weaker in the absence of Mic60 (Fig 6.24). A potential explanation for this effect is that Mic60 facilitates the optimal positioning of the respiratory complexes and Coi1, and thus contributes for their interactions (Fig 7.1). In line with my findings, recent studies have shown that the MICOS complex is required for efficient function of respiratory chain complexes in both yeast and mice (Cogliati et al., 2013; Friedman et al., 2015).

7.3   Coi1 is required for the formation of complexes III and IV and of their supercomplexes

The interaction of Coi1 with the respiratory chain complexes were confirmed by blue native PAGE. We noticed that the absence of Coi1 results in defects in the assembly of complexes III and IV. Accordingly, the non-assembled form of the complex III subunit Rip1 was detected in much higher amounts in mitochondria lacking Coi1 (Fig 6.25). Moreover, a considerable shift in the apparent molecular weight of complex III and IV supercomplexes was observed in organelles lacking Coi1, which might be a result of the accumulation of a stalled intermediate complex IV. In addition to this shift, lower amounts of the complex III and IV supercomplexes were observed (Fig 6.25). Heme was detected only at the levels of the supercomplexes suggesting that maybe the affinity of the complex subunits to heme is higher when complex IV is part of a supercomplex (Fig 6.25B). Taken together, the deletion of *COI1* leads to altered levels of complexes III and IV of the respiratory chain.

The absence of Coi1 seems to impair the final step of complex III assembly possibly leading to a dead-end assembly intermediate. Furthermore, the lack of Coi1 causes also a major reduction in the amounts of heme associated with complex IV. Considering these observations, Coi1 resembles Rcf1 and Rcf2 that mediate supramolecular interactions between complex III and IV. Interestingly, both Coi1 and Rcf2 are found only in fungi (Strogolova et al., 2012). The results from interaction studies show a clear physical and functional interaction of Coi1 with the respiratory chain complexes III and IV. Hence, Coi1 might work in a similar fashion as Rcf1 and Rcf2 to regulate the assembly and stability of respiratory chain supercomplexes.

7.3.1 Coi1 might provide heme to complex IV

The absence of Coi1 leads to a clear reduction of heme staining and heme A absorbance of complex IV. This raises the possibility that Coi1 facilitates the incorporation of heme into complex IV. Heme is a crucial cofactor of many oxidases in eukaryotic cells, and heme A, which is typical to complex IV, is synthesized with the help of Cox10 (heme O synthase) (Tzagoloff et al., 1993) and Cox15 (heme A synthase) (Barros et al., 2002). Heme A is required for the proper folding of Cox1, a core subunit of complex IV, and it also stabilizes the interaction between Cox1 and other subunits of complex IV (Kim et al., 2012). The results in this study show moderate changes in the absorbance of heme B and C whereas the absorbance of heme A was dramatically diminished (Fig 6.28). These findings suggest a dramatic loss of this redox cofactor and might indicate a potential defect in the synthesis of heme A.

The process that assures heme insertion into the mature Cox1 is not resolved yet. Cox1 is assembled co-translationally into the IM and it forms an intermediate complex with chaperones (Cox14, Cox25, and mitochondrial matrix Ssc1), assembly factors (Coa1, Coa2, Coa3, and Shy1), and complex IV subunits (Cox5a and Cox6). At this stage, heme seems to be incorporated in the vicinity of Shy1 (Bareth et al., 2013; Kim et al., 2012; Mashkevich et al., 1997). The absence of the assembly factors and chaperones mentioned above affects the assembly of the Cox1 intermediate complex (Khalimonchuk et al., 2010; Kim et al., 2012). In the current study, it is observed that in the absence of Coi1, mitochondrially encoded proteins

are normally translated (Fig 6.21), but their assembly into functional complexes is impaired (Fig 6.25).

The observed defects in the assembly of these proteins might be due to an impaired heme association. One can speculate that Coi1 might be directly or indirectly involved in the incorporation of heme into mature Cox1. A possible connection of Coi1 to heme is the sequence motif CXXXH (77- 81 aa) present in the C-terminal domain of the protein. CXXCH is known as a C-type heme binding motif, where the two cysteine residues interact with the vinyl carbon groups of heme and the single histidine binds the heme iron (Allen et al., 2004; Kim et al., 2012; Mavridou et al., 2012). It was also reported, that the presence of only a single cysteine, as it is the case in Coi1, leads to an intermediate affinity to heme (Fulop et al., 2009). The mutagenesis experiments performed in this study showed that the putative heme binding domain might not have direct functional role in heme binding. Therefore, it is possible that Coi1 is not directly involved in transferring heme to complex IV, but might be involved together with other proteins to direct heme to its final destination.

Based on the results presented above, the phenotype of the deletion of *COI1* could be explained by the following model (Fig 7.2 and 7.3). In the absence of Coi1, heme A is not incorporated into the early Cox1 containing complex which leads to a stalled intermediate complex comprising also the mitochondrial ribosome and Mss51. Due to the accumulation of the ribosome and other subunits, a size shift of complex is detectable by blue native PAGE (Fig 6.25). Mss51 is an important negative feedback regulator of Cox1 translation, which might inhibit the Cox1 translation leading to defective Cox1 intermediate assembly.

According to the experiments performed in this study, Coi1 might have a second function in assembling the supercomplexes formed between complex III and IV. Lack of Coi1 clearly leads to a growth phenotype on non-fermentable carbon sources (Fig 6.6) and a drastic reduction of complex IV activity (Fig 6.27). Furthermore, the deletion of *COI1* has a severe effect on the III_2IV_2 supercomplex and on complex IV, which can be complemented by ectopically expressed Coi1 (Fig 6.26). Considering the physical interaction between Coi1 and Rcf1, Coi1 might help Rcf1 as interface between complexes III and IV.
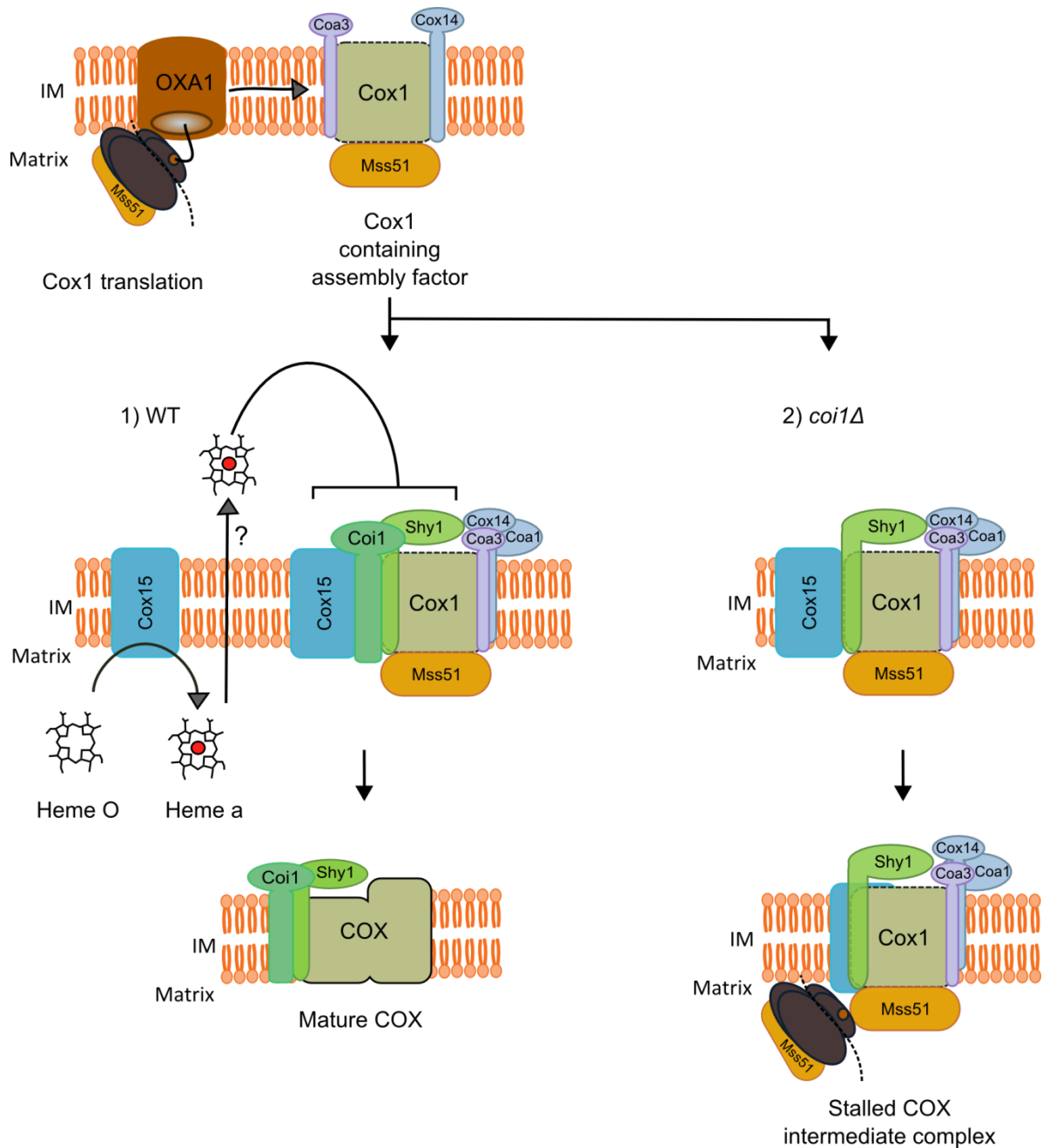
84

Figure 7.2 Coi1 is required for heme insertion in complex IV. Cox1 is synthesized in the mitochondrial matrix while the translating ribosomes are activated by the translational activator Mss51. Oxa1 inserts Cox1 into the IM and interacts with Cox14 and cytochrome c oxidase assembly 3 (Coa3) factor. Cox15 is involved in biogenesis of heme A, it converts heme O to heme A in the matrix. Cox15 interacts with crucial cofactor of COX such as Coa3, Cox14 and Shy1. **(1)** In wild type mitochondria, Coi1 interact with Cox15 and cofactor involved in Cox1 biogenesis. Coi1 might be involved in the insertion of heme A into Cox1 with cooperation with other cofactors. This pre-assembly step leads to further insertion of nuclear encoded subunits to form a mature complex IV. The export of heme A from the matrix to the IMS remains still unclear, therefore it is indicated with a question mark (?). **(2)** In absence of Coi1, heme A is not completely available to Cox1 intermediate complex suggesting a stalled COX complex with assembly cofactors and mitochondrial ribosomes.

So far it was shown that Rcf1 and Rcf2 are required for the stability of the III_2IV_2 supercomplex and for the assembly of Cox13, which might be the link between Rcf1 and the complexes III and IV (Strogolova et al., 2012; Vukotic et al., 2012). Taken together, Coi1 might assist in the assembly of complex IV and interact with Rcf1 or Rcf2 to help them to form the respiratory chain supercomplexes.

Regardless of its actual molecular mechanism, this study identifies Coi1 as a novel assembly factor essential for the proper function of the mitochondrial respiration.
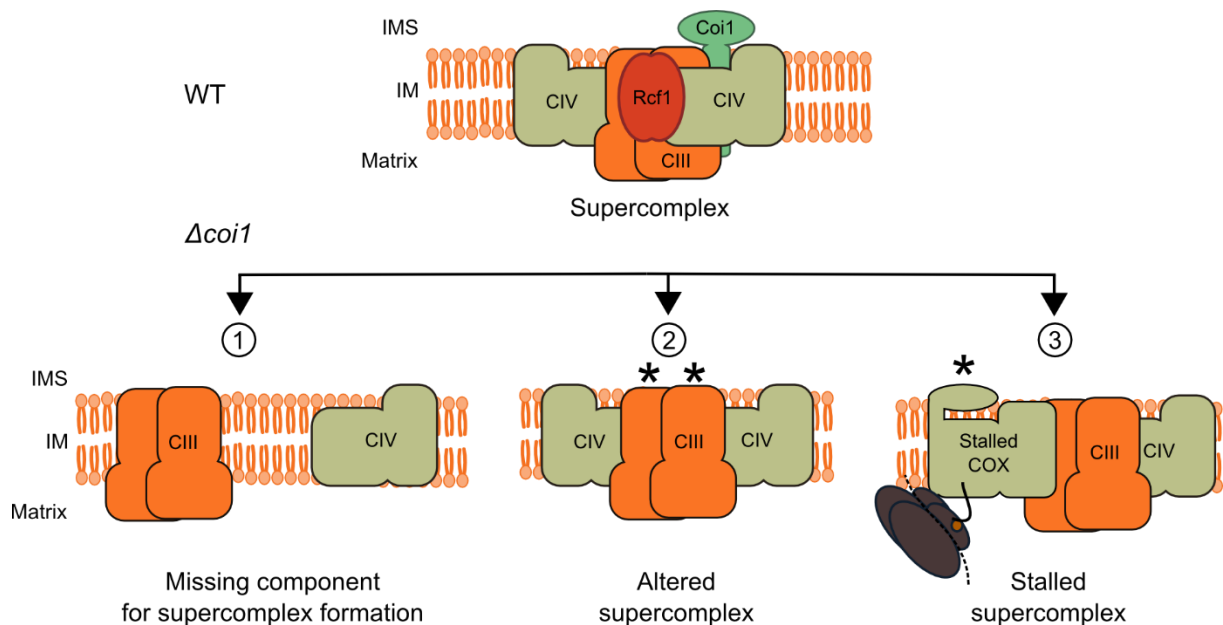

Figure 7.3 Suggested models for the involvement of Coi1 in supercomplex formation. Upper part: In WT cells Coi1 and Rcf1 help to form supercomplexes of complex III and complex IV. Lower part: Deletion of *COI1* can lead to unassembled supercomplex and the coexistence of different pools such as **(1)** partially assembled supercomplexes, **(2)** altered structure of assembled supercomplexes, or **(3)** stalled assembly of complex IV due to defects in heme integration. *, stalled complex IV; **, altered supercomplex.

8 References

Acin-Perez, R., and Enriquez, J.A. (2014). The function of the respiratory supercomplexes: the plasticity model. Biochim Biophys Acta *1837*, 444-450.

Acin-Perez, R., Fernandez-Silva, P., Peleato, M.L., Perez-Martos, A., and Enriquez, J.A. (2008). Respiratory active mitochondrial supercomplexes. Mol Cell *32*, 529-539.

Ahmed, A.U., and Fisher, P.R. (2009). Import of nuclear-encoded mitochondrial proteins: a cotranslational perspective. Int Rev Cell Mol Biol *273*, 49-68.

Allen, J.W., Ginger, M.L., and Ferguson, S.J. (2004). Maturation of the unusual single-cysteine (XXXCH) mitochondrial c-type cytochromes found in trypanosomatids must occur through a novel biogenesis pathway. Biochem J *383*, 537-542.

Althoff, T., Mills, D.J., Popot, J.L., and Kuhlbrandt, W. (2011). Arrangement of electron transport chain components in bovine mitochondrial supercomplex I1III2IV1. EMBO J *30*, 4652-4664.

Arnold, I., Pfeiffer, K., Neupert, W., Stuart, R.A., and Schägger, H. (1998). Yeast mitochondrial F1F0-ATP synthase exists as a dimer: identification of three dimer-specific subunits. EMBO J *17*, 7170-7178.

Bareth, B., Dennerlein, S., Mick, D.U., Nikolov, M., Urlaub, H., and Rehling, P. (2013). The heme a synthase Cox15 associates with cytochrome c oxidase assembly intermediates during Cox1 maturation. Mol Cell Biol *33*, 4128-4137.

Barrientos, A., Zambrano, A., and Tzagoloff, A. (2004). Mss51p and Cox14p jointly regulate mitochondrial Cox1p expression in Saccharomyces cerevisiae. EMBO J *23*, 3472-3482.

Barros, M.H., Nobrega, F.G., and Tzagoloff, A. (2002). Mitochondrial ferredoxin is required for heme A synthesis in Saccharomyces cerevisiae. J Biol Chem *277*, 9997-10002.

Becker, T., Böttinger, L., and Pfanner, N. (2012). Mitochondrial protein import: from transport pathways to an integrated network. Trends Biochem Sci *37*, 85-91.

Birnboim, H.C., and Doly, J. (1979). A rapid alkaline extraction procedure for screening recombinant plasmid DNA. Nucleic Acids Res *7*, 1513-1523.

Boekema, E.J., and Braun, H.P. (2007). Supramolecular structure of the mitochondrial oxidative phosphorylation system. J Biol Chem *282*, 1-4.

Bohnert, M., Rehling, P., Guiard, B., Herrmann, J.M., Pfanner, N., and van der Laan, M. (2010). Cooperation of stop-transfer and conservative sorting mechanisms in mitochondrial protein transport. Curr Biol *20*, 1227-1232.

Borgese, N., Brambillasca, S., and Colombo, S. (2007). How tails guide tail-anchored proteins to their destinations. Curr Opin Cell Biol *19*, 368-375.

Bottinger, L., Guiard, B., Oeljeklaus, S., Kulawiak, B., Zufall, N., Wiedemann, N., Warscheid, B., van der Laan, M., and Becker, T. (2013). A complex of Cox4 and mitochondrial Hsp70 plays an important role in the assembly of the cytochrome c oxidase. Mol Biol Cell *24*, 2609-2619.

Bradford, M.M. (1976). A rapid and sensitive method for the quantitation of microgram quantities of protein utilizing the principle of protein-dye binding. Anal Biochem *72*, 248-254.

Brix, J., Rüdiger, S., Bukau, B., Schneider-Mergener, J., and Pfanner, N. (1999). Distribution of binding sequences for the mitochondrial import receptors Tom20, Tom22, and Tom70 in a presequence-carrying preprotein and a non-cleavable preprotein. J Biol Chem *274*, 16522-16530.

Castresana, J., Lübben, M., Saraste, M., and Higgins, D.G. (1994). Evolution of cytochrome oxidase, an enzyme older than atmospheric oxygen. EMBO J *13*, 2516-2525.

Cavalier-Smith, T. (1987). The origin of eukaryotic and archaebacterial cells. Ann. N. Y. Acad. Sci. *503*, 17-54.

Chaban, Y., Boekema, E.J., and Dudkina, N.V. (2014). Structures of mitochondrial oxidative phosphorylation supercomplexes and mechanisms for their stabilisation. Biochim Biophys Acta *1837*, 418-426.

Chacinska, A., Koehler, C.M., Milenkovic, D., Lithgow, T., and Pfanner, N. (2009). Importing mitochondrial proteins: machineries and mechanisms. Cell *138*, 628-644.

Chacinska, A., Pfannschmidt, S., Wiedemann, N., Kozjak, V., Sanjuán Szklarz, L.K., Schulze-Specking, A., Truscott, K.N., Guiard, B., Meisinger, C., and Pfanner, N. (2004). Essential role of Mia40 in import and assembly of mitochondrial intermembrane space proteins. EMBO J *23*, 3735-3746.

Chen, Y.-C., Taylor, Eric B., Dephoure, N., Heo, J.-M., Tonhato, A., Papandreou, I., Nath, N., Denko, Nicolas C., Gygi, Steven P., and Rutter, J. (2012). Identification of a Protein Mediating Respiratory Supercomplex Stability. Cell Metab *15*, 348-360.

Church, C., Goehring, B., Forsha, D., Wazny, P., and Poyton, R.O. (2005). A role for Pet100p in the assembly of yeast cytochrome c oxidase: interaction with a subassembly that accumulates in a pet100 mutant. J Biol Chem *280*, 1854-1863.

Claypool, S.M., Oktay, Y., Boontheung, P., Loo, J.A., and Koehler, C.M. (2008). Cardiolipin defines the interactome of the major ADP/ATP carrier protein of the mitochondrial inner membrane. J Cell Biol *182*, 937-950.

Cogliati, S., Frezza, C., Soriano, Maria E., Varanita, T., Quintana-Cabrera, R., Corrado, M., Cipolat, S., Costa, V., Casarin, A., Gomes, Ligia C.*, et al.* (2013). Mitochondrial Cristae Shape Determines Respiratory Chain Supercomplexes Assembly and Respiratory Efficiency. Cell *155*, 160-171.

Cruciat, C.M., Brunner, S., Baumann, F., Neupert, W., and Stuart, R.A. (2000). The cytochrome bc1 and cytochrome c oxidase complexes associate to form a single supracomplex in yeast mitochondria. J Biol Chem *275*, 18093-18098.

Das, J., Miller, S.T., and Stern, D.L. (2004). Comparison of diverse protein sequences of the nuclear-encoded subunits of cytochrome C oxidase suggests conservation of structure underlies evolving functional sites. Mol Biol Evol *21*, 1572-1582.

Daum, G., Böhni, P.C., and Schatz, G. (1982). Import of proteins into mitochondria. Cytochrome b2 and cytochrome c peroxidase are located in the intermembrane space of yeast mitochondria. J Biol Chem *257*, 13028-13033.

Davies, K.M., Anselmi, C., Wittig, I., Faraldo-Gómez, J.D., and Kühlbrandt, W. (2012). Structure of the yeast F1Fo-ATP synthase dimer and its role in shaping the mitochondrial cristae. Proc Natl Acad Sci U S A *109*, 13602-13607.

Davis, A.J., Alder, N.N., Jensen, R.E., and Johnson, A.E. (2007). The Tim9p/10p and Tim8p/13p Complexes Bind to Specific Sites on Tim23p during Mitochondrial Protein Import. Mol Biol Cell *18*, 475-486.

Diekert, K., Kispal, G., Guiard, B., and Lill, R. (1999). An internal targeting signal directing proteins into the mitochondrial intermembrane space. Proc Natl Acad Sci U S A *96*, 11752-11757.

Dienhart, M.K., and Stuart, R.A. (2008). The yeast Aac2 protein exists in physical association with the cytochrome bc1-COX supercomplex and the TIM23 machinery. Mol Biol Cell *19*, 3934-3943.

Dudek, J., Rehling, P., and van der Laan, M. (2013). Mitochondrial protein import: common principles and physiological networks. Biochim Biophys Acta *1833*, 274-285.

Dudkina, N.V., Kouril, R., Peters, K., Braun, H.-P., and Boekema, E.J. (2010). Structure and function of mitochondrial supercomplexes. Biochim Biophys Acta *1797*, 664-670.

Dudkina, N.V., Kudryashev, M., Stahlberg, H., and Boekema, E.J. (2011). Interaction of complexes I, III, and IV within the bovine respirasome by single particle cryoelectron tomography. Proc Natl Acad Sci U S A *108*, 15196-15200.

Eubel, H., Jänsch, L., and Braun, H.-P. (2003). New insights into the respiratory chain of plant mitochondria. Supercomplexes and a unique composition of complex II. Plant Physiol *133*, 274-286.

Fox, T.D. (2012). Mitochondrial Protein Synthesis, Import, and Assembly. Genetics *192*, 1203-1234.

Friedman, J.R., Mourier, A., Yamada, J., McCaffery, J.M., and Nunnari, J. (2015). MICOS coordinates with respiratory complexes and lipids to establish mitochondrial inner membrane architecture. Elife *4*.

Fujiki, M., and Verner, K. (1991). Coupling of protein synthesis and mitochondrial import in a homologous yeast in vitro system. J Biol Chem *266*, 6841-6847.

Fujiki, M., and Verner, K. (1993). Coupling of cytosolic protein synthesis and mitochondrial protein import in yeast. Evidence for cotranslational import in vivo. J Biol Chem *268*, 1914-1920.

Fujiki, Y., Hubbard, A.L., Fowler, S., and Lazarow, P.B. (1982). Isolation of intracellular membranes by means of sodium carbonate treatment: application to endoplasmic reticulum. J Cell Biol *93*, 97-102.

Fulop, V., Sam, K.A., Ferguson, S.J., Ginger, M.L., and Allen, J.W. (2009). Structure of a trypanosomatid mitochondrial cytochrome c with heme attached via only one thioether bond and implications for the substrate recognition requirements of heme lyase. FEBS J *276*, 2822-2832.

Gartner, F., Voos, W., Querol, A., Miller, B.R., Craig, E.A., Cumsky, M.G., and Pfanner, N. (1995). Mitochondrial import of subunit Va of cytochrome c oxidase characterized with yeast mutants. J Biol Chem *270*, 3788-3795.

Gavin, P.D., Prescott, M., Luff, S.E., and Devenish, R.J. (2004). Cross-linking ATP synthase complexes in vivo eliminates mitochondrial cristae. J Cell Sci *117*, 2333-2343.

Geier, B.M., Schägger, H., Ortwein, C., Link, T.A., Hagen, W.R., Brandt, U., and Von Jagow, G. (1995). Kinetic properties and ligand binding of the eleven-subunit cytochrome-c oxidase from Saccharomyces cerevisiae isolated with a novel large-scale purification method. Eur J Biochem *227*, 296-302.

Genova, M.L., and Lenaz, G. (2014). Functional role of mitochondrial respiratory supercomplexes. Biochim Biophys Acta *1837*, 427-443.

Gietz, R.D., Schiestl, R.H., Willems, A.R., and Woods, R.A. (1995). Studies on the transformation of intact yeast cells by the LiAc/SS-DNA/PEG procedure. Yeast *11*, 355-360.

Glerum, D.M., Koerner, T.J., and Tzagoloff, A. (1995). Cloning and characterization of COX14, whose product is required for assembly of yeast cytochrome oxidase. J Biol Chem *270*, 15585-15590.

Grandier-Vazeille, X., Bathany, K., Chaignepain, S., Camougrand, N., Manon, S., and Schmitter, J.M. (2001). Yeast mitochondrial dehydrogenases are associated in a supramolecular complex. Biochemistry *40*, 9758-9769.

Gray, M.W., Burger, G., and Lang, B.F. (1999). Mitochondrial evolution. Science *283*, 1476-1481.

Hackenbrock, C.R., Chazotte, B., and Gupte, S.S. (1986). The random collision model and a critical assessment of diffusion and collision in mitochondrial electron transport. J Bioenerg Biomembr *18*, 331-368.

Hackenbrock, C.R., Schneider, H., Lemasters, J.J., and Höchli, M. (1980). Relationships between bilayer lipid, motional freedom of oxidoreductase components, and electron transfer in the mitochondrial inner membrane. Adv Exp Med Biol *132*, 245-263.

Heinemeyer, J., Braun, H.-P., Boekema, E.J., and Kouril, R. (2007). A structural model of the cytochrome C reductase/oxidase supercomplex from yeast mitochondria. J Biol Chem *282*, 12240-12248.

Hell, K. (2008). The Erv1-Mia40 disulfide relay system in the intermembrane space of mitochondria. Biochim Biophys Acta *1783*, 601-609.

Hell, K., Neupert, W., and Stuart, R.A. (2001). Oxa1p acts as a general membrane insertion machinery for proteins encoded by mitochondrial DNA. EMBO J *20*, 1281-1288.

Herrmann, J.M., Neupert, W., and Stuart, R.A. (1997). Insertion into the mitochondrial inner membrane of a polytopic protein, the nuclear-encoded Oxa1p. EMBO J *16*, 2217-2226.

Hoffmann, H.P., and Avers, C.J. (1973). Mitochondrion of yeast: ultrastructural evidence for one giant, branched organelle per cell. Science *181*, 749-751.

Hunte, C., Koepke, J., Lange, C., Rossmanith, T., and Michel, H. (2000). Structure at 2.3 A resolution of the cytochrome bc(1) complex from the yeast Saccharomyces cerevisiae co-crystallized with an antibody Fv fragment. Structure *8*, 669-684.

Khalimonchuk, O., Bestwick, M., Meunier, B., Watts, T.C., and Winge, D.R. (2010). Formation of the redox cofactor centers during Cox1 maturation in yeast cytochrome oxidase. Mol Cell Biol *30*, 1004-1017.

Kim, H.J., Khalimonchuk, O., Smith, P.M., and Winge, D.R. (2012). Structure, function, and assembly of heme centers in mitochondrial respiratory complexes. Biochim Biophys Acta *1823*, 1604-1616.

Kyhse-Andersen, J. (1984). Electroblotting of multiple gels: a simple apparatus without buffer tank for rapid transfer of proteins from polyacrylamide to nitrocellulose. J Biochem Biophys Methods *10*, 203-209.

Lange, C., and Hunte, C. (2002). Crystal structure of the yeast cytochrome bc1 complex with its bound substrate cytochrome c. Proc Natl Acad Sci U S A *99*, 2800-2805.

Lenaz, G. (2001). A critical appraisal of the mitochondrial coenzyme Q pool. FEBS Lett *509*, 151-155.

Levchenko, M., Wuttke, J.M., Rompler, K., Schmidt, B., Neifer, K., Juris, L., Wissel, M., Rehling, P., and Deckers, M. (2016). Cox26 is a novel stoichiometric subunit of the yeast cytochrome c oxidase. Biochim Biophys Acta *1863*, 1624-1632.

Lill, R. (2009). Function and biogenesis of iron-sulphur proteins. Nature *460*, 831-838.

Mashkevich, G., Repetto, B., Glerum, D.M., Jin, C., and Tzagoloff, A. (1997). SHY1, the yeast homolog of the mammalian SURF-1 gene, encodes a mitochondrial protein required for respiration. J Biol Chem *272*, 14356-14364.

Mavridou, D.A., Stevens, J.M., Monkemeyer, L., Daltrop, O., di Gleria, K., Kessler, B.M., Ferguson, S.J., and Allen, J.W. (2012). A pivotal heme-transfer reaction intermediate in cytochrome c biogenesis. J Biol Chem *287*, 2342-2352.

Mayer, A., Lill, R., and Neupert, W. (1993). Translocation and insertion of precursor proteins into isolated outer membranes of mitochondria. J Cell Biol *121*, 1233-1243.

McCaldon, P., and Argos, P. (1988). Oligopeptide biases in protein sequences and their use in predicting protein coding regions in nucleotide sequences. Proteins *4*, 99-122.

McKenzie, M., Lazarou, M., Thorburn, D.R., and Ryan, M.T. (2006). Mitochondrial respiratory chain supercomplexes are destabilized in Barth Syndrome patients. J Mol Biol *361*, 462-469.

Melton, D.A., Krieg, P.A., Rebagliati, M.R., Maniatis, T., Zinn, K., and Green, M.R. (1984). Efficient in vitro synthesis of biologically active RNA and RNA hybridization probes from plasmids containing a bacteriophage SP6 promoter. Nucleic Acids Res *12*, 7035-7056.

Mick, D.U., Fox, T.D., and Rehling, P. (2011). Inventory control: cytochrome c oxidase assembly regulates mitochondrial translation. Nat Rev Mol Cell Biol *12*, 14-20.

Mick, D.U., Vukotic, M., Piechura, H., Meyer, H.E., Warscheid, B., Deckers, M., and Rehling, P. (2010). Coa3 and Cox14 are essential for negative feedback regulation of COX1 translation in mitochondria. J Cell Biol *191*, 141-154.

Mileykovskaya, E., Penczek, P.A., Fang, J., Mallampalli, V.K., Sparagna, G.C., and Dowhan, W. (2012). Arrangement of the respiratory chain complexes in Saccharomyces cerevisiae supercomplex III2IV2 revealed by single particle cryo-electron microscopy. J Biol Chem *287*, 23095-23103.

Moreno-Lastres, D., Fontanesi, F., García-Consuegra, I., Martín, M.A., Arenas, J., Barrientos, A., and Ugalde, C. (2012). Mitochondrial complex I plays an essential role in human respirasome assembly. Cell Metab *15*, 324-335.

Neupert, W., and Herrmann, J.M. (2007). Translocation of proteins into mitochondria. Annu Rev Biochem *76*, 723-749.

Nobrega, F.G., Nobrega, M.P., and Tzagoloff, A. (1992). BCS1, a novel gene required for the expression of functional Rieske iron-sulfur protein in Saccharomyces cerevisiae. EMBO J *11*, 3821-3829.

Okamoto, K., and Shaw, J.M. (2005). Mitochondrial morphology and dynamics in yeast and multicellular eukaryotes. Annu Rev Genet *39*, 503-536.

Ott, M., Prestele, M., Bauerschmitt, H., Funes, S., Bonnefoy, N., and Herrmann, J.M. (2006). Mba1, a membrane-associated ribosome receptor in mitochondria. EMBO J *25*, 1603-1610.

Pagliarini, D.J., Calvo, S.E., Chang, B., Sheth, S.A., Vafai, S.B., Ong, S.-E., Walford, G.A., Sugiana, C., Boneh, A., Chen, W.K.*, et al.* (2008). A mitochondrial protein compendium elucidates complex I disease biology. Cell *134*, 112-123.

Paschen, S.A., Waizenegger, T., Stan, T., Preuss, M., Cyrklaff, M., Hell, K., Rapaport, D., and Neupert, W. (2003). Evolutionary conservation of biogenesis of beta-barrel membrane proteins. Nature *426*, 862-866.

Pfeiffer, K., Gohil, V., Stuart, R.A., Hunte, C., Brandt, U., Greenberg, M.L., and Schägger, H. (2003). Cardiolipin stabilizes respiratory chain supercomplexes. J Biol Chem *278*, 52873-52880.

Prokisch, H., Andreoli, C., Ahting, U., Heiss, K., Ruepp, A., Scharfe, C., and Meitinger, T. (2006). MitoP2: the mitochondrial proteome database--now including mouse data. Nucleic Acids Res *34*, D705-711.

Rapaport, D., Neupert, W., and Lill, R. (1997). Mitochondrial protein import. Tom40 plays a major role in targeting and translocation of preproteins by forming a specific binding site for the presequence. J Biol Chem *272*, 18725-18731.

Rehling, P., Model, K., Brandner, K., Kovermann, P., Sickmann, A., Meyer, H.E., Kuhlbrandt, W., Wagner, R., Truscott, K.N., and Pfanner, N. (2003). Protein insertion into the mitochondrial inner membrane by a twin-pore translocase. Science *299*, 1747-1751.

Saiki, R.K., Gelfand, D.H., Stoffel, S., Scharf, S.J., Higuchi, R., Horn, G.T., Mullis, K.B., and Erlich, H.A. (1988). Primer-directed enzymatic amplification of DNA with a thermostable DNA polymerase. Science *239*, 487-491.

Sambrook J., F.E.F., Maniatis T. , NY (1989). Molecular Cloning: A Laboratory Manual. Cold Spring Harbor Laboratory Press; Plainview.

Saraste, M. (1999). Oxidative phosphorylation at the fin de siècle. Science *283*, 1488-1493.

Schagger, H. (2001a). Blue-native gels to isolate protein complexes from mitochondria. Methods Cell Biol *65*, 231-244.

Schagger, H. (2001b). Respiratory chain supercomplexes. IUBMB life *52*, 119-128.

Schägger, H. (2002). Respiratory chain supercomplexes of mitochondria and bacteria. Biochim Biophys Acta *1555*, 154-159.

Schägger, H., and Pfeiffer, K. (2000). Supercomplexes in the respiratory chains of yeast and mammalian mitochondria. EMBO J *19*, 1777-1783.

Schagger, H., and von Jagow, G. (1991). Blue native electrophoresis for isolation of membrane protein complexes in enzymatically active form. Anal Biochem *199*, 223-231.

Scheffler, I.E. (2001). A century of mitochondrial research: achievements and perspectives. Mitochondrion *1*, 3-31.

Schmidt, O., Pfanner, N., and Meisinger, C. (2010). Mitochondrial protein import: from proteomics to functional mechanisms. Nat Rev Mol Cell Biol *11*, 655-667.

Schnell, D.J., and Hebert, D.N. (2003). Protein translocons: multifunctional mediators of protein translocation across membranes. Cell *112*, 491-505.

Shoubridge, E.A. (2012). Supersizing the mitochondrial respiratory chain. Cell Metab *15*, 271-272.

Smith, P.M., Fox, J.L., and Winge, D.R. (2012). Biogenesis of the cytochrome bc1 complex and role of assembly factors. Biochim Biophys Acta *1817*, 276-286.

Soll, J., and Schleiff, E. (2004). Protein import into chloroplasts. Nat Rev Mol Cell Biol *5*, 198-208.

Soto, I.C., Fontanesi, F., Liu, J., and Barrientos, A. (2012). Biogenesis and assembly of eukaryotic cytochrome *c* oxidase catalytic core. Biochim Biophys Acta *1817*, 883-897.

Stiburek, L., Vesela, K., Hansikova, H., Pecina, P., Tesarova, M., Cerna, L., Houstek, J., and Zeman, J. (2005). Tissue-specific cytochrome *c* oxidase assembly defects due to mutations in SCO2 and SURF1. Biochem J *392*, 625-632.

Strecker, V., Kadeer, Z., Heidler, J., Cruciat, C.M., Angerer, H., Giese, H., Pfeiffer, K., Stuart, R.A., and Wittig, I. (2016). Supercomplex-associated Cox26 protein binds to cytochrome *c* oxidase. Biochim Biophys Acta *1863*, 1643-1652.

Strogolova, V., Furness, A., Robb-McGrath, M., Garlich, J., and Stuart, R.A. (2012). Rcf1 and Rcf2, Members of the Hypoxia-Induced Gene 1 Protein Family, Are Critical Components of the Mitochondrial Cytochrome bc1-Cytochrome c Oxidase Supercomplex. Mol Cell Biol *32*, 1363-1373.

Stuart, R.A. (2008). Supercomplex organization of the oxidative phosphorylation enzymes in yeast mitochondria. J Bioenerg Biomembr *40*, 411-417.

Towbin, H., Staehelin, T., and Gordon, J. (1979). Electrophoretic transfer of proteins from polyacrylamide gels to nitrocellulose sheets: procedure and some applications. Proc Natl Acad Sci U S A *76*, 4350-4354.

Trochimchuk, T., Fotheringham, J., Topp, E., Schraft, H., and Leung, K.T. (2003). A comparison of DNA extraction and purification methods to detect Escherichia coli O157:H7 in cattle manure. J Microbiol Methods *54*, 165-175.

Tsukihara, T., Aoyama, H., Yamashita, E., Tomizaki, T., Yamaguchi, H., Shinzawa-Itoh, K., Nakashima, R., Yaono, R., and Yoshikawa, S. (1996). The whole structure of the 13-subunit oxidized cytochrome c oxidase at 2.8 A. Science *272*, 1136-1144.

Turakhiya, U., von der Malsburg, K., Gold, V.A., Guiard, B., Chacinska, A., van der Laan, M., and Ieva, R. (2016). Protein Import by the Mitochondrial Presequence Translocase in the Absence of a Membrane Potential. J Mol Biol *428*, 1041-1052.

Tzagoloff, A., Nobrega, M., Gorman, N., and Sinclair, P. (1993). On the functions of the yeast COX10 and COX11 gene products. Biochem Mol Biol Int *31*, 593-598.

van der Laan, M., Hutu, D.P., and Rehling, P. (2010). On the mechanism of preprotein import by the mitochondrial presequence translocase. Biochim Biophys Acta *1803*, 732-739.

Vukotic, M., Oeljeklaus, S., Wiese, S., Vögtle, F.N., Meisinger, C., Meyer, H.E., Zieseniss, A., Katschinski, D.M., Jans, D.C., Jakobs, S*., et al.* (2012). Rcf1 mediates cytochrome oxidase assembly and respirasome formation, revealing heterogeneity of the enzyme complex. Cell Metab *15*, 336-347.

Wach, A., Brachat, A., Alberti-Segui, C., Rebischung, C., and Philippsen, P. (1997). Heterologous HIS3 marker and GFP reporter modules for PCR-targeting in Saccharomyces cerevisiae. Yeast *13*, 1065-1075.

Wessel, D., and Flugge, U.I. (1984). A method for the quantitative recovery of protein in dilute solution in the presence of detergents and lipids. Anal Biochem *138*, 141-143.

Westermann, B., and Neupert, W. (2000). Mitochondria-targeted green fluorescent proteins: convenient tools for the study of organelle biogenesis in Saccharomyces cerevisiae. Yeast *16*, 1421-1427.

Winge, D.R. (2012). Sealing the mitochondrial respirasome. Mol Cell Biol *32*, 2647-2652.

Yoshida, M., Muneyuki, E., and Hisabori, T. (2001). ATP synthase--a marvellous rotary engine of the cell. Nat Rev Mol Cell Biol *2*, 669-677.

Youle, R.J., and Karbowski, M. (2005). Mitochondrial fission in apoptosis. Nat Rev Mol Cell Biol *6*, 657-663.

Zahedi, R.P., Sickmann, A., Boehm, A.M., Winkler, C., Zufall, N., Schönfisch, B., Guiard, B., Pfanner, N., and Meisinger, C. (2006). Proteomic analysis of the yeast mitochondrial outer membrane reveals accumulation of a subclass of preproteins. Mol Biol Cell *17*, 1436-1450.

Zickermann, V., Angerer, H., Ding, M.G., Nübel, E., and Brandt, U. (2010). Small single transmembrane domain (STMD) proteins organize the hydrophobic subunits of large membrane protein complexes. FEBS Lett *584*, 2516-2525.

9 Acknowledgements

10 Curriculum Vitae

Ravi Kumar Singhal

May 30, 1987	Born Jind, Haryana India
2003 - 2005	Senior Secondary, Bangalore India
2005 - 2009	Bachelor of Engineering in Biotechnology, Bangalore India
2009 - 2010	Research trainee at National centre of biological science, Bangalore India
2010 - 2012	Masters in cell and molecular biology, Uppsala University, Sweden
2012 - 2017	PhD research in the laboratory of Prof. Dr. Doron Rapaport at the Interfaculty institute of biochemistry, University of Tuebingen, Germany